1

MASSACHUSETTS INSTITUTE OF TECHNOLOGY
DEPARTMENT OF NUCLEAR ENGINEERING
Cambridge, Massachusetts 02139

MIT-2344-4 MITNE-65

HEAVY WATER LATTICE PROJECT ANNUAL REPORT

September 30, 1965

Contract AT (30-1)-2344
U.S. Atomic Energy Commission

MASSACHUSETTS INSTITUTE OF TECHNOLOGY
DEPARTMENT OF NUCLEAR ENGINEERING
Cambridge, Massachusetts 02139

MIT-2344-4 MITNE-65
AEC Research and Development Report
UC-34 Physics
(TID-4500, 45th Edition)

HEAVY WATER LATTICE PROJECT ANNUAL REPORT

September 30, 1965

Contract AT(30-1)2344
U.S. Atomic Energy Commission

Editors:

T. J. Thompson
I. Kaplan
F. M. Clikeman
M. J. Driscoll

Contributors:

J. Barch
N. Berube
H. Bliss
F. M. Clikeman
W. H. D'Ardenne
M. J. Driscoll
D. M. Goebel
J. W. Gosnell
H. M. Guéron
J. Harrington, III
S. P. Hellman
I. Kaplan
B. Kelley
D. D. Lanning
L. T. Papay
E. E. Pilat
C. Robertson
E. Sefchovich
A. Supple
T. J. Thompson
G. L. Woodruff

DISTRIBUTION

MIT-2344-4 MITNE-65

AEC Research and Development Report

UC-34 Physics

(TID-4500, 45th Edition)

1. USAEC, New York Operations Office (D. Richtmann)
2. USAEC, Division of Reactor Development (P. Hemmig)
3-5. USAEC, Division of Reactor Development (I. Zartman)
6. USAEC, New York Patents Office (H. Potter)
7. USAEC, Division of Reactor Development, Washington, D.C. (S. Strauch)
8. USAEC, New York Operations Office, Research and Development Division
9. USAEC, Division of Reactor Development, Reports and Statistics Branch
10. USAEC, Maritime Reactors Branch
11. USAEC, Civilian Reactors Branch
12. USAEC, Army Reactors Branch
13. USAEC, Naval Reactors Branch
14. Advisory Committee on Reactor Physics (E. R. Cohen)
15. ACRP (G. Dessauer)
16. ACRP (D. de Bloisblanc)
17. ACRP (M. Edlund)
18. ACRP (R. Ehrlich)

19. ACRP (I. Kaplan)

20. ACRP (J. Chernick)

21. ACRP (F. C. Maienschein)

22. ACRP (R. Avery)

23. ACRP (P. F. Zweifel)

24. ACRP (P. Gast)

25. ACRP (G. Hansen)

26. ACRP (S. Krasik)

27. ACRP (L. W. Nordheim)

28. ACRP (T. M. Snyder)

29. ACRP (J. J. Taylor)

30-32. O. T. I. E., Oak Ridge, for Standard Distribution

33-100. Internal Distribution

ABSTRACT

An experimental and theoretical program on the physics of heavy water moderated, partially enriched lattices is being conducted at the Massachusetts Institute of Technology. Experimental methods have been adapted or developed for research on buckling, fast fission, resonance capture, and thermal capture. In the past year, measurements have been made on lattices of 0.25-inch rods containing 1.143% enriched fuel and on 0.75-inch rods containing 0.947% enriched fuel. Research is also under way in the areas of single-rod measurements, two-region-lattice studies, studies of lattices with added neutron absorbers, fast neutron distribution measurements, miniature lattice work, and pulsed neutron methods.

TABLE OF CONTENTS

LIST OF FIGURES

LIST OF TABLES

1. INTRODUCTION

1. FORWARD

This report is the fifth annual progress report of the Heavy Water Lattice Project of the Massachusetts Institute of Technology. The first four progress reports describe the details of the facility and the development and testing of experimental methods, and report initial results (1, 2, 3, 4). This report is concerned mainly with the summary and analysis of data obtained by continued application of the methods developed. Although complete descriptions of facilities, apparatus and experimental methods are given in the reports listed in Appendix A, the various sections of this report have been written so that a reader having general familiarity with subcritical facility methods can understand and apply the results reported.

This report covers work done primarily in the period, October 1, 1964 through September 30, 1965; and covers specifically that which was not covered in the preceding annual report (4).

2. LATTICE FUEL ENRICHMENT

It appears appropriate to note recent information on the U^{235} concentration of some of the fuel rods used in our experiments. This information may have a slight effect on some of the data reported in the following sections. In a letter of June 14, 1965, L. Clark, Jr. of M.I.T. requested from the Brookhaven National Laboratory, the original user of this fuel, clarification of some inconsistencies in the accountability records for the Lattice Project's 1.027% enriched, one-quarter-inch-diameter fuel rods. In a reply dated September 15, 1965, Dr. G. A. Price of B.N.L. indicated that a thorough investigation had revealed that the true enrichment of this material averaged 1.016% instead of 1.027%. The B.N.L. letter also includes an analysis showing a small reduction of about 0.0035 in k_{eff} for some of their lattice work with this fuel. The 1.143% material supplied by B.N.L. to M.I.T. at the same time was also rechecked and the value of 1.143% confirmed.

Because this information has just become available, while most of the M.I.T. work on this fuel was published in last year's annual report, we have continued to describe the fuel as 1.027% enriched in this report to avoid further confusion. The use of 1.027% will also serve to remind the reader that this value was used in any calculations involved, and thus to identify uncorrected results. Any data eventually corrected and reported will be described as being for 1.016% fuel.

3. STAFF

The project staff during the report period was as follows:

I. Kaplan, Professor of Nuclear Engineering*

T. J. Thompson, Professor of Nuclear Engineering*

D. D. Lanning, Associate Professor of Nuclear Engineering (prior to July 1, 1965)

F. M. Clikeman, Assistant Professor of Nuclear Engineering*

M. J. Driscoll, Research Associate (since July 1, 1965)*

H. E. Bliss, Hertz Fellow*+

H. S. Cheng, Research Assistant

D. M. Goebel, Naval Postgraduate Student (JLOASEP)+

J. W. Gosnell, Research Associate*+

H. M. Guéron, Research Assistant

J. Harrington III, AEC Fellow*+

S. P. Hellman, Research Assistant

B. K. Malaviya, DSR Staff

L. T. Papay, AEC Fellow+

E. E. Pilat, Research Assistant*

C. G. Robertson, AEC Fellow+

E. Sefchovich, Research Assistant*

C. Stassis, Research Assistant*

G. Woodruff, Research Assistant*+

J. H. Barch, Senior Technician*

A. T. Supple, Jr., Senior Technician*

N. L. Berube, Technician*

Miss B. Kelley, Technical Assistant*

D. A. Gwinn, Part-time Electronics Supervisor*

---

*Continuing on staff as of October 1, 1965.
+Not charged to contract.

4. REFERENCES

(1) "Heavy Water Lattice Research Project Annual Report," NYO-9658, September 30, 1961.

(2) "Heavy Water Lattice Project Annual Report," NYO-10208 (MITNE-26), September 30, 1962.

(3) "Heavy Water Lattice Project Annual Report," NYO-10212 (MITNE-46), September 30, 1963.

(4) "Heavy Water Lattice Project Annual Report," MIT-2344-3 (MITNE-60), September 30, 1964.

2. MATERIAL BUCKLING AND INTRACELLULAR THERMAL NEUTRON DISTRIBUTIONS

J. Barch
N. Berube
B. Kelley
A. Supple
F. M. Clikeman

1. INTRODUCTION

Standard methods have been developed to measure the material buckling and the intracellular thermal neutron distributions for the lattices studied in the M.I.T. Lattice Facility (1, 2, 3, 4, 5, 6). Since the last annual report (4), results have been obtained by using these techniques on three lattices of uranium rods in D_2O. The results given in this report are for 1.143% U^{235} enriched, 0.25-inch-diameter rods in triangular lattice spacings of 1.75 and 2.50 inches and 0.947% U^{235} enriched, 0.75-inch-diameter uranium rods in a 2.50-inch triangular spacing.

2. BUCKLING MEASUREMENTS

2.1 Experimental Methods

Neutron flux distributions are measured throughout the lattice assembly by activating gold foils, both bare and cadmium-covered. Special aluminum foil holders are used to accurately position the foils throughout the lattice assembly. The relative gold activity is measured in both the radial and axial directions in the tank. The gold-cadmium ratio is then calculated as a function of position to locate that region of the lattice assembly which has an equilibrium neutron spectrum. The relative activities of both the bare and cadmium-covered foils from the equilibrium region are then fitted by least squares to the functional relationship:

$$\phi = AJ_o(\alpha r) \sinh \gamma(H-Z) , \qquad (2.1)$$

where:

α^2 is the radial buckling in the r direction,

γ^2 is the axial buckling in the Z direction,

and

H is the extrapolated height of the assembly.

The material buckling B_m^2 is then given by,

$$B_m^2 = \alpha^2 - \gamma^2 . \tag{2.2}$$

Corrections to the measured foil activities for counter deadtime, activity decay times and foil weights, together with the least-squares fitting to Eq. 2.1, are accomplished using an IBM 7094 computer.

A more detailed account of the experimental techniques may be found in Refs. 1, 2, 3, 4, and 6.

2.2 Results

The results of the measurements of α^2 and γ^2 for three lattices are given in Tables 2.1, 2.2 and 2.3.

The errors quoted for the buckling measurements are the standard deviation of the individual measurements of the buckling. The larger than usual standard deviation associated with the radial buckling of the 1.143% U^{235} enriched rods in the 2.50-inch-pitch lattice cannot be explained at the present time but is still under investigation.

3. INTRACELLULAR THERMAL NEUTRON DISTRIBUTIONS

Intracellular thermal neutron distributions are used to determine the thermal utilization of a lattice cell. The usual procedure is to measure the subcadmium gold activity in a representative cell. The measured distribution is then compared with the relative activity predicted by the computer code THERMØS. If the two activity distributions agree, then the thermal utilization computed by THERMØS is assumed to be a good value.

TABLE 2.1

Buckling Values for 0.25-Inch-O.D., 1.143% U^{235} Enriched Uranium Rods (Density of 18.898 gm/cm^3) in a 2.50-Inch Triangular Pitch Lattice

D_2O Temperature (°C)	Type of Run	Type of Detector	Run Number	Radial Buckling a^2 ($cm^{-2} \times 10^6$)	Axial Buckling γ^2 ($cm^{-2} \times 10^6$)	Material Buckling B_m^2 ($cm^{-2} \times 10^6$)
29	Axial	Bare Au	92		1390	
			93		1362	
			96		1415	
			98		1413	
			Average		1395 ± 12	
		Cd-covered Au	88		1374	
			90		1410	
			94		1418	
			A-2		1386	
			Average		1397 ± 11	
25		Bare Au	A-7		1368	
60			A-8		1430	
			A-9		1425	
29	Radial	Bare Au	87	2473		
			89	2389		
			97	2466		
			99	2422		
			Average	2438 ± 20		
		Cd-covered Au	91	2373		
			95	2401		
			A-0	2320		
			A-1	2339		
			A-3	2433		
			A-6	2413		
			Average	2380 ± 17		
Grand average of all 29°C axial measurements					1396 ± 7	
Grand average of all radial measurements				2403 ± 16		
Material Buckling = $a^2 - \gamma^2$ =						1007 ± 17

TABLE 2.2

Buckling Values for 0.25-Inch-O.D., 1.143% U^{235} Enriched Uranium Rods (Density of 18.898 gm/cm^3) in a 1.75-Inch Triangular Pitch Lattice

D_2O Temperature (°C)	Type of Run	Type of Detector	Run Number	Radial Buckling a^2 ($cm^{-2} \times 10^6$)	Axial Buckling γ^2 ($cm^{-2} \times 10^6$)	Material Buckling B_m^2 ($cm^{-2} \times 10^6$)
26	Axial	Bare Au	B-0		1000	
			B-5		985	
			B-7		979	
			B-9		976	
			Average		985 ± 5	
		Cd-covered Au	B-1		1090	
			C-2		1043	
			C-4		1058	
			D-2		1004	
			D-4		1002	
			D-0		990	
			Average		1031 ± 15	
	Radial	Bare Au	B-2	2427		
			B-6	2434		
			B-4	2416		
			B-8	2433		
			C-0	2426		
			Average	2427 ± 3		
		Cd-covered Au	C-3	2422		
			C-6	2414		
			C-9	2398		
			D-1	2411		
			D-5	2394		
			Average	2408 ± 5		
Grand average of all axial measurements					1013 ± 12	
Grand average of all radial measurements				2418 ± 4		
Material buckling = $a^2 - \gamma^2$ =						1405 ± 13

TABLE 2.3

Buckling Values for 0.75-Inch-O.D., 0.947% U^{235} Enriched Uranium Rods (Density of 18.9 gm/cm^3) in a 2.50-Inch Triangular Pitch Lattice

D_2O Temperature (°C)	Type of Run	Type of Detector	Run Number	Radial Buckling a^2 ($cm^{-2} \times 10^6$)	Axial Buckling γ^2 ($cm^{-2} \times 10^6$)	Material Buckling B_m^2 ($cm^{-2} \times 10^6$)
24	Axial	Bare Au	E-2		1441	
			E-9		1404	
			F-9		1385	
			G-0		1376	
			G-2		1404	
			G-8		1371	
			Average		1397 ± 10	
		Cd-covered Au	D-8		1405	
			E-6		1378	
			E-7		1394	
			Average		1392 ± 8	
24	Radial	Bare Au	D-6	2350		
			D-7	2385		
			Average	2368 ± 18		
		Cd-covered Au	E-0	2347		
			E-1	2378		
			E-8	2362		
			Average	2362 ± 9		
Grand average of all axial measurements					1395 ± 7	
Grand average of all radial measurements				2364 ± 8		
Material buckling = $a^2 - \gamma^2$ =						969 ± 11

3.1 Experimental Methods

The experimental techniques used were the same as those reported by Simms et al. (5). The gold foils used as detectors were 1/16 inch in diameter and either 0.0025, 0.0043, or 0.010 inch thick. The cadmium boxes were the same as used by Simms. The foil holders were similar to those used by Simms.

Both bare and cadmium-covered foils were irradiated in the lattice at the same time but in slightly different axial positions, as shown in Fig. 2.1. The activity of both the bare and cadmium-covered foils was counted on automatic sample-changing scintillation counters set to count the 0.411-Mev gamma ray in the $Au^{198} \xrightarrow{\beta} Hg^{198*} \xrightarrow{\gamma} Hg^{198}$ decay. The measured activity was corrected for background, counter deadtime, and the 2.7-day half-life of the Au^{198} activity.

The foil activity was also corrected for the different axial positions of the foils by using the equation,

$$\phi_i = \sinh \gamma(H-Z_i) ,$$

where Z_i is the height of the foil position above the bottom of the fuel. H and γ are the extrapolated height and the axial component of the buckling, respectively, and were measured in a separate experiment, as reported previously in this section.

After all of the corrections have been applied to the activities, the activities of the cadmium-covered foils are plotted as a function of radial position from the center of one fuel rod. A smooth curve is then drawn through the points by eye and the epicadmium activity is determined at each point. The epicadmium activities are then subtracted from the bare foil activities to yield the subcadmium or thermal activities. The thermal activities are then also plotted as a function of radial position.

In all cases, two rod-to-rod and one rod-to-moderator foil holders were used. In the moderator, no statistically significant difference in the activity could be observed between the gold foils irradiated in corresponding positions relative to the fuel rods. Therefore, in order to get better counting statistics, the activity of all of the foils irradiated in the same relative position in the cell were averaged together. It is this average that is plotted in Figs. 2.2, 2.3, and 2.4. The error due to the counting statistics is about the size of the points.

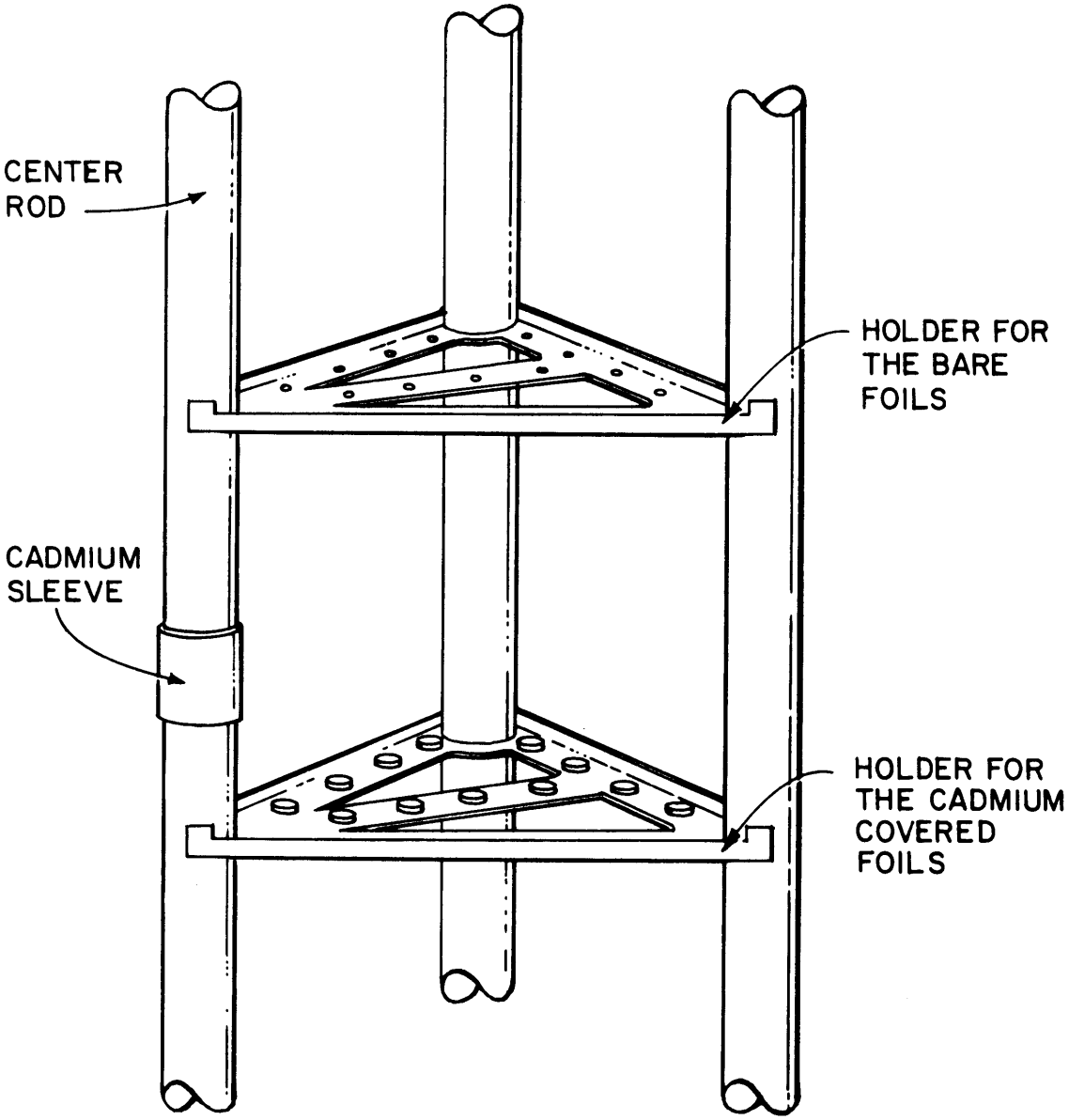

FIG. 2.1 FOIL HOLDER ARRANGEMENT FOR MICROSCOPIC FLUX MEASUREMENTS.

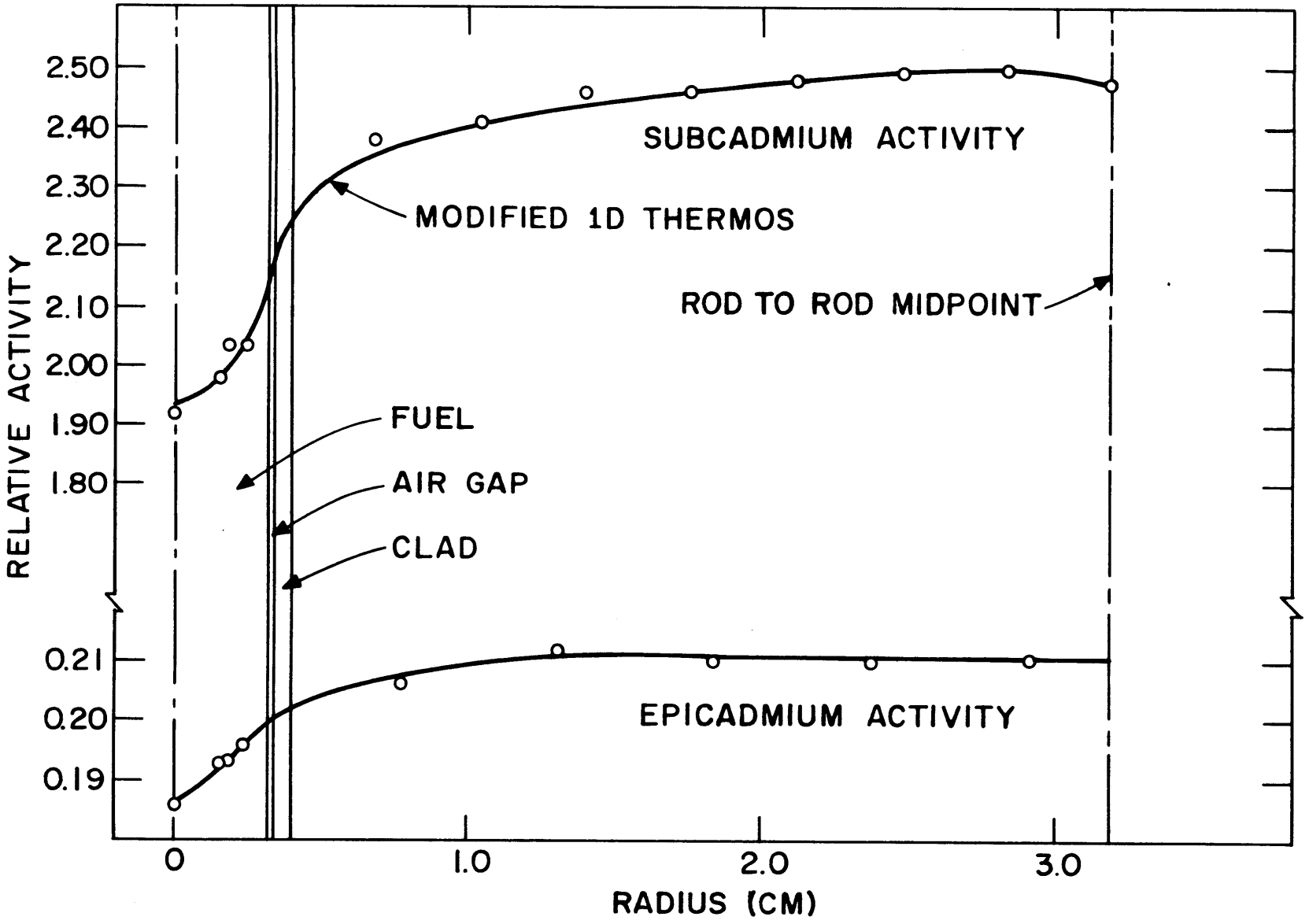

FIG. 2.2 MICROSCOPIC GOLD ACTIVITY DISTRIBUTION IN LATTICE OF 1/4-INCH DIAMETER 1.143% U^{235} URANIUM RODS ON A 2.50-INCH TRIANGULAR PITCH

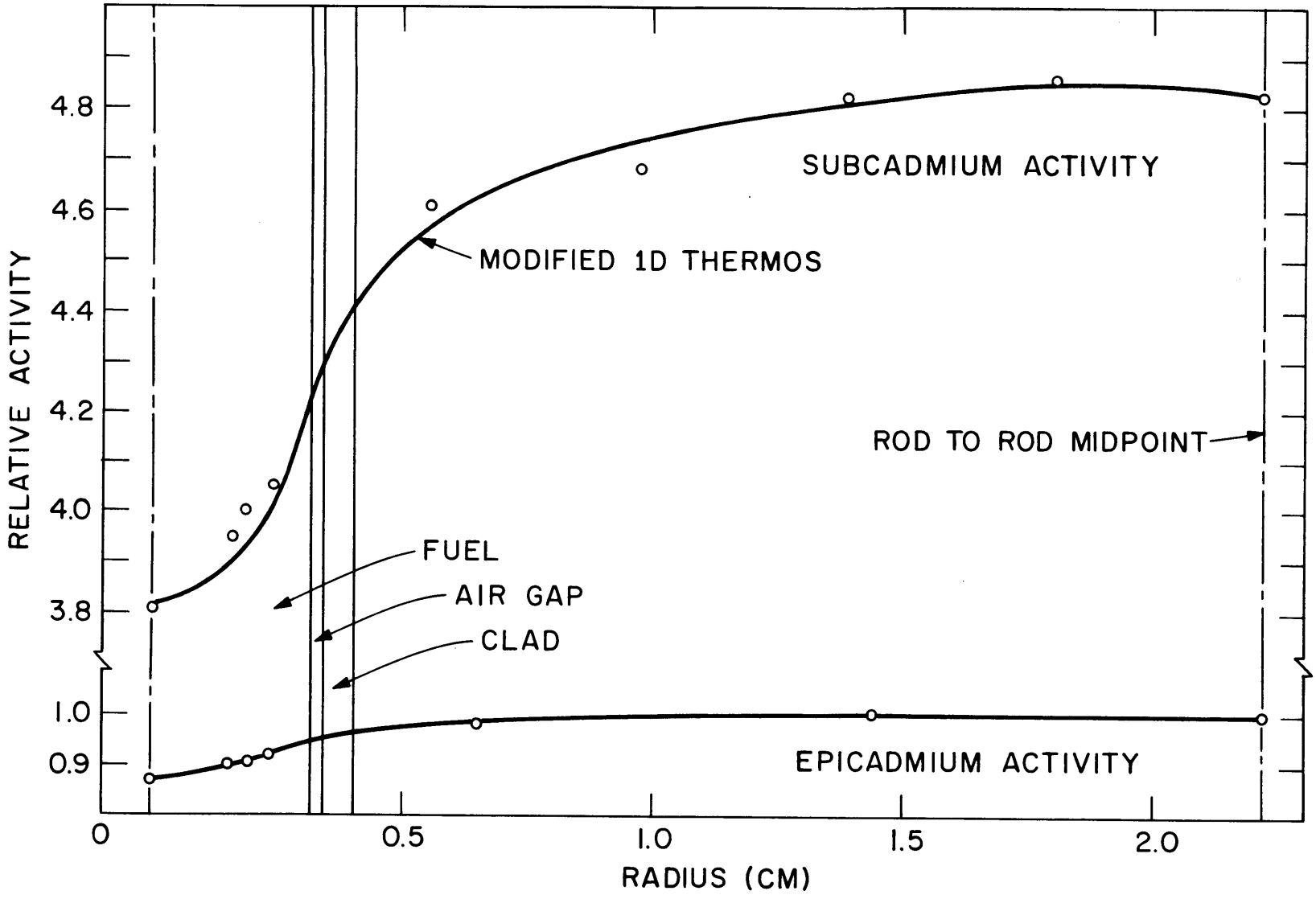

FIG. 2.3 MICROSCOPIC GOLD ACTIVITY DISTRIBUTION IN LATTICE OF 1/4 INCH DIAMETER 1.143% U^{235} URANIUM RODS ON A 1.75-INCH TRIANGULAR PITCH

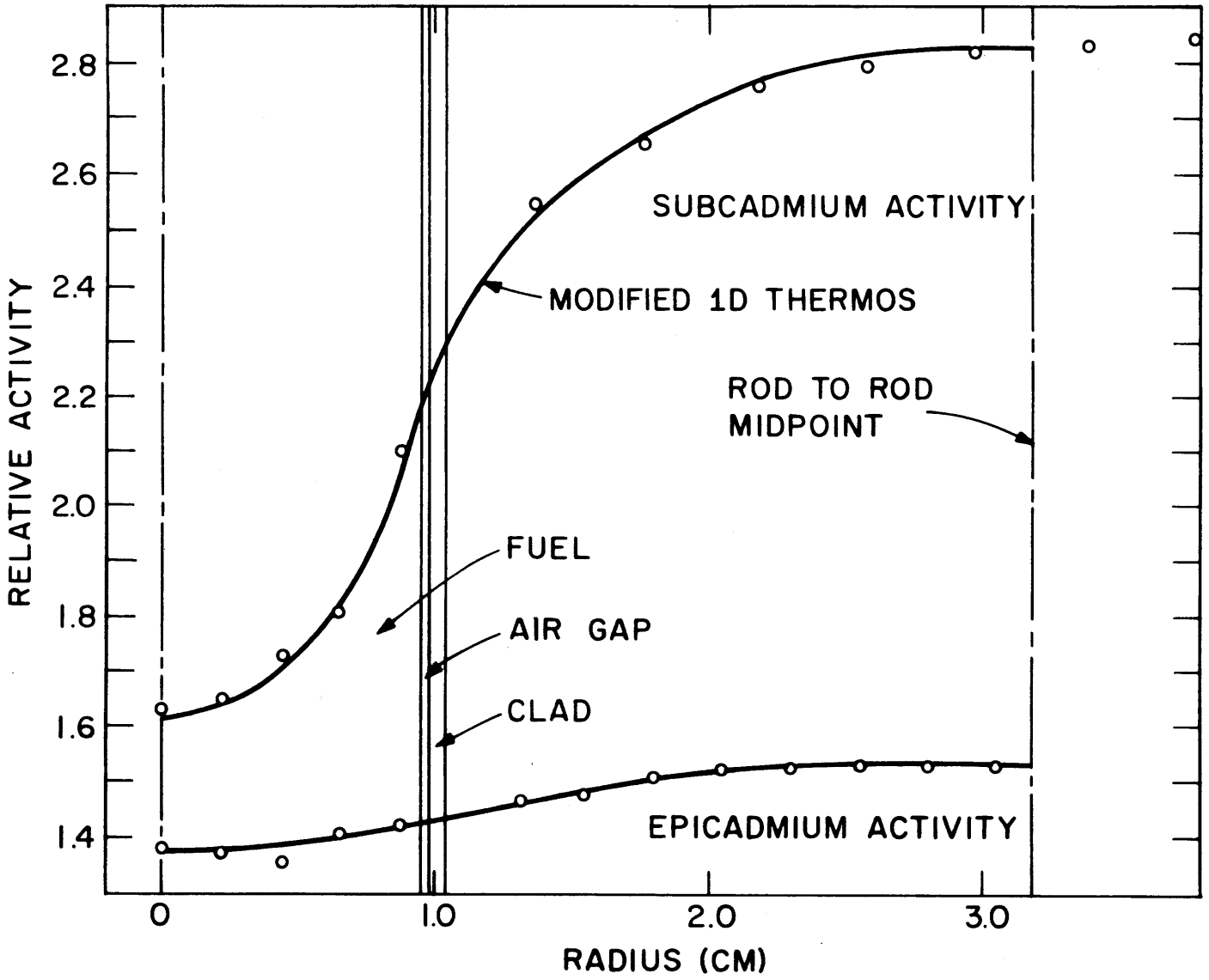

FIG. 2.4 MICROSCOPIC GOLD ACTIVITY DISTRIBUTION IN LATTICE OF 3/4 INCH DIAMETER 0.947% U^{235} URANIUM RODS ON A 2.50-INCH TRIANGULAR PITCH

3.2 Theoretical Calculations

The one-dimensional computer code THERMØS, as modified and reported by Simms et al., was used to compute the neutron flux distribution in a unit cell consisting of five regions: the fuel, a small air gap between the fuel and cladding, the cladding, the moderator, and a scattering region at the cell boundary. The computer code then used the computed flux distribution and the Au^{197} activation cross section to compute the relative activity of Au^{198} for gold placed in the cell. The Au^{198} cross section used was modified to take into account any self-shielding caused by using a finite thickness of gold.

THERMØS also computes the total absorption of neutrons in the cell for a number of different integrated energies. By using the energy range from 0.0 ev to 0.415 ev (the cadmium cutoff energy), the ratio of the number of neutrons absorbed in the fuel to the total number absorbed in the cell was determined, and this value is reported as f, the thermal utilization.

3.3 Results

Both the experimental and theoretical subcadmium gold activities are shown in Figs. 2.2, 2.3, and 2.4 for the three lattices studied. As shown in the figures, the agreement between the computed curves and experimental points is good. This leads one to believe that the modified 1D THERMØS code is a reasonably accurate description of the lattice cells and that the values of the thermal utilization that it computes are accurate. The results of THERMØS are given in Table 2.4. It might be noted that the sum of the absorptions does not equal 1.0000. This is because the code was programmed to consider absorption up to 0.785 ev, and the results given here are only for neutron energies up to 0.415 ev.

The error given for f is the same as that given by Brown, et al. (7) and comes primarily from uncertainties in the cross sections of aluminum and D_2O. The quoted error has no relationship to the degree of fit between the theoretical THERMØS calculation and the experimental points or to the uncertainties in the experimental points.

TABLE 2.4

Relative Absorption Rates Computed with THERMØS

Region	1.143% U^{235} 1.75-Inch Spacing		1.143% U^{235} 2.50-Inch Spacing		0.947% U^{235} 2.50-Inch Spacing	
	Volume	Total Absorption in Region	Volume	Total Absorption in Region	Volume	Total Absorption in Region
Fuel	0.3167	0.96215	0.3167	0.94924	2.8502	0.96639
Air gap	0.0311	0.00002	0.0311	0.00002	0.0611	0.00005
Cladding	0.1646	0.01548	0.1646	0.01527	0.4461	0.00603
Moderator	16.598	0.01651	34.407	0.03258	31.563	0.00518
f =	0.9678 ± 0.0010		0.9520 ± 0.0010		0.9885 ± 0.0010	

4. REFERENCES

(1) "Heavy Water Lattice Research Project Annual Report," NYO-9658, September 30, 1961.

(2) "Heavy Water Lattice Research Project Annual Report," NYO-10,208 (MITNE-26), September 30, 1962.

(3) "Heavy Water Lattice Research Project Annual Report," NYO-10,212 (MITNE-46), September 30, 1963.

(4) "Heavy Water Lattice Project Annual Report," MIT-2344-3 (MITNE-60), September 30, 1964.

(5) Simms, R., I. Kaplan, T. J. Thompson, and D. D. Lanning, "Analytical and Experimental Investigations of the Behavior of Thermal Neutrons in Lattice of Uranium Metal Rods in Heavy Water," NYO-10,211 (MITNE-33), October 1963.

(6) Palmedo, P. F., I. Kaplan, and T. J. Thompson, "Measurements of the Material Bucklings of Lattice of Natural Uranium Rods in D_2O," NYO-9660 (MITNE-13), January 1962.

(7) Brown, P. S., T. J. Thompson, I. Kaplan, and A. E. Profio, "Measurements of the Spatial and Energy Distributions of Thermal Neutrons in Uranium Heavy Water Lattices," NYO-10,205 (MITNE-17), August 1962.

3. FAST NEUTRON DISTRIBUTIONS

G. L. Woodruff

Fast neutron distributions have been measured with threshold detector foils in seven different lattices. The results for the first five lattices were reported in Ref. 1. These lattices included 1.25-inch, 1.75-inch, and 2.50-inch triangular spacings of 1.027% U^{235}, 0.25-inch-diameter fuel rods, and 1.25-inch and 2.50-inch spacings of 1.143% U^{235}, 0.25-inch-diameter fuel rods. Recent work has included a lattice of 1.75-inch spacing, 1.143% U^{235}, 0.25-inch-diameter fuel rods and a lattice of 2.50-inch spacing, 0.947% U^{235}, 0.75-inch-diameter fuel rods. All the above lattices have also been studied theoretically with two computer codes. The first code, UNCOL, is an uncollided flux approximation written especially for the recent work. The second code, HEETR (High Energy Events in Thermal Reactors) was written by H. K. Clark at the Savannah River Laboratory.

1. THE UNCOL CODE

1.1 Introduction

Methods making use of transport theory can be divided into three general types: kernel methods, integral transport theory methods, and general transport theory methods. The relative merits of each type are discussed elsewhere (2). The kernel methods are characterized by simplicity and directness. They have the disadvantages of being limited in their applicability and of requiring, in most cases, experimental data. Kernel methods are particularly suitable for treating fast neutrons in the present work because the cross sections involved are small and the number of interactions of interest are limited. For these reasons, a kernel method was selected for use in developing a theoretical representation of the fast flux. This effort resulted in the UNCOL code, which computes the spatial distribution and magnitude of the uncollided fast flux.

The computation consists of integrating a modified form of the single collision transport kernel for cylindrical shell sources. The integration is over the radius of all fuel rods in the assembly. The results are multiplied by the appropriate weighting coefficients (usually a J_o Bessel function distribution) and then summed to give the relative fast flux at points of interest.

The following assumptions are made:

(1) that the use of a kernel derived for cylinders of infinite length may be used for cylinders of finite length;

(2) that the homogeneous medium kernel may be used for two-region configurations by suitable adjustments in cross sections;

(3) that the spatial distribution of the fission reaction rate within a fuel rod may be expressed by the relation,

$$S(r') = C_o + C_1 r'^2 .$$

1.2 Applicability

The fast neutrons treated in the present work are not a well defined group. Some restrictions on the group can be specified, however, and qualitative energy boundaries can be defined.

Consider a source of fast neutrons with some energy spectrum, S(E). We are interested in the neutrons above some energy level, E_L. We assume that all neutrons with energies above this level are either source neutrons which have experienced no interaction or neutrons which have undergone interactions that did not significantly affect their direction of travel. It is clear that this assumption is valid provided E_L is sufficiently large. The cross sections of interest are then of the "removal" type used in multigroup calculations. Conversely, if E_L is too small, the approach will fail. If E_L is too small, a significant fraction of the neutrons will have experienced interactions (notably, inelastic scattering and large angle elastic scattering) which significantly changed their direction of travel. Since no provision for treating changes in direction is included in the model, the multiply scattered group cannot be accurately calculated.

In the case considered, the source group S(E) is the fission neutron spectrum. The assemblies studied are cylindrical and are composed primarily of uranium and heavy water. Although the magnitude of E_L is not required for calculations, a rough estimate is useful in order to gauge the applicability of the results. For this purpose, it is convenient to consider uranium and heavy water separately.

Murley (3) has considered in detail the energy spectrum of the neutrons which have had one or two collisions in uranium. The spectra of these neutrons and of fission neutrons are given in Fig. 3.1. Over 70% of the once-collided neutrons have energies below 1 Mev. In addition, some neutrons are captured in their first collision and some of the once-collided neutrons with energies greater than 1 Mev will have changed their direction of travel only slightly. It is therefore reasonable to conclude that a large fraction of the neutrons above 1 Mev (perhaps 90% or more) are adequately covered in the model described above.

The treatment of the heavy water is more difficult. While, in uranium, elastic scattering can be almost completely ignored and the effects of inelastic scattering are not complicated, in heavy water this is not the case. Except for some inelastic scattering by oxygen (which poses no problem), the reaction of primary interest is elastic scattering. The analysis is complicated by the fact that elastic scattering in heavy water is a function of both incident neutron energy, E, and energy transfer, ΔE. Furthermore, there is no fixed value of the scattering angle below which the model can be said to be valid and above which the model fails. Accordingly, it is not particularly profitable to attempt a detailed analysis for determination of E_L in heavy water. Instead, the model can be evaluated by comparison with experiments and some qualitative observations noted.

The first observation is that both the fission spectrum and the elastic scattering cross section of heavy water decrease rapidly with energy for energies greater than about 1 Mev. Both of these factors tend to limit the fraction of neutrons above 1 Mev which have been scattered through "large" angles. The second observation is that small angle scattering is favored by both high Z nuclides and low Z nuclides, the former because of the higher cross section for small angles and the

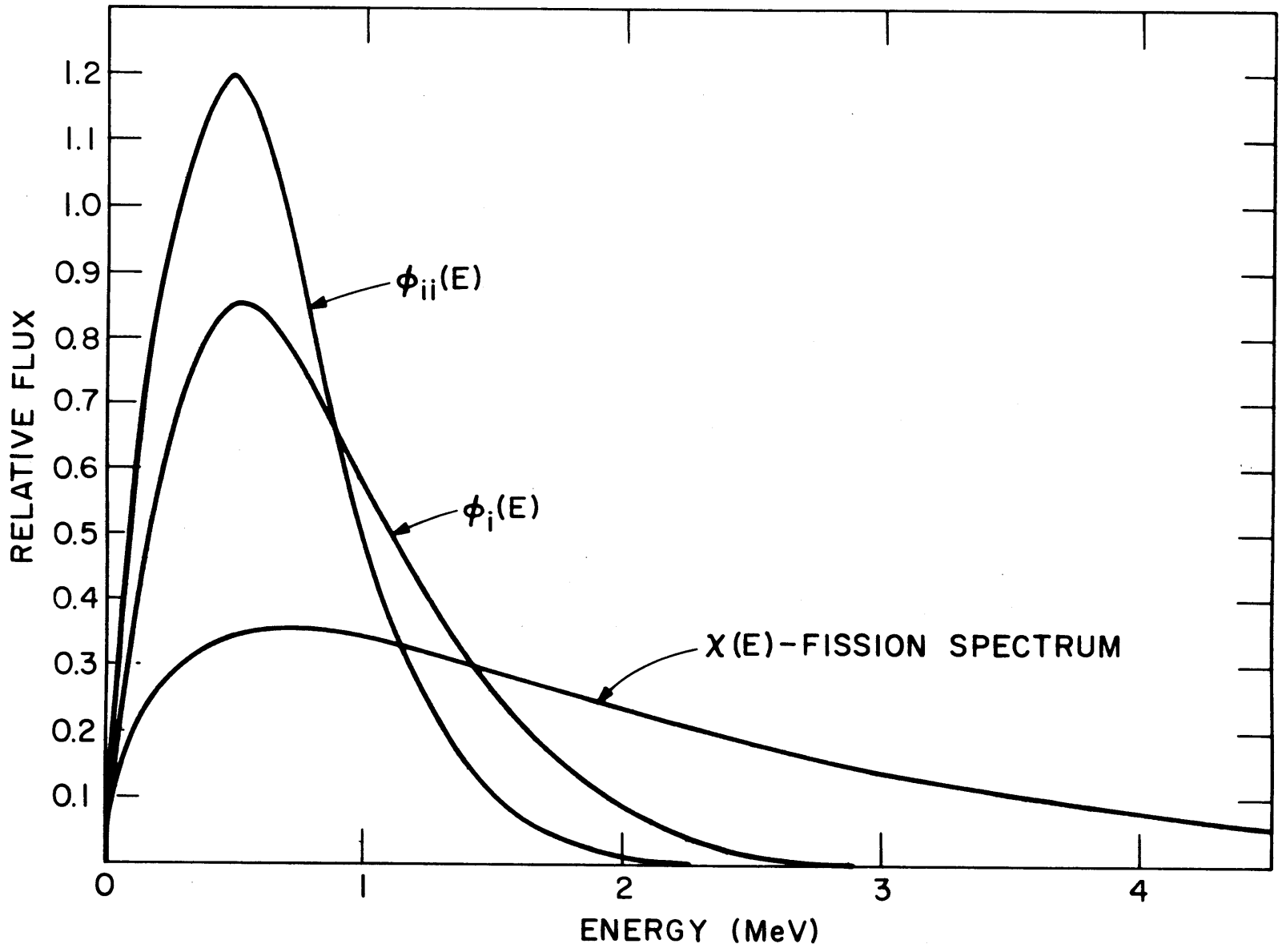

FIG. 3.1 ENERGY SPECTRA OF ONCE AND TWICE-COLLIDED NEUTRONS IN URANIUM

latter because of the translation from center-of-mass coordinates to laboratory coordinates.

In view of the above arguments, it appears on theoretical grounds that the lower energy bound for the group of neutrons treated by the present model is probably somewhere in the vicinity of 1 Mev.

1.3 Derivation

The single collision transport kernel expresses the first collision neutron density at a point r, resulting from a cylindrical shell source of infinite length and of radius r'. The kernel has been tabulated by Weinberg and Wigner (2); it has also been derived from the point kernel by Cady (4):

$$\overline{Tc}(r,r') = \frac{\Sigma}{2\pi} \int_1^\infty K_o(\Sigma r y)\, I_o(\Sigma r' y)\, dy\,, \quad r > r'\,, \tag{3.1}$$

$$\overline{Tc}(r,r') = \frac{\Sigma}{2\pi} \int_1^\infty K_o(\Sigma r' y)\, I_o(\Sigma r y)\, dy\,, \quad r < r'\,. \tag{3.2}$$

If we are interested not in the first collision density but rather in the fast neutron flux, we need only divide $\overline{Tc}(r,r')$ by Σ, the total cross section, to give the uncollided flux transport kernel, $Tc(r,r')$. This is a straightforward procedure for monoenergetic source neutrons in a homogeneous medium. The consideration of an energy-dependent source in a multiregion assembly requires a definition of what is meant by the uncollided flux and an appropriate calculation of the cross section used. In this case, the uncollided flux is the integrated flux above a minimum energy, E_L. Then, to be consistent, the cross section used must be an effective removal cross section.

If the source shape is not a cylindrical shell, but a cylindrical rod, the uncollided flux at point r is obtained by integrating $Tc(r,r')$ over the radius of the rod:

$$T_R(r) = \int_{R_1}^{R_2} dr'\, 2\pi r' Tc(r,r')\,. \tag{3.3}$$

Equation 3.3 is valid only if the source is constant over the radius of the rod. This restriction can be removed by the introduction of a source term, S(r'), suitably normalized, which gives the radial dependence of the source. Then,

$$T_R(r) = \int_{R_1}^{R_2} dr'\ 2\pi r' S(r')\ Tc(r,r') . \tag{3.4}$$

The form of the source term S(r') is arbitrary. The only requirement is that it should give a reasonable approximation to the source distributions of interest. It is mathematically convenient to express S(r') in the form of a polynomial in even powers of r' :

$$S(r') = C_o + C_1 r'^2 + C_2 r'^4 + \ldots + C_n r'^{2n} . \tag{3.5}$$

The radially symmetric fission distribution implied by Eq. 3.5 is a good representation of the real physical situation inside a fuel rod. In fact, as comparison with experimental data will show, truncation after the first two terms of Eq. 3.5 provides an excellent approximation for cases of interest.

Truncating Eq. 3.5 after two terms and substituting into 3.4 gives:

$$T_{R_a}(r) = \int_{R_1}^{R_2} dr'[C_o r' + C_1 r'^3] \int_1^\infty K_o(\Sigma r y)\ I_o(\Sigma r' y)\ dy , \quad r > r' , \tag{3.6}$$

$$T_{R_b}(r) = \int_{R_1}^{R_2} dr'[C_o r' + C_1 r'^3] \int_1^\infty K_o(\Sigma r' y)\ I_o(\Sigma r y)\ dy , \quad r < r' . \tag{3.7}$$

Reversing the order of integration in both cases gives:

$$T_{R_a}(r) = \int_1^\infty dy\ K_o(\Sigma r y) \int_{R_1}^{R_2} dr'[C_o r' + C_1 r'^3]\ I_o(\Sigma r' y) , \tag{3.8}$$

$$T_{R_b}(r) = \int_1^\infty dy\ I_o(\Sigma r y) \int_{R_1}^{R_2} dr'[C_o r' + C_1 r'^3]\ K_o(\Sigma r' y) . \tag{3.9}$$

The integrations over r′ can be performed analytically with the aid of the following relations*:

$$\int xI_o(x)\,dx = xI_1(x)\,, \tag{3.10}$$

$$\int xK_o(x)\,dx = -xK_1(x)\,, \tag{3.11}$$

$$\int x^3 I_o(x)\,dx = -4\int xI_o(x)\,dx + [x^3 I_1(x)+2x^2 I_o(x)]\,, \tag{3.12}$$

$$\int x^3 K_o(x)\,dx = 4\int xK_o(x)\,dx - [x^3 K_1(x)+2x^2 K_o(x)]\,. \tag{3.13}$$

Making the appropriate change of variables and using Eqs. 3.10 through 3.13 gives:

$$T_{R_a}(r) = \int_1^\infty dy\, K_o(\Sigma r y)\, P_{R_a}(R_1, R_2, \Sigma, y)\,, \tag{3.14}$$

$$T_{R_b}(r) = \int_1^\infty dy\, I_o(\Sigma r y)\, P_{R_b}(R_1, R_2, \Sigma, y)\,, \tag{3.15}$$

where,

$$P_{R_a}(R_1,R_2,\Sigma,y) = \frac{I_1(\Sigma R_2 y)}{\Sigma y}\left[C_o R_2 + C_1 R_2^3 - \frac{4C_1 R_2}{(\Sigma y)^2}\right] + \frac{2C_1 R_2^2}{(\Sigma y)^2} I_o(\Sigma R_2 y)$$
$$- \frac{I_1(\Sigma R_1 y)}{\Sigma y}\left[C_o R_1 + C_1 R_1^3 - \frac{4C_1 R_1}{(\Sigma y)^2}\right] - \frac{2C_1 R_1^2}{(\Sigma y)^2} I_o(\Sigma R_1 y)\,, \tag{3.16}$$

$$P_{R_b}(R_1,R_2,\Sigma,y) = \frac{K_1(\Sigma R_1 y)}{\Sigma y}\left[C_o R_1 + \frac{4C_1 R_1}{(\Sigma y)^2} + C_1 R_1^3\right] + \frac{2C_1 R_1^2}{(\Sigma y)^2} K_o(\Sigma R_1 y)$$
$$- \frac{K_1(\Sigma R_2 y)}{\Sigma y}\left[C_o R_2 + \frac{4C_1 R_2}{(\Sigma y)^2} + C_1 R_2^3\right] - \frac{2C_1 R_2^2}{(\Sigma y)^2} K_o(\Sigma R_2 y)\,. \tag{3.17}$$

---

*Equations 3.12 and 3.13 are special cases of a general reduction formula due to Watson (5).

The integrations in Eqs. 3.14 and 3.15 are performed numerically in UNCOL. The parabolic rule for integration is used, but the mesh spacing is left arbitrary to be included as input to the code. In the present case, 242 mesh points were used near and inside the fuel and 21 mesh points were used for other locations. Halving or doubling the number of mesh points was found to affect the results by less than 0.5%.

For points inside the fuel rod, the uncollided flux is the sum of integrals of three types. Equation 3.14 with $R_1 = 0$ and $R_2 = r$ gives the contribution from the cylindrical portion of the rod from the center out to the radius r. Equation 3.15 with $R_1 = r$ and $R_2 = R_o$ gives the contribution of the annular section of the fuel rod "outside" the point of interest. The third type of integral gives the contribution from fuel rods other than the one in which the point is located. For this, Eq. 3.14 is used repeatedly with $R_1 = 0$, $R_2 = R_o$ and with r equal to the distance to the center of each rod.

For points outside the fuel, Eq. 3.14 is used repeatedly for each rod with $R_1 = 0$, $R_2 = R_o$ and r the distance to the center of each rod calculated.

Up to this point, the procedure for the calculation of the cross section, Σ, has been left open. For a homogeneous medium, Σ should be the effective removal cross section consistent with the arguments of section 1.1. It is probably best determined by experiment, but it should be closely approximated by the removal cross section of the highest energy group in a set of multigroup constants. As stated in section 1.1, the group should be one with a lower boundary at approximately 1 Mev.

The extension to two regions requires further definition of Σ. The accuracy of the method is improved if the values of Σ for each of the two regions are not very different. Fortunately, fast neutron cross sections (especially if averaged over an energy interval) do not show the extreme variations that are often encountered in thermal cross sections. In UNCOL, Σ is treated as a function of distance from the center of the fuel rod for which the calculation is made. For points in the moderator, Σ is taken as the weighted average of the fuel removal cross section Σ_f and the moderator removal cross section Σ_m:

$$\Sigma(r) = \frac{\Sigma_f R_o + \Sigma_m (r - R_o)}{r} . \qquad (3.18)$$

For points inside the fuel rods, $\Sigma = \Sigma_f$.

2. THE HEETR CODE

The HEETR code is an integral transport code used to calculate high energy events in thermal reactors. It was written by H. K. Clark and is described in Refs. 6 and 7. A brief description follows.

HEETR is a multigroup, multiregion code for cylindrical geometry written in FORTRAN II. The basic assumptions used in the code are:

(1) scattering in the laboratory system is isotropic;

(2) the distribution of secondary neutrons is uniform within each region;

(3) the distribution of currents at interfaces is uniform over the interface;

(4) the number of neutrons passing through an interface per unit solid angle is proportional to the cosine of the angle that the direction of travel makes with the normal to the interface;

(5) the reactor is infinite.

The neutron current leaving a region is expressed in terms of the current entering the region by means of transmission probabilities, and in terms of sources within the region by means of escape probabilities. For regular lattice arrays, a unit cell boundary condition is used (net current at outer interface of outer region equals zero). For clusters of cylindrical fuel elements, Dancoff factors are used to approximate the interaction between elements.

The code requires, as input, values of microscopic group cross sections, cell dimensions and nuclide concentrations. The relative spatial distribution of thermal fissions is also required. For each neutron group, the code computes disadvantage factors in each region. The spatially averaged flux integrated over energy, and spatial averages of nuclear parameters are also calculated. In particular, the ratio of U^{238} fissions to U^{235} fissions, δ_{28}, is calculated for each fuel region as well as for the entire fuel rod.

The lower energy bound for which the code is applicable is not specified, but the code is probably useful down to the energies at which resonance self-shielding becomes significant.

Some minor modifications were made in the code for use at M.I.T., so that the program used is somewhat different from the one listed in Ref. 7. The modifications are primarily concerned with control sequencing and parameter dimensions.

3. THE RATIO CODE

The RATIO code was written to analyze the energy spectra calculated by the HEETR code in terms of various fast reactions. It calculates a matrix of the ratios of the fast reaction rates. It also calculates for each reaction and spectrum the relative contribution by each energy group to the total activation. The boundaries of the energy groups are variable. The code was written for a five-group structure, but the extension to a greater number of groups is straightforward.

In RATIO, the multigroup energy spectrum is converted into an "N-mesh" differential energy spectrum as follows. In all except the highest energy group, the spectrum is treated as a histogram consistent with the relative values of the different groups; i.e., the flux is assumed constant over the energy range of each individual group. The highest energy group is treated as a portion of the fission neutron energy spectrum. The highest energy group is normalized so that its integral is consistent with the relative fluxes in the groups computed by HEETR. This procedure involves the assumption, of course, that the lower bound of the highest energy group is sufficiently high so that the spectrum above this point does, in fact, correspond to part of a fission spectrum. Some sort of special treatment along these lines is needed for the first group since this group has no upper energy bound. The choice of the fission spectrum shape is not only logical on physical grounds but is required for consistent calculations.

With the above procedure, a fine-mesh flux is computed in increments of 0.25 Mev. The saturated specific activation for each reaction, i, is then:

$$A_i = \int_0^\infty \phi(E)\, \sigma_i(E)\, dE \ . \tag{3.19}$$

The integration of Eq. 3.19 is performed by using the trapezoidal rule. The cross-section data used are identical with those compiled by Rydin (8) except for the $Rh^{103}(n,n')Rh^{103m}$ data which were compiled from the theoretical curve by Vogt and Cross (9).

4. RESULTS

The intracell spatial distributions for the $In^{115}(n,n')In^{115m}$, $U^{238}(n,f)$, $Ni^{58}(n,p)Co^{58}$, and $Zn^{64}(n,p)Cu^{64}$ reactions are given in Figs. 3.2 through 3.5 for the 0.25-inch-diameter, 1.027% enriched lattices. The distributions for the 0.25-inch-diameter, 1.143% enriched lattices are given in Figs. 3.6 through 3.9. For both enrichments, the 0.25-inch-diameter rods were studied at spacings of 1.25, 1.75, and 2.50 inches. Results for the one lattice of 0.75-inch-diameter, 0.947% enriched rods are given in Figs. 3.10 through 3.13. The spacing in this case was 2.50 inches.

The experimental data are normalized at the cell edge in all cases. While normalization in the fuel might be preferred on physical grounds, the greater accuracy of the moderator foils (due primarily to their larger size) provides a normalization that is more representative of the distribution. It is important to keep this in mind when interpreting the results. For example, in Fig. 3.2, it might be concluded that for a given thermal flux level, the magnitude of the fast flux inside the fuel rods of the 2.50-inch-spaced lattice is greater than the fast flux inside the fuel for the 1.25-inch-spacing case. In fact, the contrary is true. Since the interaction effect between rods increases as the rod spacing decreases, the magnitude of the fast flux also increases.* The magnitude of the fast flux in the fuel for the 1.25-inch-spacing case is therefore greater than for the 2.50-inch-spacing case.

---

*In practice, the actual magnitude of the thermal flux and, consequently, the fast flux is also a function of the multiplication constant of the lattice, the reactor power, the height of the reactor regulating rod, and the fuel loading of the reactor, as well as height and radial location in the lattice tank and fuel rod size.

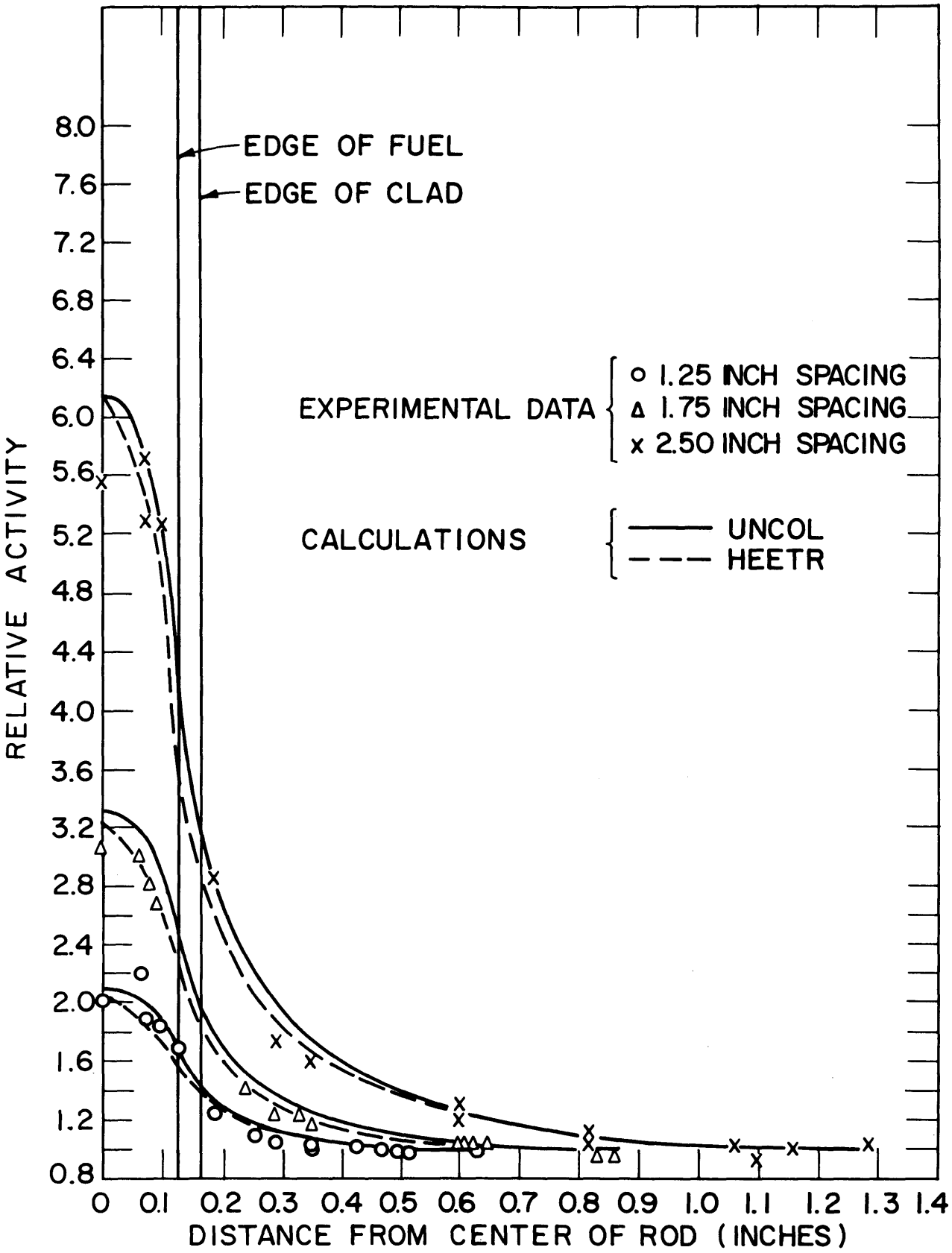

FIG. 3.2 $In^{115}(n,n^{1})\ In^{115m}$ ACTIVITY DISTRIBUTION FOR 0.25 INCH DIAMETER - 1.027% ENRICHED LATTICES

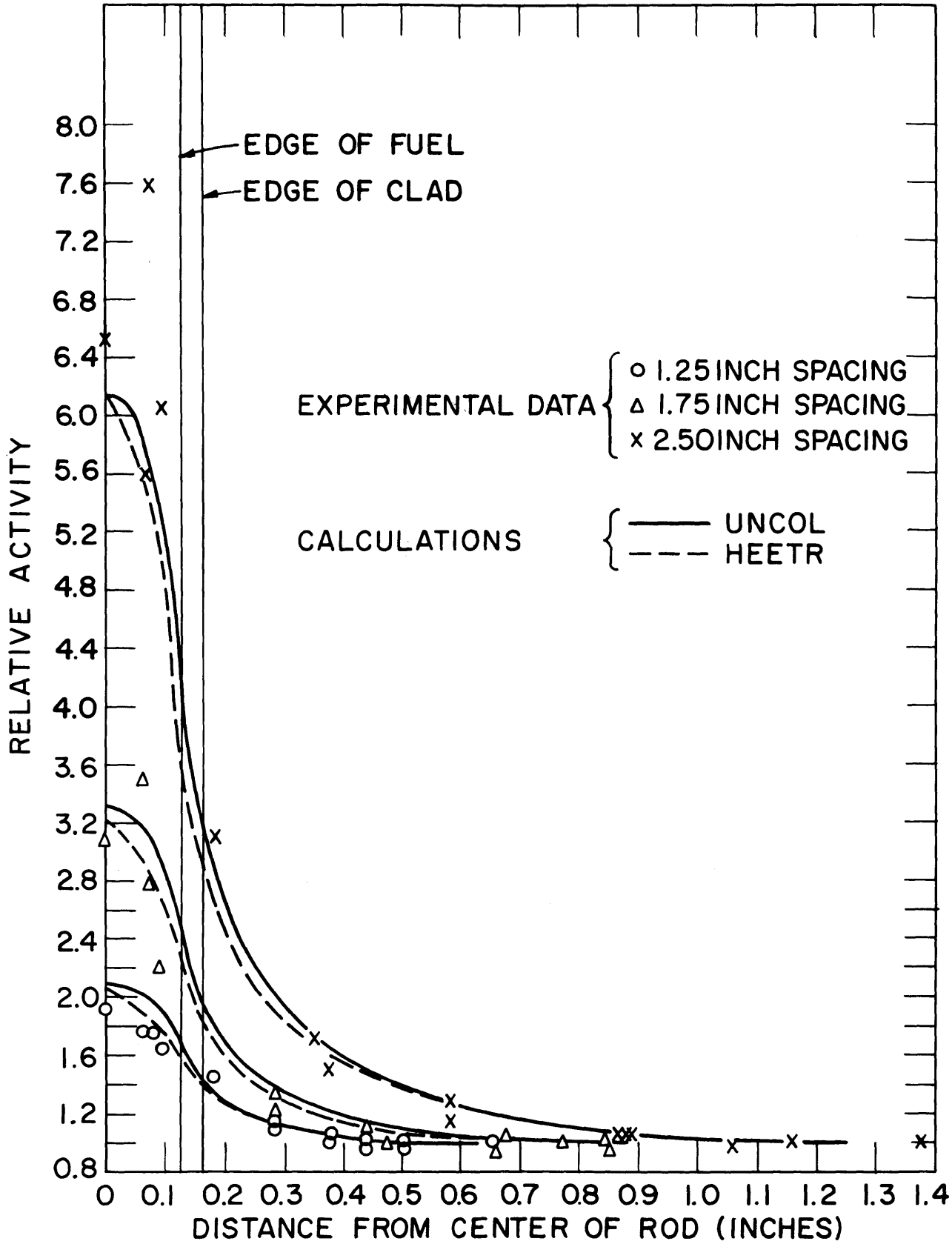

FIG. 3.3 $U^{238}(n,f)$ ACTIVITY DISTRIBUTION FOR 0.25 INCH DIAMETER - 1.027% ENRICHED LATTICES

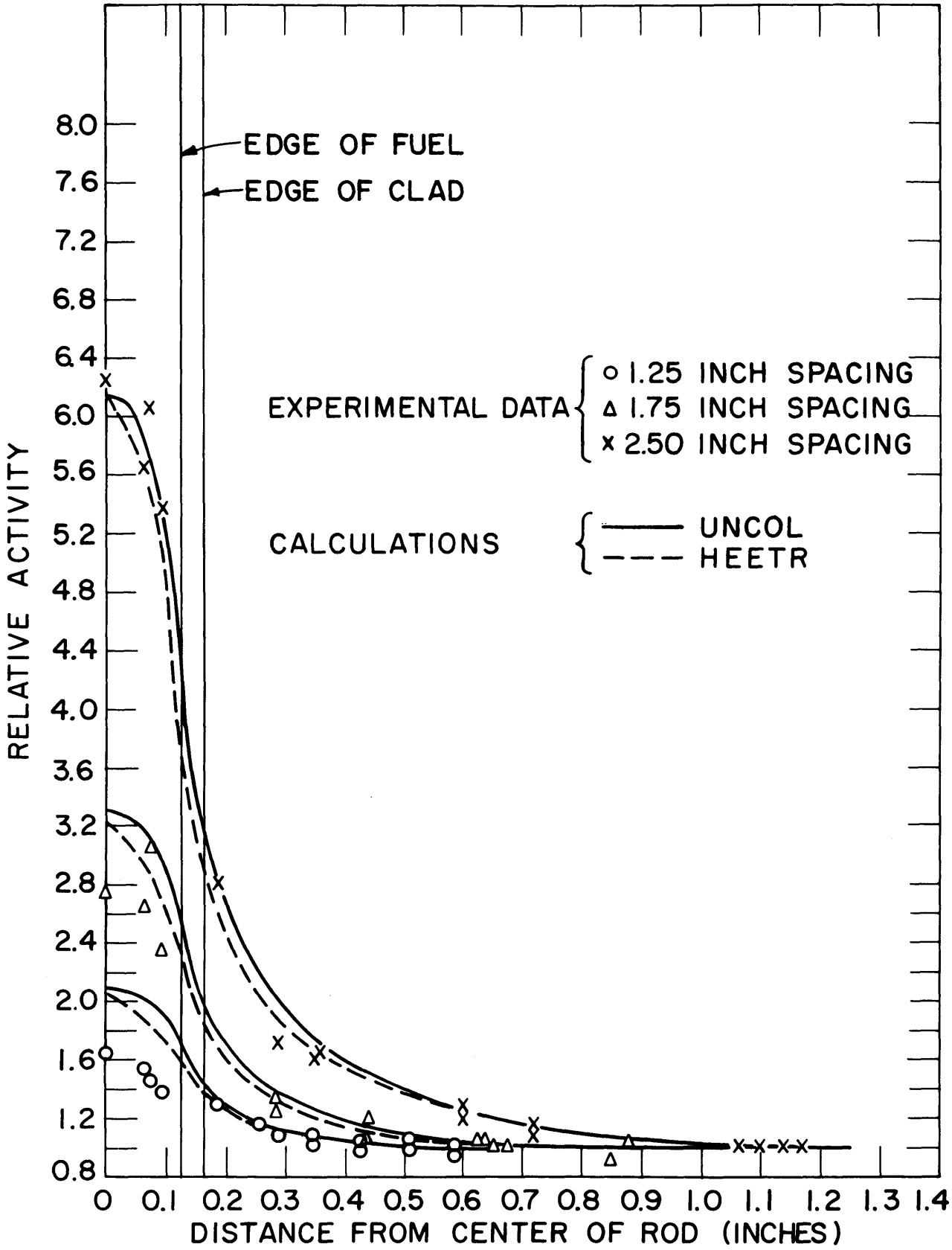

FIG. 3.4 $Ni^{58}(n,p)$ ACTIVITY DISTRIBUTION FOR 0.25 INCH DIAMETER -1.027% ENRICHED LATTICES

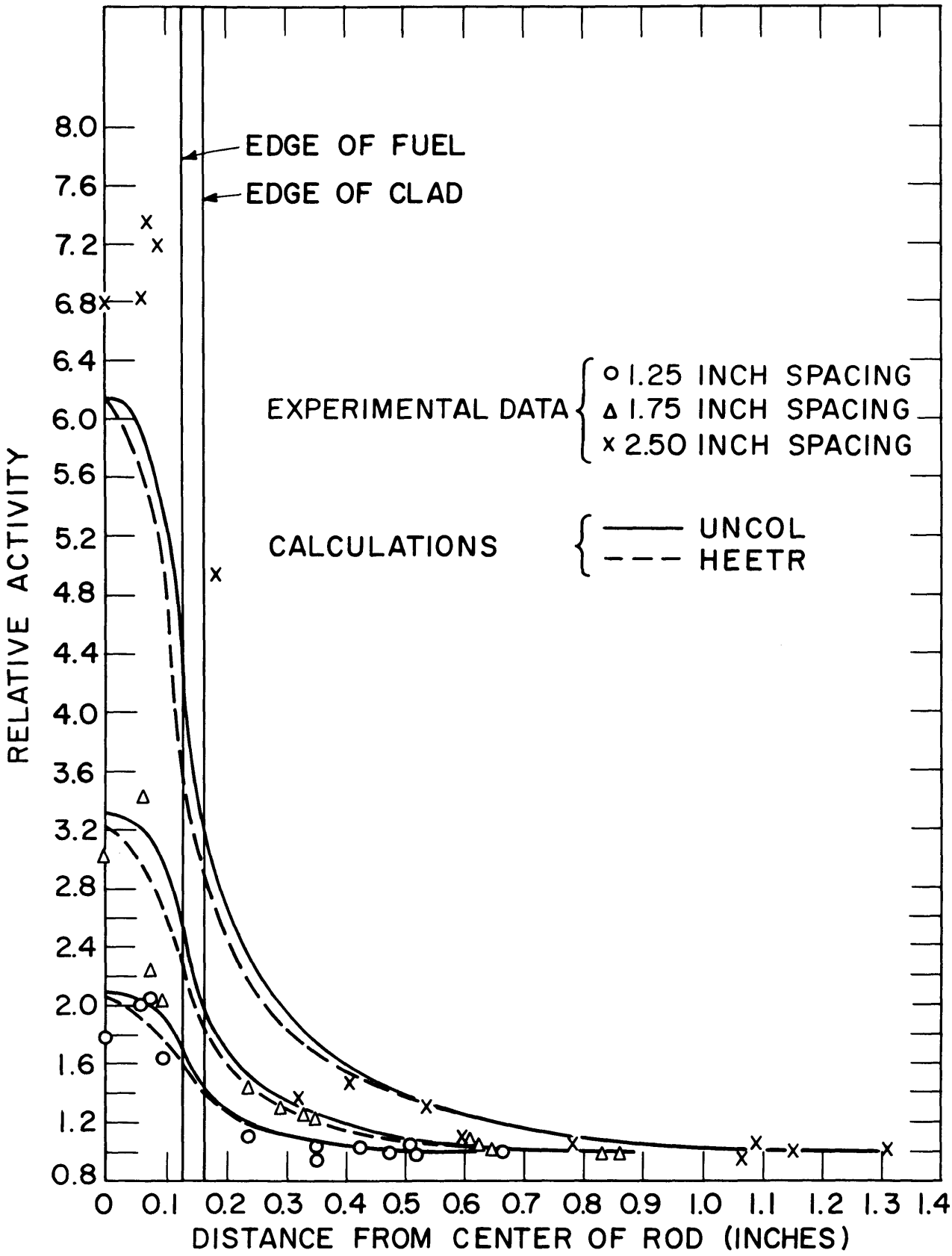

FIG. 3.5 $Zn^{64}(n,p)Cu^{64}$ ACTIVITY DISTRIBUTION FOR 0.25 INCH DIAMETER - 1.027 % ENRICHED LATTICES

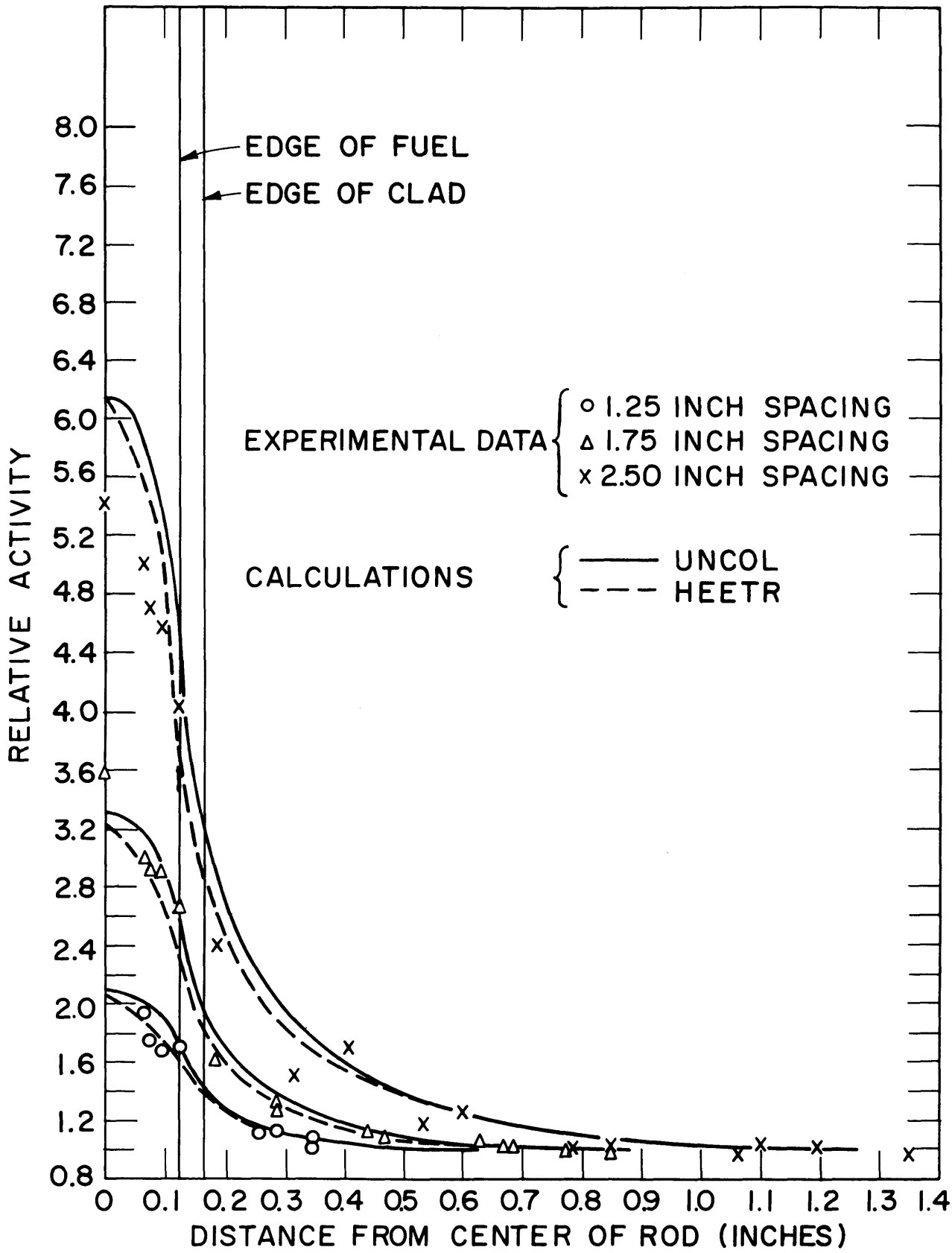

FIG. 3.6 $In^{115}(n,n^{1})\ In^{115m}$ ACTIVITY DISTRIBUTION FOR 0.25 INCH DIAMETER - 1.143% ENRICHED LATTICES

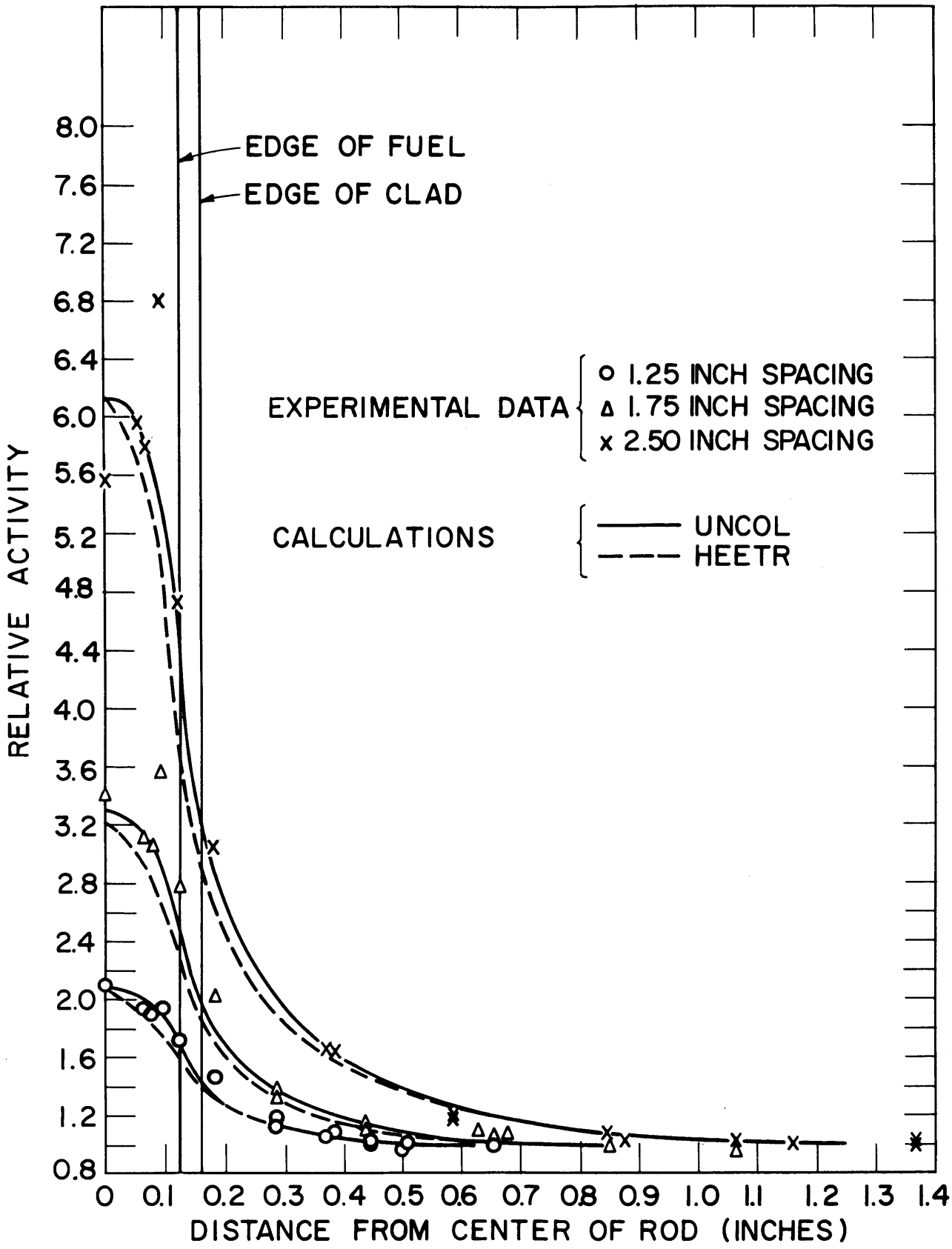

FIG. 3.7 $U^{238}(n,f)$ ACTIVITY DISTRIBUTION FOR 0.25 INCH DIAMETER - 1.143% ENRICHED LATTICES

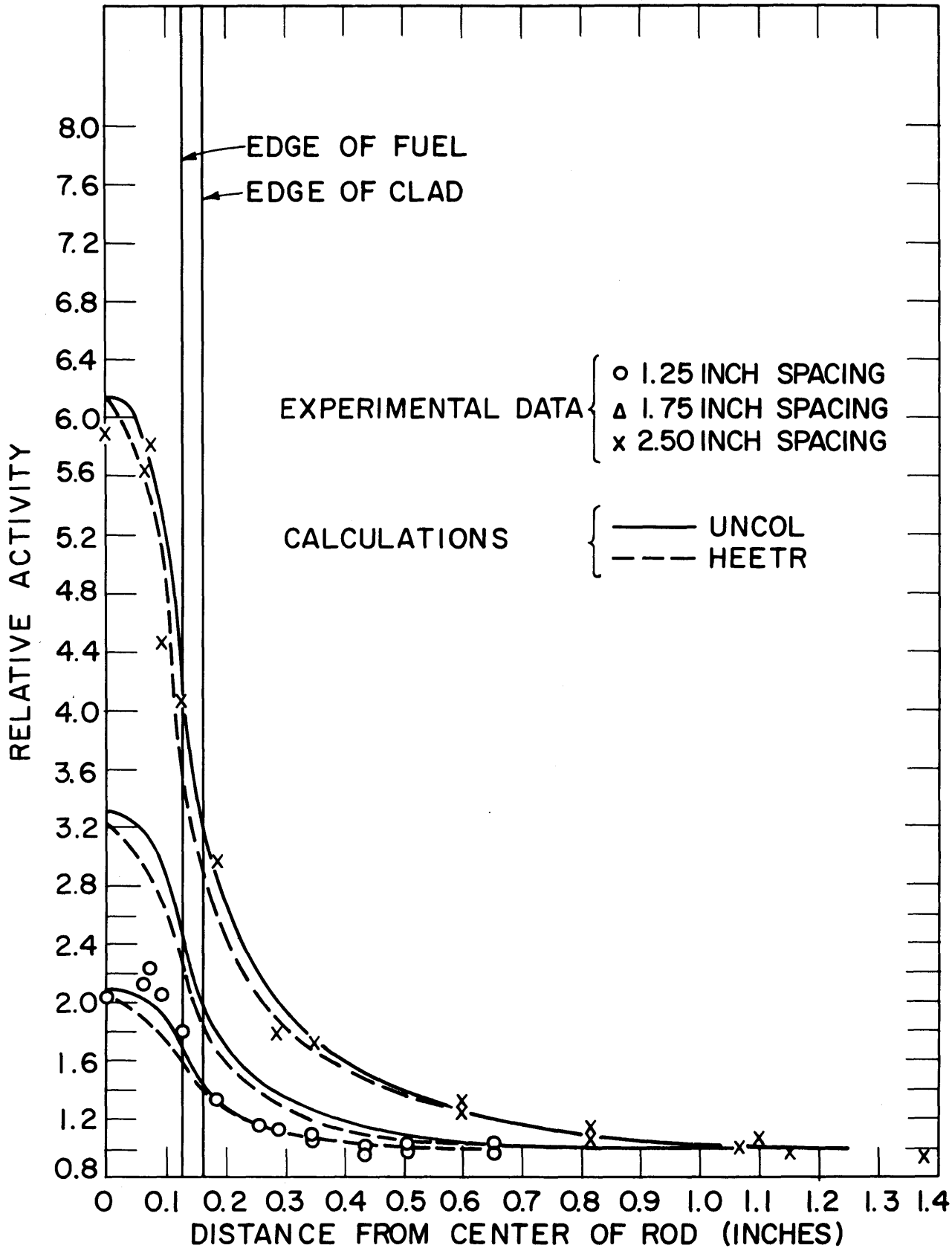

FIG. 3.8 $Ni^{58}(n,p)Co^{58}$ ACTIVITY DISTRIBUTION FOR 0.25 INCH DIAMETER - 1.143% ENRICHED LATTICES

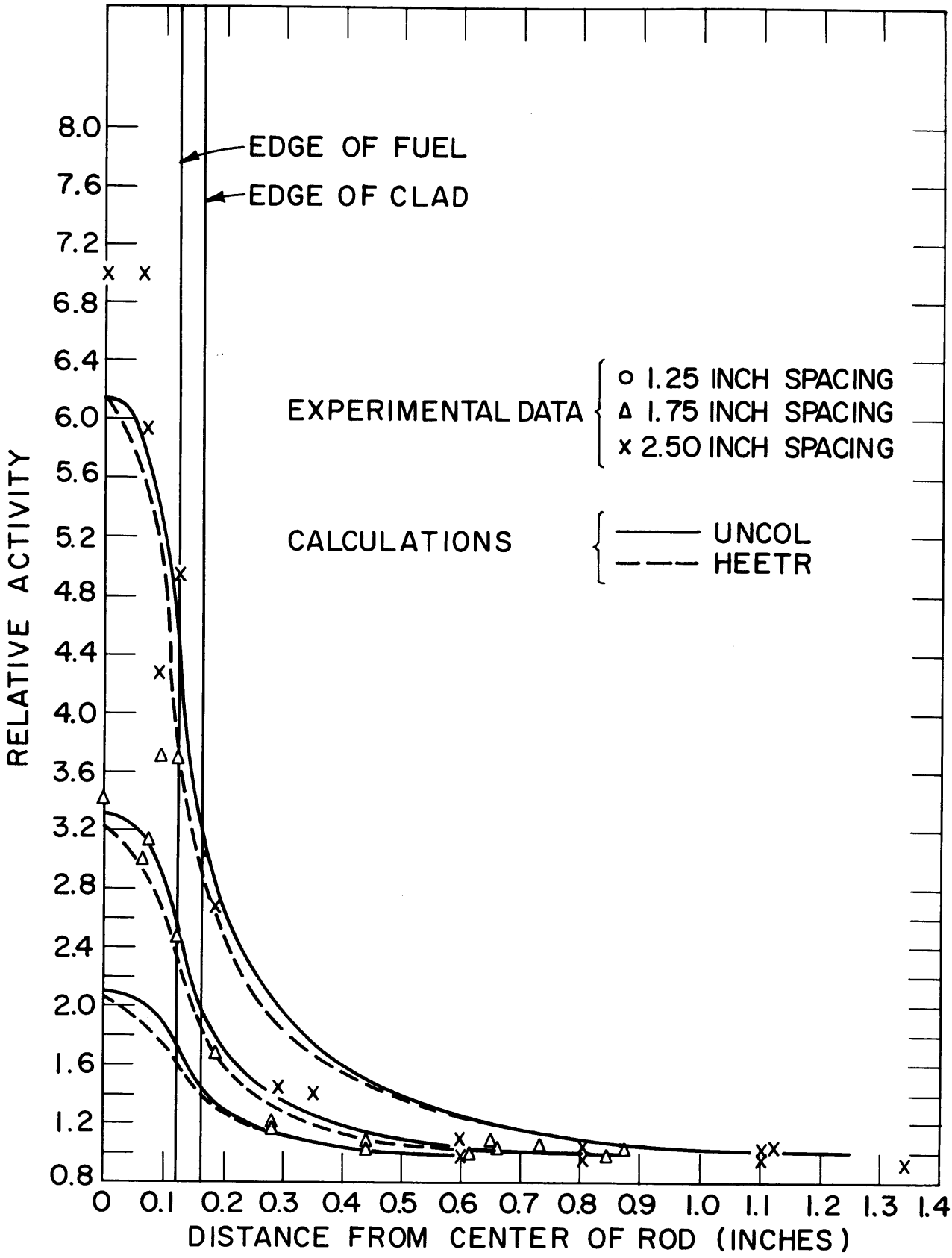

FIG. 3.9 $Zn^{64}(n,p)Cu^{64}$ ACTIVITY DISTRIBUTION FOR 0.25 INCH DIAMETER - 1.143% ENRICHED LATTICES

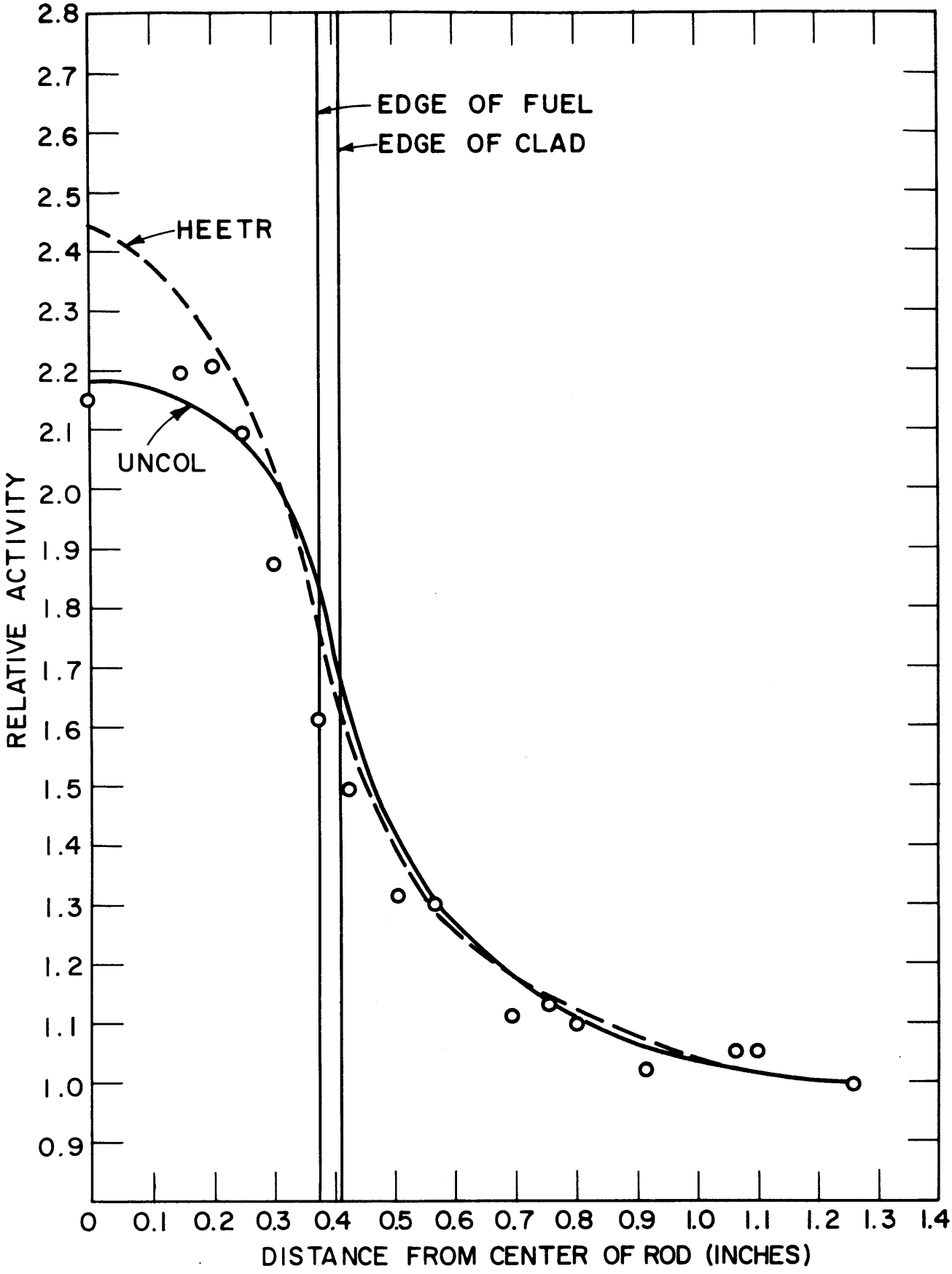

FIG. 3.10 $In^{115}(n,n')In^{115m}$ ACTIVITY DISTRIBUTION FOR 0.75 INCH DIAMETER - 2.5 INCH SPACING 0.947% ENRICHED LATTICE

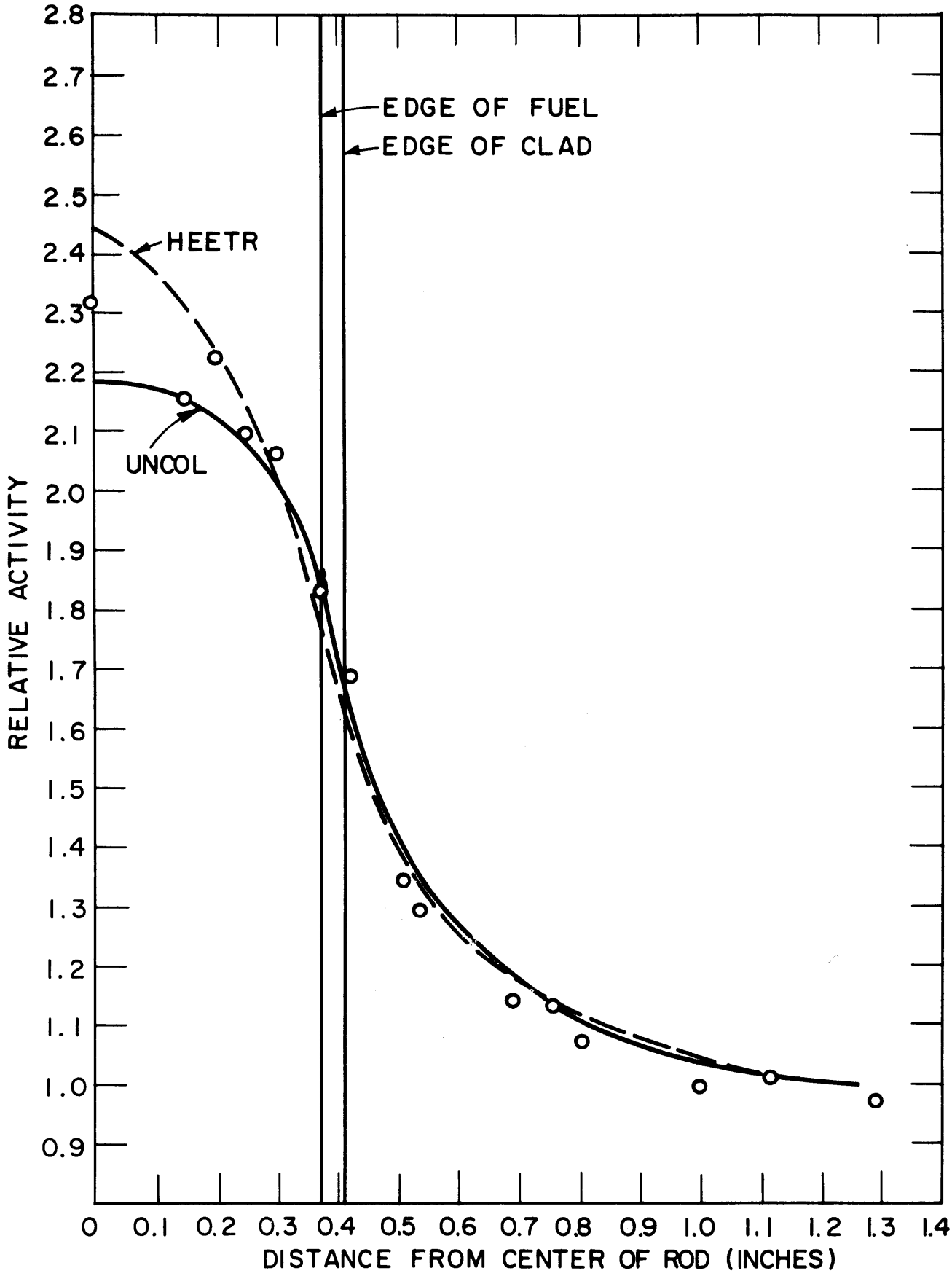

FIG. 3.11 $U^{238}(n,f)$ ACTIVITY DISTRIBUTION FOR
0.75 INCH DIAMETER - 2.5 INCH SPACING
0.947% ENRICHED LATTICE

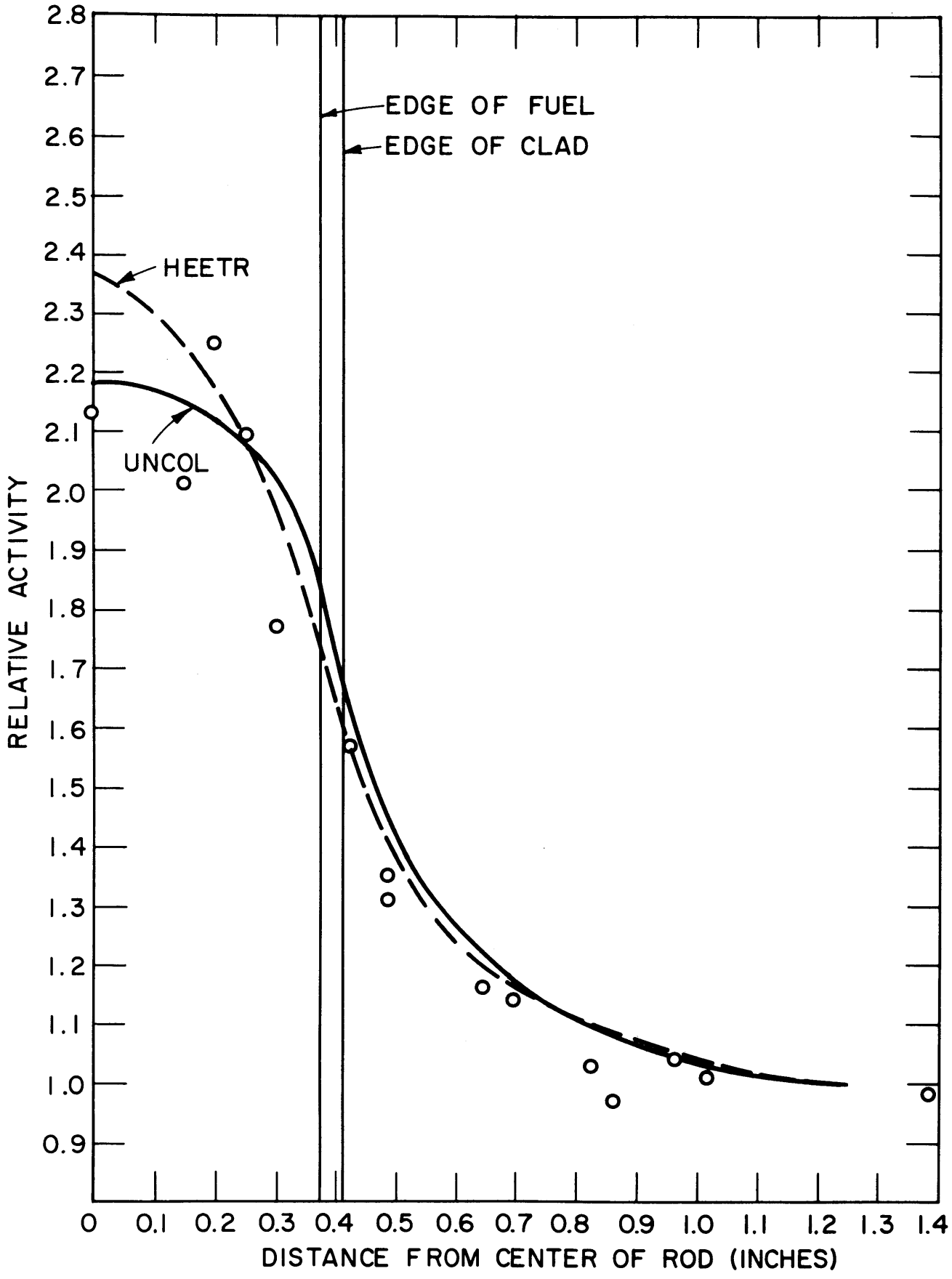

FIG. 3.12 Ni^{58} (n,p) Co^{58} ACTIVITY DISTRIBUTION FOR 0.75 INCH DIAMETER - 2.5 INCH SPACING 0.947% ENRICHED LATTICE

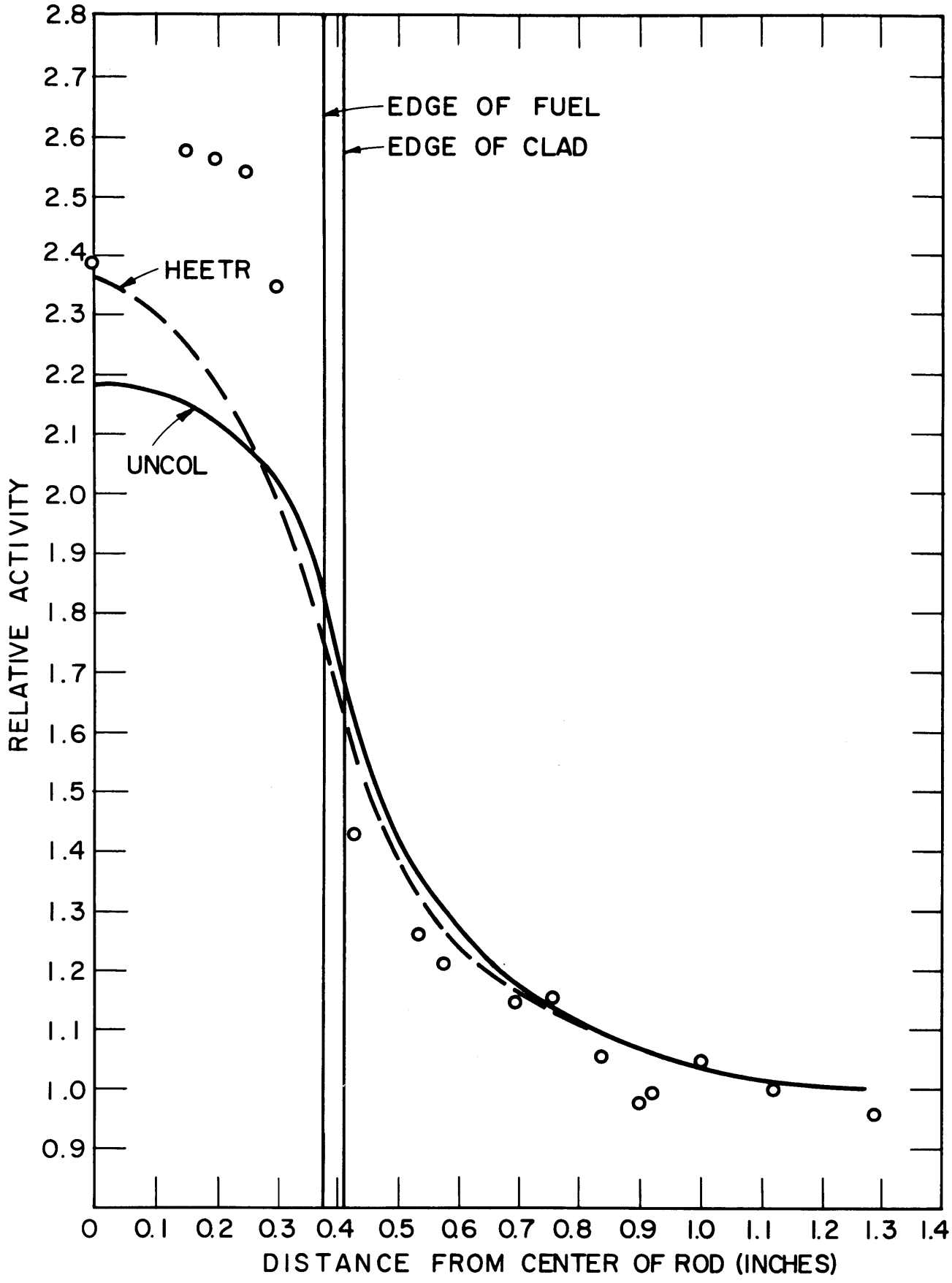

FIG. 3.13 $Zn^{64}(n,p)\ Cu^{64}$ ACTIVITY DISTRIBUTION FOR 0.75 INCH DIAMETER - 2.5 INCH SPACING 0.947% ENRICHED LATTICE

Plotted along with the experimental data in each case are the results of UNCOL and HEETR calculations. The results are also normalized at the cell edge in order to be consistent with the experimental data.

The UNCOL results plotted in Figs. 3.2 through 3.13 are those for a consistent set of removal cross sections as discussed in section 1.2. For all these cases, the macroscopic fuel removal cross section was 0.1 cm^{-1}, and the macroscopic moderator removal cross section was 0.093 cm^{-1}. Calculations were made with UNCOL for a large variety of combinations of cross sections. Both the fuel and the moderator removal cross sections were independently varied from 0.05 cm^{-1} to 0.2 cm^{-1}. The above combination (Σ_f = 0.1 cm^{-1}, Σ_m = 0.093 cm^{-1}) proved to be the optimum for correlating data from widely varying experimental conditions. Furthermore, this set of values also provides a satisfactory comparison with data from the M.I.T. Reactor core and experimental facilities. The reactor and the experimental facilities provide comparisons which contrast sharply with the lattices studied, both with respect to dimensions involved and moderator-to-fuel ratio. It is also of interest to note that the above removal cross-section values approximate rather closely some published group removal cross sections. For example, A.N.L. few-group calculations give,for a single group lying above 1.35 Mev, a removal cross section of 0.0899 cm^{-1} for D_2O and 0.1039 for U^{238} (10, 7).

The only other input data for the UNCOL calculations that require explanation are the polynomial coefficients for the fission spatial distribution. As discussed in section 1.2, it has been assumed that the fission distributions within a fuel rod can be expressed by a polynomial of the form:

$$S(r') = C_o + C_1 r'^2 . \qquad (3.20)$$

It is convenient to normalize in such a way that C_o is equal to unity; then only C_1 need be determined. For a first approximation, S(r') could be expressed by the thermal flux distribution within a fuel rod as determined either experimentally or by calculation with THERMØS (11), for example. For the more closely packed lattices, however, there is significant fast and resonance fission. The resonance fission can be assumed

to be a constant, independent of position within the fuel rod. The fast fission distribution is the same as that being calculated. Thus, we have:

$$S(r') = 1.0 + C_1 r'^2 \simeq \phi_{TH}(r') + \delta_{25} + \delta_{28}\phi_F(r') . \qquad (3.21)$$

This formulation assumes δ_{28} to be constant within the fuel rod. This is a poor assumption, but its use leads to negligible error. Since Eq. 3.21 involves $\phi_F(r')$, the distribution being calculated, the procedure is an iterative one. An estimate is made of $\phi_F(r')$, C_1 is then calculated (by least-squares methods, for example), then $\phi_F(r')$ is calculated. If the assumed distribution differs from the one calculated, it is corrected and the process repeated. Since δ_{28} is always much less than unity, the process rapidly converges and at most only a few iterations are involved. The procedure described here was used in the present work because it gives a more accurate fission distribution when the experimental values of δ_{25} and δ_{28} are available. In cases of interest, the omission of fast and resonance fission does not lead to large errors in the calculation of the fast flux distribution. Hence, if δ_{25} and δ_{28} are not known, they can be estimated or taken as zero without introducing large errors. On the other hand, assuming the fission rate to be constant inside the fuel rod (setting C_1 to zero) will, in general, significantly affect the results. It is fairly important, therefore, to obtain some estimate of the thermal flux distribution inside the fuel rod. In the present work, THERMØS was used to calculate the thermal flux distribution and experimentally measured values of δ_{28} and δ_{25} were used.

The HEETR results are actually the calculated activity distributions for each reaction considered. This is in contrast to the UNCOL calculations which are fast flux distributions consistent with the assumptions of section 1.1. The HEETR results were obtained in the following manner. A HEETR calculation was made for the lattice being studied. This calculation provided the neutron energy spectrum for the lattice cell and the spatial distribution within the lattice cell for each of the five energy groups described in Table 3.1. In Table 3.1, the fission spectrum component for each group is also given. The fission spectrum is normalized so that the integral is unity. With the HEETR energy spectrum as input, the RATIO code computed for each reaction the percentage of the

TABLE 3.1

Energy Group Structure for HEETR Calculations

Group	E_L (Mev)	Normalized* Fission Spectrum, N(E)
1	3.679	0.14659
2	2.231	0.20703
3	1.353	0.22383
4	0.8208	0.17596
5	0.4979	0.11346

*The sum of groups 1 through 5 plus neutrons below 0.4979 Mev totals 1.0.

total activation due to each of the five energy groups. These results were then used with the spatial distribution of the five energy groups to compute the activity distributions. The spatial distributions of the first four energy groups are similar. Since these four groups contribute substantially all the activation for the reactions studied, there is very little variation in the different activity distributions. This is particularly true for the 0.25-inch-rod-diameter lattices.

The HEETR results are for calculations with the cell boundary approximation and the transport cross section option. The results of calculations involving total cross sections rather than the transport approximation showed no significant differences. The microscopic cross section input data were from a 15 energy group set supplied by H. K. Clark from data in Refs. 12, 13, and 14. The calculations reported here used the first five groups (i.e., the high energy range) of the fifteen-group structure for which the data were compiled. It was necessary, therefore, to change only the transfer cross sections. The transfer cross sections affected were those of the type $(i \rightarrow j)$, where i includes groups 1 through 5 and j includes all values greater than 5. The 5 group $(i \rightarrow 6)$ transfer cross section values are the sum of all the 15 group $(i \rightarrow j)$ values for j greater than 5.

In comparing the experimental and calculated results, there are two conspicuous examples of poor agreement. These two examples are the zinc results for lattices of 2.5-inch spacing and the nickel results

for the lattice of 1.027% enriched, 0.25-inch-diameter rods and 1.25-inch spacing. The zinc results show a higher peaking in the fuel for the lattices of 2.5-inch spacing than predicted by calculations. This could be due in part to the perturbation effects resulting from flux depression associated with the cadmium-covered moderator foils. However, this effect is too small to account for the difference and, in any event, should affect the results of all the reactions equally. More to the point, there are two experimental factors that are unique with the zinc reaction as compared with the others utilized. The first is the necessity for correcting for the Zn^{69} activity produced by the $Zn^{68}(n,\gamma)Zn^{69}$ reaction. The second factor is the low statistical accuracy attainable with the zinc reaction. The cross section for the $Zn^{64}(n,p)Cu^{64}$ reaction has a relatively high energy threshold and never reaches a high value for any energy. Both the Zn^{69} correction and the statistical inaccuracy are greatest in the 2.5-inch-spaced lattices. The ratio of Zn^{69} activity to Cu^{64} activity is higher because the ratio of thermal flux to fast flux is higher. The combination of the small cross section and the reduced fast flux level results in experimental uncertainty which is relatively large in comparison with that for the other reactions and closer lattice spacings studied. Further work is required before the zinc results for the lattices of 2.5-inch-spaced rods can be fully explained.

The discrepancy between theory and experiment for the $Ni^{58}(n,p)Co^{58}$ data for the 0.25-1.25-1.027% lattice is considered anomalous. Judging from the computed curves and the other distributions, it appears that the experimental points in the fuel are all too low by a factor of approximately 1.3. This is too large a factor to be caused by a mistake in the correction for radial location in the lattice tank. These corrections are usually less than 5%. Furthermore, since the rod supporting the moderator foils was always farther from the center of the lattice than the rod containing the fuel foils, the radial correction factor tends to reduce slightly the relative peaking in the fuel. In this case, the rod containing the fuel foils would have had to have been located in the seventh ring rather than in the center position in order to account for the difference. A much more likely explanation is that the moderator foil holder slipped at some point before or during the run. If the moderator foils

were actually located about 6 inches lower than assumed, an error of this magnitude would result. The possibility of such an event was recognized after the first two lattices were studied. On subsequent runs, the position of the moderator holder was measured both before and after the lattice run. The data in question, however, resulted from the second lattice studied, and the height of the moderator holder was measured only before the run.

In addition to the zinc results discussed above, there is some indication that the results for the other reactions show a greater peaking than the calculations predict. As with the zinc data, this tendency is more pronounced for the lattices with larger spacings. This result can be explained in terms of the perturbation effects of the cadmium-covered foils. The thermal flux in the fuel rod supporting the moderator foils was locally depressed by approximately 10%. This, in turn, caused the effective source strength for the fast flux originating in this rod and irradiating the moderator foils to be reduced by some smaller value, perhaps 5%.* The precise magnitude of the net reduction in moderator foil activity would be difficult to compute but should be even smaller because not all the activation of the moderator foils is due to the nearest rod. The fuel foils are located in a separate rod and should not be significantly influenced by this perturbation. This means, therefore, that the moderator foil activation is decreased and the fuel foil activation is not. On a relative plot, this has the effect of erroneously increasing the peaking within the rod.

If the magnitude of the local thermal flux depression due to the cadmium covers is roughly the same for the various spacings, the error so introduced must be larger for the wider spacings. Although the reduction in activation from the nearest rod is about the same for the various spacings, the interaction effect is smallest for the wider spacings. Thus,

---

*In contrast to the thermal case, the effects of a purely local flux depression are dampened somewhat, due to the long mean-free path for fast neutrons. Thus, a local depression of 10%, when combined with unperturbed contributions from elsewhere in the same rod, will produce a net effect of less than 10%.

the nearest rod contributes a greater percentage of the activation for the wider spacings. The reduction in activation, therefore, has greater effect in those cases.

The accuracy attained in the 0.75-inch-rod-diameter lattice is generally higher than that for the 0.25-inch-rod-diameter lattices. This is to be expected for two reasons. All other factors being equal, the magnitude of the fast flux increases with increasing rod size. The increase in the fraction of the fuel area per unit cell by a factor of 9 significantly increased the fast flux. Furthermore, the larger rods permitted the use of 0.125-inch-diameter foils inside the fuel, whereas only 0.0625-inch-diameter foils could be used inside the 0.25-inch-diameter rods: the total activity per foil was thereby increased by a factor of 4.

Wolberg (15) measured the microscopic distribution of the $U^{238}(n,f)$ reaction in and about a single 1.01-inch-diameter, natural uranium rod in D_2O. The results, along with the UNCOL calculation for this case, are plotted in Fig. 3.14. In this case, the points inside the fuel rods are more accurate and the normalization is therefore made at the center of the rod.

Except as discussed above, there appear to be no significant differences between the experimental data, the UNCOL calculation and the HEETR calculations. The HEETR results give distributions with a steeper slope inside the fuel than the UNCOL results. The HEETR results show some slight variations among the different reactions, at least in the 0.75-inch-rod-diameter lattice. The UNCOL calculations, on the other hand, represent flux distributions and do not discriminate among the different reactions. These differences between UNCOL and HEETR are not large, however, and the two methods can be said to match the data with comparable accuracy.

At the present time, the experimental part of this investigation has been completed, the theoretical analysis is nearly finished and drafting of a final report is well under way. It is expected that a topical report will be issued early in the coming annual report period.

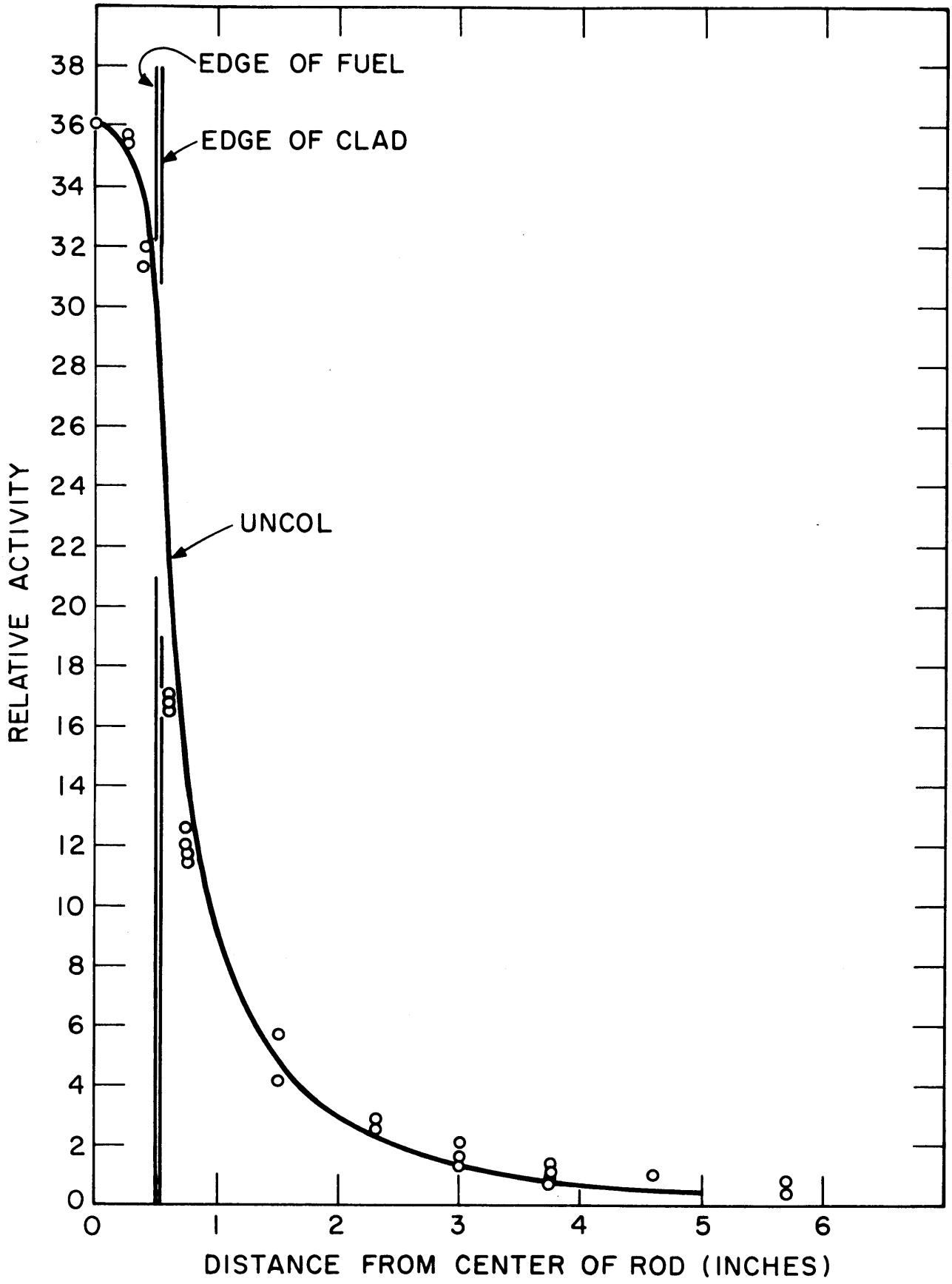

FIG. 3.14 U^{238} (n,f) ACTIVITY DISTRIBUTION FOR 1.0 INCH DIAMETER SINGLE ROD (W4) OF NATURAL URANIUM

5. REFERENCES

(1) "Heavy Water Lattice Research Project Annual Report," MIT-2344-3 (MITNE-60), September 30, 1964.

(2) Weinberg, A. M., and E. P. Wigner, The Physical Theory of Neutron Chain Reactors, Univ. of Chicago Press, 1958.

(3) Murley, T. M., "Calculation of δ_{28} for Isolated Rods," M.I.T. unpublished memo, March 1965.

(4) Cady, K. B., "Neutron Transport in Cylindrical Rods," Ph.D. Thesis, M.I.T. Nuclear Engineering Department, September 1962.

(5) Watson, G. N., The Theory of Bessel Functions, (Second Edition), Cambridge Univ. Press, London, 1958.

(6) Clark, H. K., "Calculation of High Energy Events in Thermal Reactors," DP-609, September 1961.

(7) Clark, H. K., "Calculation of High Energy Events in Thermal Reactors, II. A Computer Code - HEETR," DP-928, November 1964.

(8) Rydin, R. A., N. C. Rasmussen, and G. L. Brownell, "Fast Neutron Spectroscopy and Dosimetry of the M.I.T. Reactor Medical Therapy Facility Beam," AFCRL-64-404 (MITNE-47), May 1964.

(9) Vogt, E. W., and W. G. Cross, published in "Measurement of Fission Neutron Fluxes and Spectra with Threshold Detectors," by J. C. Roy, R. W. Durham, A. G. Fowler, and J. J. Hawton, AECL-1994, May 1964.

(10) Reactor Physics Constants, ANL-5800 (Second Edition), July 1963.

(11) Honeck, H. C., "THERMØS, A Thermalization Transport Theory Code for Reactor Lattice Calculations," BNL-5826, September 1961.

(12) Yiftah, S., D. Okrent, and P. A. Moldauer, Fast Reactor Cross Sections, Pergamon Press, New York, 1960.

(13) O'Shea, D. M., H. H. Hummel, W. B. Loewenstein, and D. Okrent, "Twenty-Six-Group Cross Sections," Trans. Am. Nucl. Soc., 7 (2), 242-243, November 1964.

(14) Okrent, D., private communication to H. K. Clark, 1965.

(15) Wolberg, J. R., T. J. Thompson, and I. Kaplan, "A Study of the Fast Fission Effect in Lattices of Uranium Rods in Heavy Water," NYO-9661 (MITNE-15), February 1962.

4. MEASUREMENT OF INTEGRAL PARAMETERS IN FUEL RODS

L. T. Papay
C. G. Robertson
S. P. Hellman
M. J. Driscoll

Four important reactor physics parameters are measured in lattices studied at M.I.T. by irradiating bare and cadmium-covered foil packets in the lattice fuel rods:

(1) δ_{28}, the ratio of the average U^{238} fission rate in the fuel rod to the average U^{235} fission rate in the fuel rod.

(2) R_{28}, the ratio of the average total U^{238} capture rate to the average epicadmium U^{238} capture rate.

(3) δ_{25}, the ratio of the average epicadmium U^{235} fission rate to the average subcadmium U^{235} fission rate.

(4) C^*, the ratio of the average U^{238} capture rate to the average U^{235} fission rate.

This set of experimentally measurable parameters can be related to conventional theoretical reactor physics parameters such as resonance escape probability and fast fission factor, which contribute to k_∞, the infinite multiplication factor. Reference 1 considers the pertinent relations in detail. In this section, we shall confine attention to the experimental parameters: δ_{28}, R_{28}, δ_{25} and C^*.

The results of earlier work at M.I.T. on 1.01-inch-diameter, natural uranium rods and 0.25-inch-diameter, 1.027% and 1.143% enriched rods have been reported previously in Refs. 1 through 5. This report gives additional results for 0.25-inch, 1.143% enriched lattices plus results obtained to date on a series of 0.75-inch-diameter-rod lattices of 0.947% enriched uranium. This section reports data only for standard, clean lattices with uniform spacing. Sections 6 and 8 of this report discuss measurements of parameters in lattices with added neutron absorbers and in two-region lattices. Detailed descriptions of the work summarized in this section are presented in the M.S. theses of the authors, Refs. 6 through 8.

1. δ_{28} MEASUREMENTS

Theoretical analysis of the fast fission phenomenon leads to the following equation for δ_{28} (1):

$$\delta_{28} = P(t) \frac{(EC)a\gamma(t) - S}{1 - a\gamma(t)} . \qquad (4.1)$$

The quantities EC and S are calculated constants depending only on the U^{235} and U^{238} concentrations in the lattice fuel and the detector foils. The constant a also contains experimentally determined correction factors for foil weights and for replacement of fuel by the detector packets.

P(t) = counter calibration factor, the ratio of the counts per U^{235} fission to the counts per U^{238} fission at time t after irradiation.

$\gamma(t)$ = ratio of fission product activities measured in detector foils of two different enrichments: at M.I.T., depleted (18 ppm U^{235}) and natural uranium foils are used.

Thus, two separate experiments are involved in δ_{28} measurements. The first is to calibrate the foil counting system – that is, to obtain the function P(t); and the second is to measure $\gamma(t)$ for a specific lattice configuration using the calibrated counting system.

In the present work, the standard procedures previously developed and described (3, 5, 6) were employed throughout.

Values measured for P(t) during the past year (6, 7) agree favorably with our previously reported values for this quantity (3, 4, 5). The results obtained also confirm that P(t) is indeed constant, within the experimental uncertainties, and independent of both time and foil diameter for the procedures and equipment employed at M.I.T. Table 4.1 displays the results of four determinations for a variety of experimental conditions. The results agree within the error estimates.

Once P(t) has been determined, measurement of detector foil activity ratios, $\gamma(t)$, permits one to calculate δ_{28} using Eq. 4.1. In this manner, δ_{28} measurements were made for three different experimental conditions:

TABLE 4.1

Average Values of P(t) Measured in the M.I.T. Lattice Facility

Rod Diameter (inches)	Fuel Enrichment	Moderator	P(t)[(a)]	(Ref.)
0.250	1.027	Void	1.16 ± 0.02[(a)]	(6)
0.750	0.947	Void	1.19 ± 0.03	(6)
0.750	0.947	D_2O	1.207 ± 0.034	(7)
1.01	Natural	Void	1.15 ± 0.03	(6)

(a) Uncertainties represent the estimated total error in P(t).

(a) Single rod measurements:
  (1) Single rods in the graphite-lined lattice facility cavity,
  (2) Single rods immersed in D_2O in the lattice tank.
(b) Rods which were members of D_2O-moderated lattices.

1.1 Single Rod Results

Single rod results are given in Table 4.2. They agree favorably with earlier M.I.T. experiments (3, 4, 5) and with data from H_2O-moderated lattices reported by the Brookhaven National Laboratory (9), except for the 0.25-inch, 1.027% enriched rod. Efforts to explain this disagreement have, so far, been inconclusive.

Table 4.2 also provides information on the neutron backscattering effect, which refers to the probability that fission neutrons escape from a fuel rod, scatter back into the rod, and still have sufficient energy to cause fission in U^{238}. The backscattering effect is masked by the larger interaction effect in multi-rod lattices, but the present single rod measurements provide an ideal opportunity to isolate and examine this phenomenon. The table lists four measurements made in a void. These were carried out in a large, air-filled, graphite-lined region (hohlraum) in a uniform thermal flux. The backscatter probability is effectively zero for these cases. Thus, the backscatter effect can be studied by comparing the D_2O-moderated δ_{28} single rod measurements to the hohlraum δ_{28}

TABLE 4.2

Single Rod δ_{28} Results

Average Values of δ_{28} Measured in the Graphite-Lined Cavity and Lattice Facility

Rod Diameter (inches)	Enrichment	Moderator	δ_{28}	Standard Deviation of the Mean[(b)]	Number of Determinations	Total Error[(c)]
0.250	1.027	Void	0.0146[(a)]	0.0002	7	0.0004
0.250	1.027	D_2O	0.0151	0.0002	6	0.0004
0.250	1.143	Void	0.0129	0.0002	6	0.0004
0.250	1.143	D_2O	0.0133	0.0002	6	0.0004
0.750	0.947	Void	0.0390[(a)]	0.0005	5	0.0010
0.750	0.947	D_2O	0.0409[(d)]	0.0006	6	0.0012
1.01	Natural	Void	0.0521[(a)]	0.0007	6	0.0015
1.01	Natural	D_2O	0.0551	0.0009	5	0.0017

(a) Absolute value of δ_{28} determined in the graphite-lined cavity.

(b) The standard deviation of the mean is a measure of the statistical error involved in the counting process, i.e., reproducibility, and includes the appropriate Student's t factor to account for small sample size.

(c) The total error is meant to reflect the total uncertainty in the listed values of δ_{28}. It includes the standard deviation of the mean listed and the uncertainty in P(t) and the depleted foil correction factors.

(d) A repeat determination by a second experimenter (7) gave 0.0420 ± 0.0020.

measurements. This is shown in Fig. 4.1 in which the ratio of δ_{28} for a lattice to δ_{28} for a single rod in the cavity is plotted. A curve based on the Monte Carlo results of Rief (10) is also shown for comparison. Since the effect is small, the error limits are large; but the experimental data confirm the predicted trend fairly well.

1.2 Measurement of δ_{28} in Lattices

In addition to the preceding single rod measurements, δ_{28} was also determined for three different lattices of 0.25-inch-diameter, 1.143% enriched uranium metal fuel rods. A value is also available for the initial spacing, 2.5 inches, in the current series of studies on 0.75-inch-diameter, 0.947% enriched rods. The pertinent results are shown in Table 4.3 and plotted in Fig. 4.2. Figure 4.2 also shows the 1.027% lattice data obtained during the preceding report period. As expected, the functional dependence is quite similar for the two sets of data. The consistency and linearity of the results is sufficient to provide a basis for interpolation for δ_{28} values over a wide range of lattices.

The preceding two paragraphs provide a good example of how the three-way, lattice-single rod-hohlraum comparisons, possible with the M.I.T. lattice facility, can isolate for study self-induced effects and interaction effects among lattice rods.

TABLE 4.3

Average Values of δ_{28} Measured in the M.I.T. Lattice Facility

Rod Spacing (inches)	δ_{28}	Standard Deviation of the Mean**	Number of Determinations
(a) 0.250-inch-diameter, 1.143% enriched rods*			
1.25	0.0265	±0.007	9
1.75	0.0204	±0.003	3
2.50	0.0164	±0.001	12
(b) 0.750-inch-diameter, 0.947% enriched rods			
2.50	0.0615	±0.0021	7

*Measurements performed by H. Smidt-Olsen and H. M. Guéron.

**The standard deviation of the mean includes Student's t factor to account for small sample size in all cases.

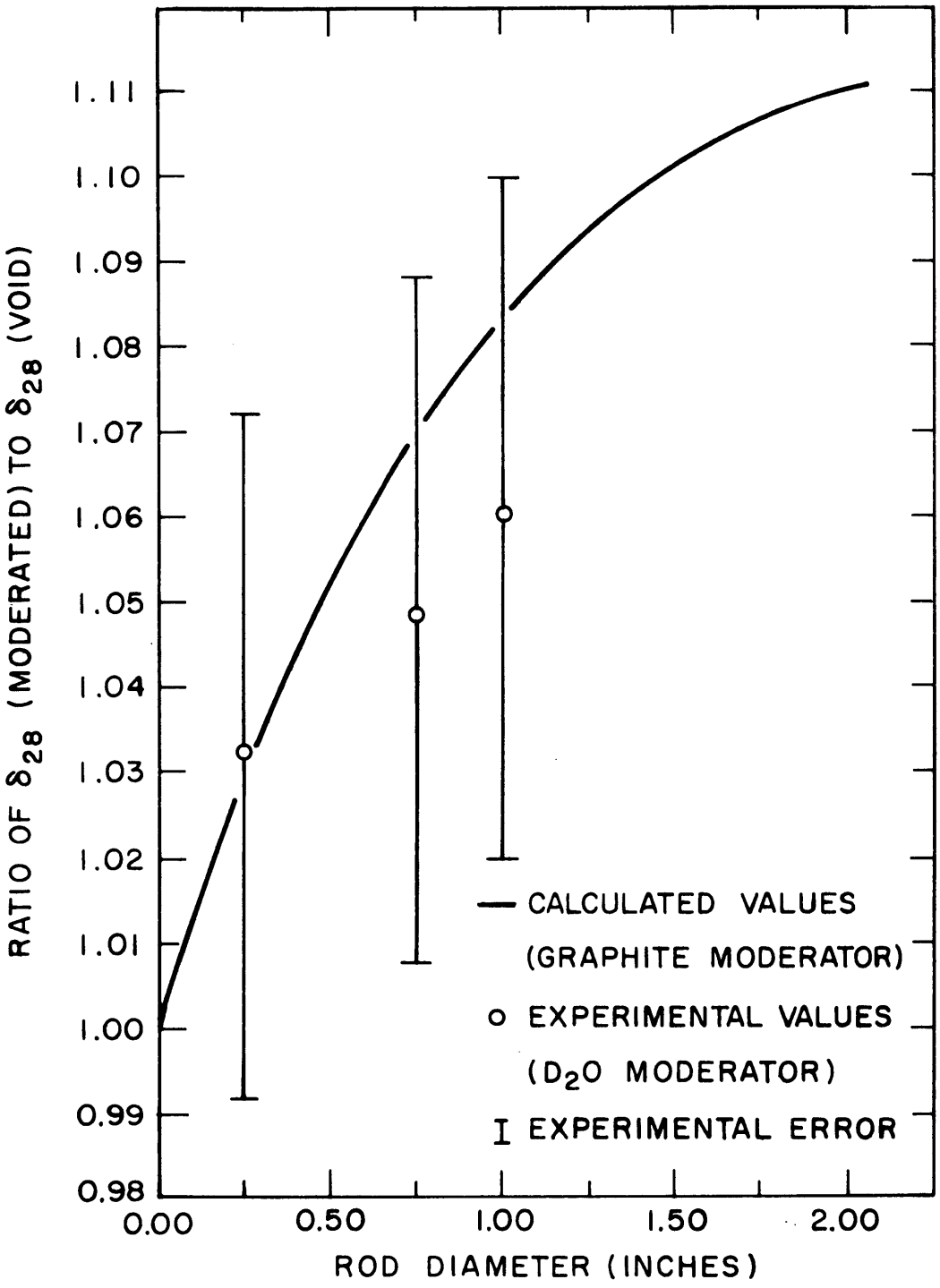

FIG. 4.1 BACKSCATTERING EFFECT FOR SMALL DIAMETER SINGLE RODS

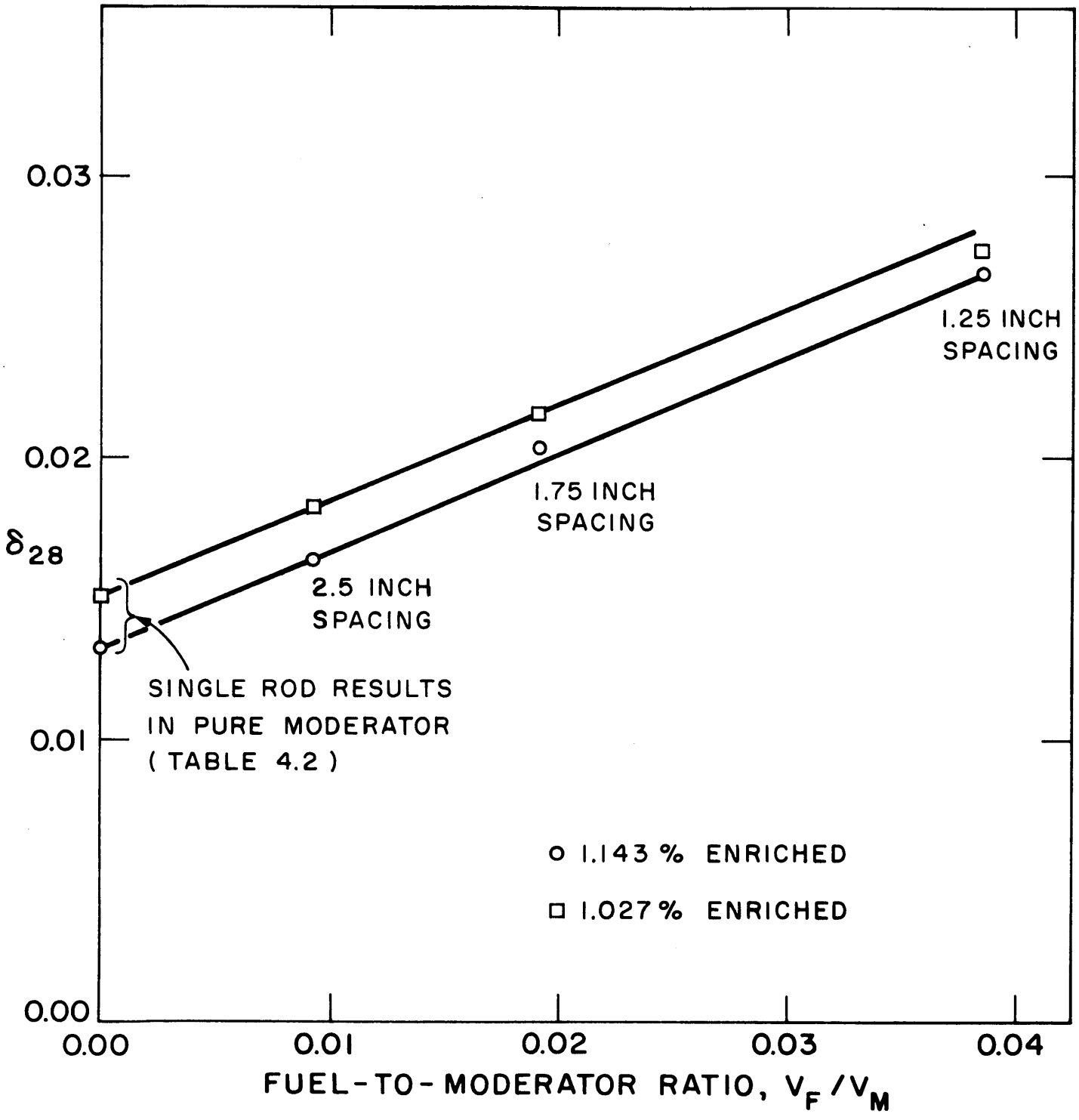

FIG. 4.2 VARIATION OF δ_{28} WITH FUEL-TO-MODERATOR RATIO

2. R_{28} MEASUREMENTS

The quantity R_{28} is just the ratio of total U^{238} activation to the epicadmium U^{238} activation. It is measured by counting the activity of the Np^{239} daughter produced when U^{238} captures a neutron, for both bare and cadmium-covered depleted uranium detector foils.

Table 4.4 lists the values obtained for the lattices investigated during the past year.

TABLE 4.4

Average Values of R_{28} Measured in the M.I.T. Lattice Facility

Rod Spacing (inches)	R_{28}	Standard Deviation of the Mean*	Number of Determinations
	(a) 0.250-inch-diameter, 1.143% enriched rods		
1.25	2.230	±0.018	6
1.75	3.105	±0.023	11
2.50	5.268	±0.094	4
	(b) 0.750-inch-diameter, 0.947% enriched rods		
2.50	1.736	±0.014	7

*The standard deviation of the mean includes Student's t factor in all cases.

The parameter R_{28} was also measured as a function of axial and radial position in the 0.250-inch-rod, 1.75-inch-pitch lattice to investigate the extent of the asymptotic region over which representative measurements can be obtained. Figure 4.3 shows the results, which validate the standard procedure of making all measurements 16 to 24 inches from the bottom of the fuel and in the first ring of rods about the center rod.

The measured values of R_{28} vary as expected. The results agree well with results obtained by W. D'Ardenne in three similar lattices of 1.027% enriched fuel (1). A check for the consistency of the data can be made in the following way. As may be inferred from the work reported in Ref. 1, a plot of ρ_{28} vs. the fraction, volume of fuel over volume of

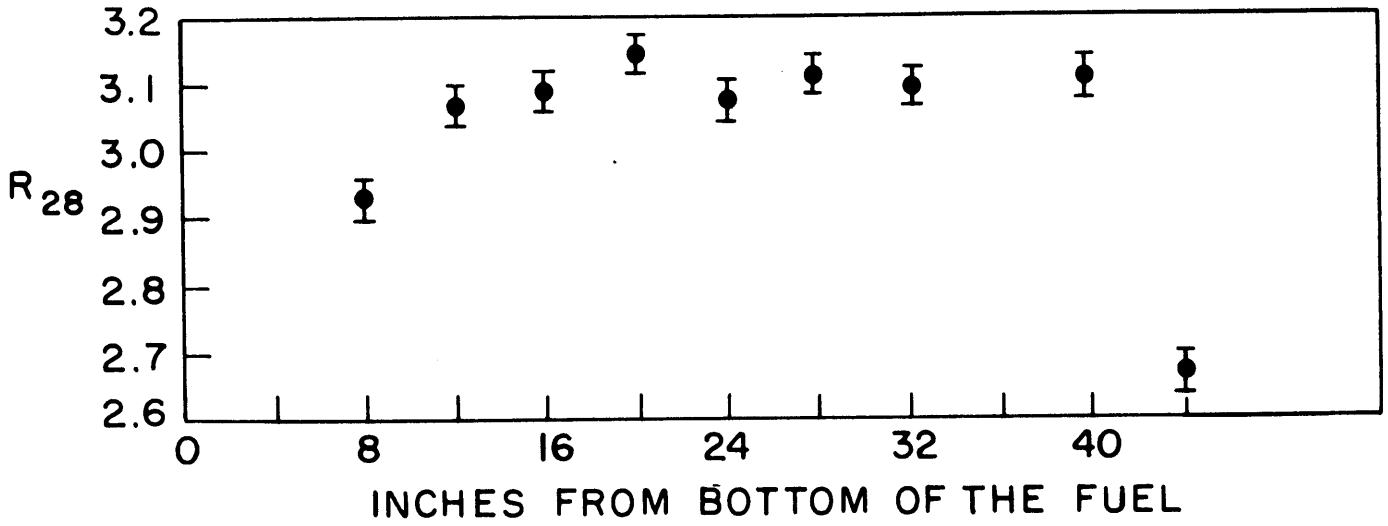

VALUES OF R_{28} AS A FUNCTION OF HEIGHT NEAR 1.75-INCH LATTICE CENTER

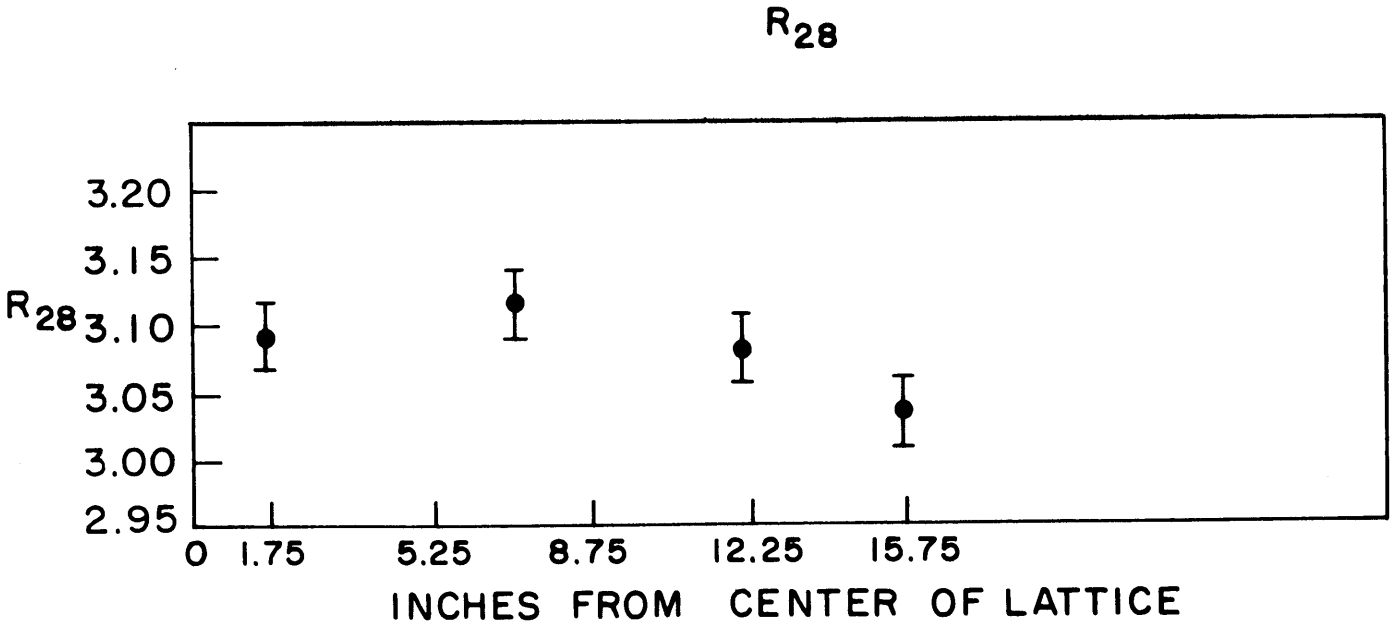

VALUES OF R_{28} AS A FUNCTION OF RADIUS, 1.75-INCH LATTICE, 16 INCHES FROM BOTTOM OF FUEL RODS

FIG. 4.3 R_{28} AS A FUNCTION OF POSITION

moderator should approximate a straight line, where $\rho_{28} = 1/(R_{28}-1)$. Figure 4.4 shows these values plotted for the 1.027% enriched and the 1.143% enriched fuel. As indicated in Fig. 4.4, the data fall very nearly on a straight line.

3. δ_{25} MEASUREMENTS

As noted in the introduction, δ_{25} is the ratio of epicadmium to subcadmium U^{235} fission rates. The values measured in the set of three lattices composed of 0.25-inch-diameter, 1.143% enriched fuel rods are shown in Table 4.5. The values reported vary as expected; as the lattice pitch increases, the δ_{25} values decrease.

TABLE 4.5

Average Values of δ_{25} Measured in the M.I.T. Lattice Facility
0.250-inch-diameter rods, 1.143% enriched

Rod Spacing (inches)	δ_{25}	Standard Deviation of the Mean*	Number of Determinations
1.25	0.0579	±0.0011	6
1.75	0.0334	±0.0016	3
2.50	0.0163	±0.0073	6

*The standard deviation of the mean includes Student's t factor in all cases.

As shown in Fig. 4.5, the variation of δ_{25} with the fuel-to-moderator ratio is linear within the accuracy of the experimental measurements for both the present set of lattices and the 1.027% enriched set reported last year, which is included for comparison.

4. C^* MEASUREMENTS

C^* is the ratio of U^{238} capture to U^{235} fission. The measured values for the set of three 1.143% lattices are reported in Table 4.6. As the lattice pitch increases, the value of C^* decreases. The values of Table 4.6 show the same trend as the values of C^* reported last year for

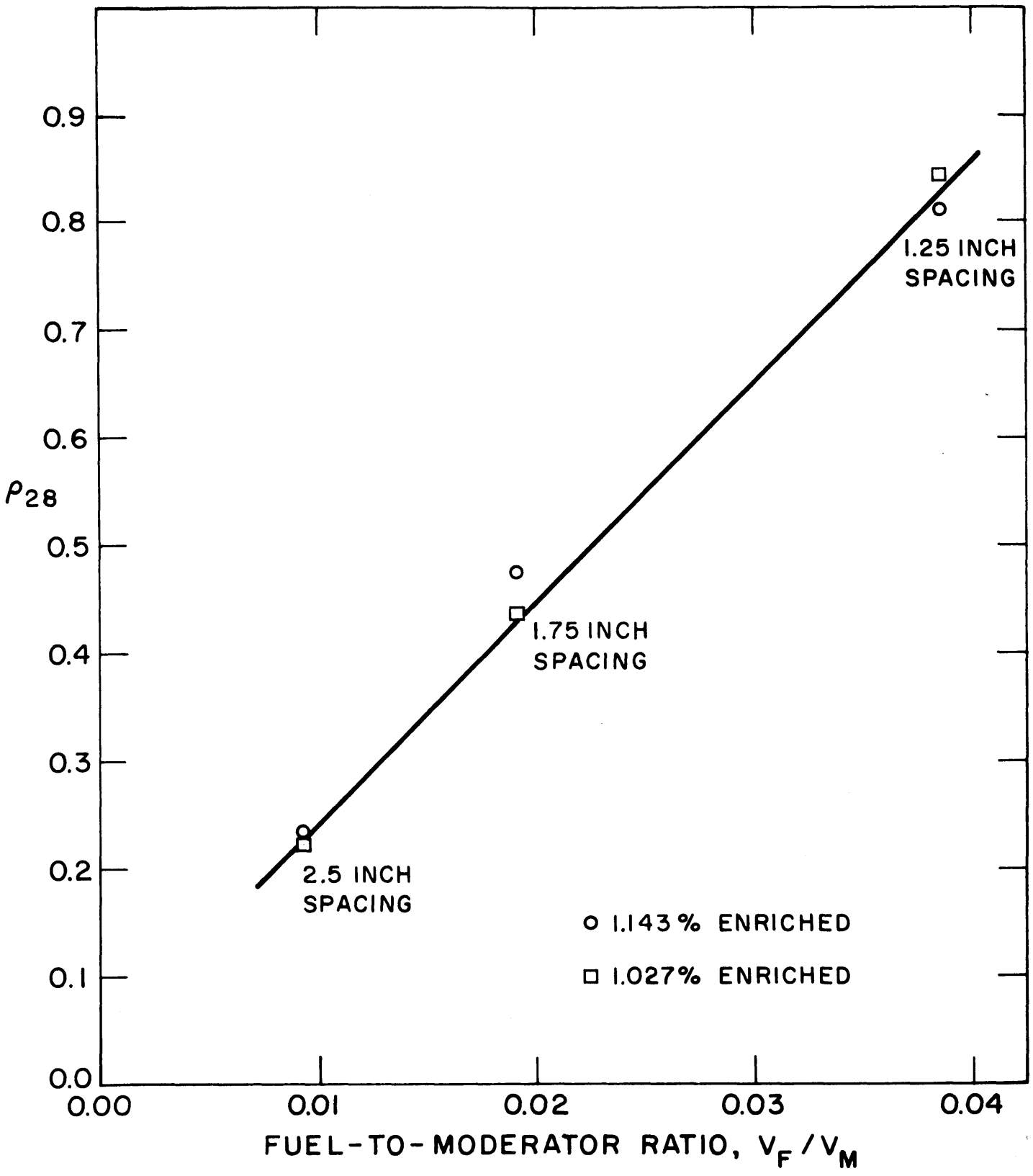

FIG. 4.4 VARIATION OF ρ_{28} WITH FUEL-TO-MODERATOR RATIO

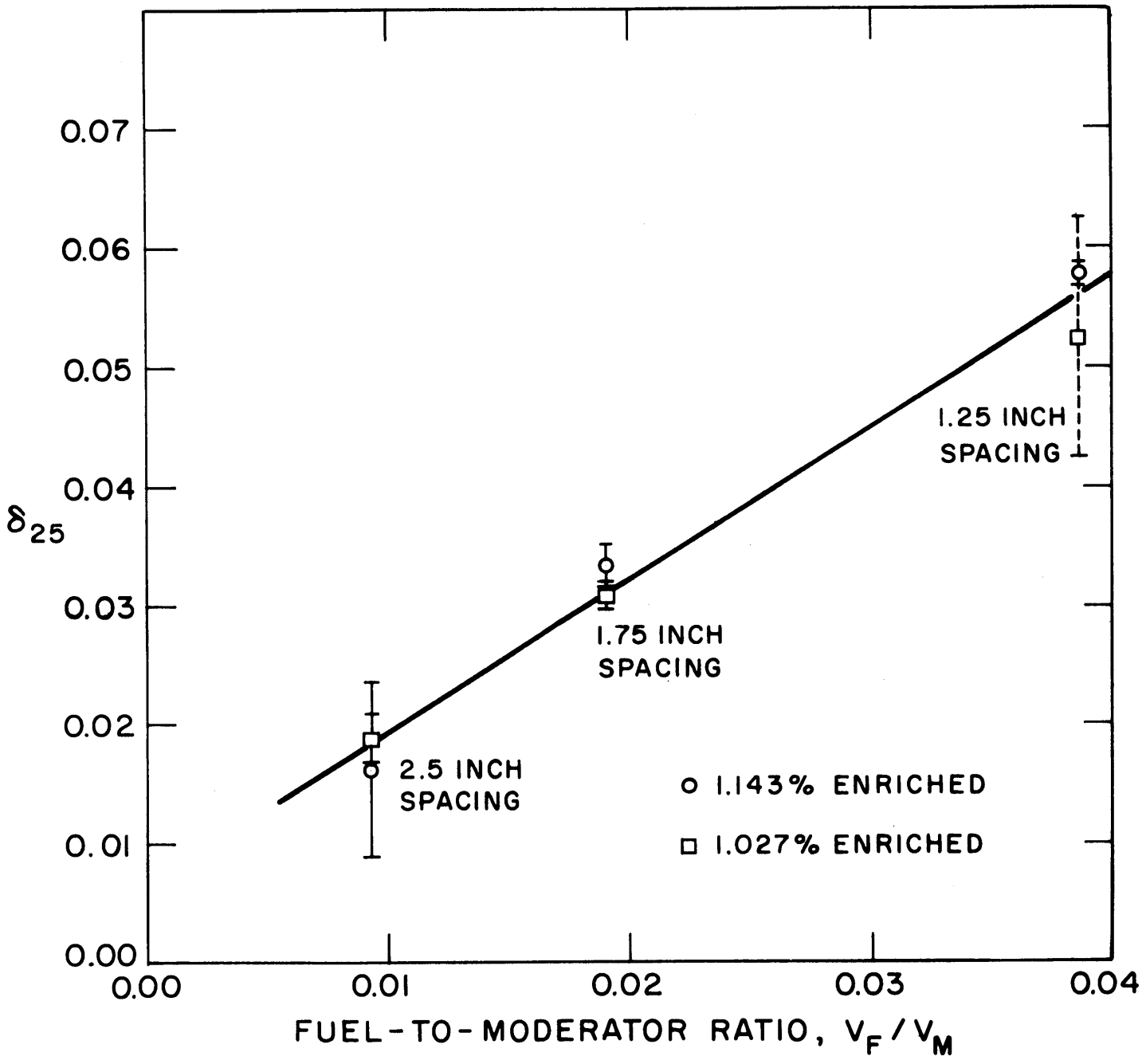

FIG. 4.5 VARIATION OF δ_{25} WITH FUEL-TO-MODERATOR RATIO

TABLE 4.6

Average Values of C^* Measured in the M.I.T. Lattice Facility

0.25-inch-diameter rods, 1.143% enriched

Rod Spacing (inches)	C^*	Standard Deviation of the Mean*	Number of Determinations
1.25	0.789	±0.040	4
1.75	0.625	±0.027	4
2.50	0.486	±0.016	6

*The standard deviation of the mean includes Student's t factor in all cases.

the 1.027% lattices (0.814, 0.644, 0.554) and are slightly lower. As shown in Fig. 4.6, the variation of C^* with the fuel-to-moderator ratio is approximately linear.

The set of measurements, δ_{28}, R_{28}, δ_{25} and C^*, reported in this section will continue to be made on future lattices. The development phase in this area, carried out mostly in thesis investigations, is now practically complete, and the procedures are now being standardized for regular performance by full-time project personnel. There are several areas meriting further study, however, including systematization of foil packet correction factors for fuel displacement. It will also be of interest to make single rod measurements of δ_{25} and C^* in order to obtain the ordinate intercept in Figs. 4.3 and 4.4. If the linearity is confirmed and the slope can be determined by experiment or theory, it appears quite likely that useful estimates can be obtained for the subject parameters in lattices through single rod measurements.

5. REFERENCES

(1) D'Ardenne, W. H., "Studies of Epithermal Neutrons in Uranium, Heavy Water Lattices," Ph.D. Thesis, M.I.T. Nuclear Engineering Department, August 1964.

(2) "Heavy Water Lattice Project Annual Report," MIT-2344-3 (MITNE-60), September 30, 1964.

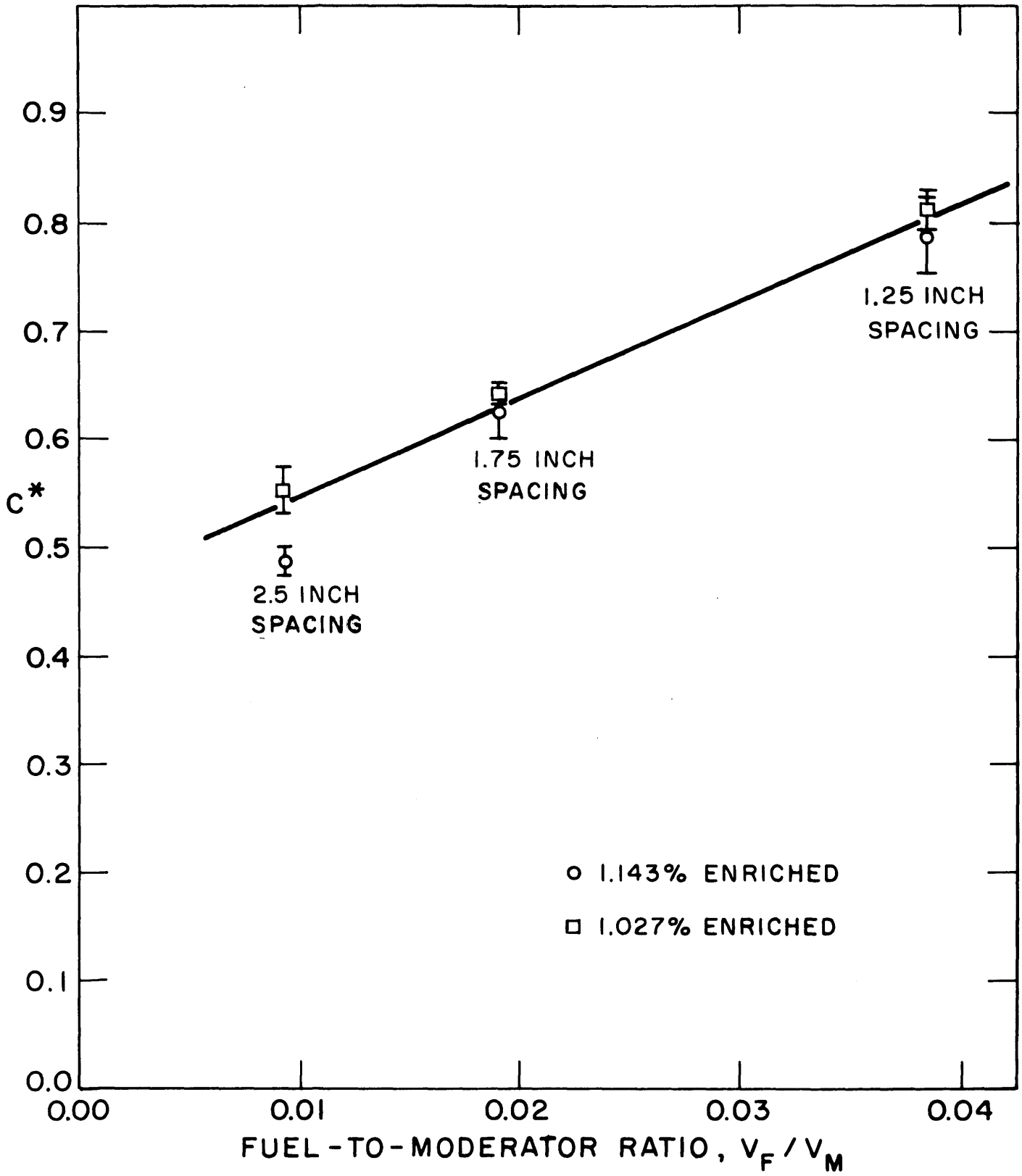

FIG. 4.6 VARIATION OF C* WITH FUEL-TO-MODERATOR RATIO

(3) Wolberg, J. R., T. J. Thompson, and I. Kaplan, "A Study of the Fast Fission Effect in Lattices of Uranium Rods in Heavy Water," NYO-9661 (MITNE-15), February 1962.

(4) Peak, J., I. Kaplan, and T. J. Thompson, "Theory and Use of Small Subcritical Assemblies for the Measurement of Reactor Parameters," NYO-10204 (MITNE-16), April 1962.

(5) Bliss, H., "Measurement of the Fast Fission Effect in Heavy Water, Partially Enriched Uranium Lattices," M.S. Thesis, M.I.T. Nuclear Engineering Department, June 1964.

(6) Papay, L. T., "Fast Neutron Fission Effect for Single Slightly Enriched Uranium Rods in Air and Heavy Water," M.S. Thesis, M.I.T. Nuclear Engineering Department, June 1965.

(7) Hellman, S. P., "Measurements of δ_{28} and ρ_{28} in a 2.5-Inch Triangular Lattice of 0.75-Inch Metallic Uranium Rods (0.947 wt % U-235) in a Heavy Water Moderator," M.S. Thesis, M.I.T. Nuclear Engineering Department, September 1965.

(8) Robertson, C. G., "Measurements of Neutron Utilization for Lattices of Slightly Enriched Uranium Rods," M.S. Thesis, M.I.T. Nuclear Engineering Department, June 1965.

(9) Hellens, R. L., and H. C. Honeck, "A Summary and Preliminary Analysis of the BNL Slightly Enriched Uranium Water Moderated Lattice Measurements," Proc. of the IAEA Conf. on Light Water Lattices, Vienna, June 1962.

(10) Rief, H., "The Fast Effect in Uranium and Beryllium Systems," Nucl. Sci. Eng., 10, 83 (1961).

5. PULSED NEUTRON STUDIES

H. E. Bliss

The pulsed neutron source research described in previous annual reports (1, 2) has been extended to several new lattices. The basic theoretical models used and the experimental equipment employed have been reported elsewhere (1, 3) and only details pertinent to the present work will be described here. Work has been done in three areas: (1) pulsed neutron source die-away measurements to determine lattice parameters have been made in clean, poisoned and substituted lattices; (2) the data analysis is being improved to obtain a more accurate value of the fundamental mode die-away constant and, possibly, estimates for one or more higher harmonics; and (3) measurements have been made with and without a cadmium plate in the bottom of the lattice tank in an attempt to determine an effective return coefficient (albedo) for the lattice cavity.

1. MEASUREMENT OF LATTICE PARAMETERS

The lattice configurations investigated with the pulsed neutron source technique during the past year are listed in Table 5.1.

The space-time dependence of the neutron density in a subcritical multiplying assembly, irradiated by a burst of fast neutrons, is given by the expression:

$$n(\bar{r}, t) = \sum_{n=1}^{\infty} A_n R_n(\bar{r})\, e^{-\lambda_n t}, \tag{5.1}$$

where $R_n(\bar{r})$ satisfies the Helmholtz equation with appropriate boundary conditions, A_n is determined by the initial conditions, and λ_n can be shown to be given by (3):

$$\lambda_n = \overline{v\Sigma}_a + \overline{vD}B^2 - \overline{v\Sigma}_a(1-\bar{\beta})\, k_\infty P(B_n^2) . \tag{5.2}$$

If a Fermi slowing-down kernel is used for the fast nonleakage probability, $P(B_n^2) = e^{-B_n^2\tau} \approx 1 - \tau B_n^2 + \frac{1}{2}\tau^2 B_n^4$, Eq. 5.2 may be written:

TABLE 5.1

Lattice Configurations Studied with the Pulsed Neutron Source Technique

Lattice Type	Pitch (inches)	Rod Diameter (inches)	Tank Diameter (feet)	Enrichment (%)	Remarks
Clean core	1.25	0.25	3	1.143	
Clean core	1.75	0.25	3	1.143	
Poisoned core	1.75	0.25	3	1.143	One 0.188-in. Cu rod/unit cell
Poisoned core	1.75	0.25	3	1.143	One 0.188-in. Cu rod/unit cell One 0.144-in. Cu rod/unit cell
Clean core	2.50	0.25	3	1.143	
Poisoned core	2.50	0.25	3	1.143	One 0.144-in. Cu rod/unit cell
Poisoned core	2.50	0.25	3	1.143	Two 0.144-in. Cu rods/unit cell
Substituted	1.75	0.25	3	1.143	Central 5 rings + central rod = 1.027% Remainder = 1.143%
Clean core	2.50	0.75	3	0.947	
Poisoned core	2.50	0.75	3	0.947	Two 0.188-in. Cu rods/unit cell One 0.144-in. Cu rod/unit cell
Clean core	5.00	0.75	4	0.947	2 runs without cadmium plate 1 run with cadmium plate
Pure Moderator	∞	–	3	–	
Pure Moderator	∞	–	4	–	1 run without cadmium plate 1 run with cadmium plate

$$\lambda_n = m + nB_n^2 - qB_n^4 , \tag{5.3}$$

where

$$m = \overline{v\Sigma}_a[1-(1-\bar{\beta})k_\infty] , \tag{5.4a}$$

$$n = \overline{vD} + \overline{v\Sigma}_a(1-\bar{\beta})\, k_\infty\tau , \tag{5.4b}$$

$$q = \frac{1}{2}\,\overline{v\Sigma}_a(1-\bar{\beta})\, k_\infty\tau^2 , \tag{5.4c}$$

In Eqs. 5.4a, b, and c, Σ_a is the total absorption cross section, D is the diffusion coefficient, τ is the neutron age to thermal energy, and the other symbols have their usual meaning. The quantity B_n^2 in Eq. 5.3 is the separation constant arising in the solution of the time-dependent thermal neutron diffusion equation. In a bare, cylindrical assembly, B_n^2 is given by:

$$B_n^2 = \left(\frac{an}{R+d}\right)^2 + \left(\frac{n\pi}{H+2d}\right) , \tag{5.5}$$

where R and H are physical dimensions and d is the extrapolation distance. For n = 1 (fundamental mode), the familiar geometric buckling results.

For each lattice listed in Table 5.1, the neutron density was measured as a function of time for each of several heights. The higher modes decay more rapidly than the fundamental mode, so that eventually the time dependence of the neutron density follows a single exponential (the fundamental mode). A least-squares fit of the observed fundamental mode decay constants as a function of the geometric buckling then yields the coefficients m, n, and q.

2. DATA ANALYSIS

In the initial pulsed neutron experiments, the observed data were fitted by an iterative, least-squares technique to an expression of the form,

$$n(t) = Ae^{-\lambda t} + b , \tag{5.6}$$

where λ is the fundamental mode decay constant and b is a constant background which includes delayed neutron effects. Since higher

harmonics contribute to data taken in the beginning time channels, these initial channels are successively dropped from the data and the fit to Eq. 5.6 repeated. When the higher harmonics no longer make a significant contribution to the data, the fit values of parameters A, b, and λ approach constants characteristic of the fundamental mode of the medium.

However, for some sets of data, a constant value of λ could not easily be ascertained, as illustrated in Fig. 5.1. The lower curve, corresponding to a D_2O height of 129 cm, exhibits a relatively constant value of 970 sec^{-1}, beginning about 1.5 msec after the burst of fast neutrons enters the system. The upper curve, corresponding to a D_2O height of 119 cm, shows no such constant value. The reasons for this behavior are currently being studied and will be reported subsequently.

As part of this investigation, a new method of data analysis is now being examined. Basically, this method involves assuming that the observed data can be represented as the sum of two exponential functions, after subtraction of a constant background. An initial "best estimate" value for the longer-lived exponential (fundamental) is then subtracted from the data and a semilogarithmic least-squares fit made to the difference to obtain a value for the shorter-lived exponential. This value is then subtracted from the initial data and a semilogarithmic least-squares fit applied to the difference to obtain a second estimate of the fundamental. The process is repeated until a desired convergence criterion is satisfied.

This technique shows considerable promise. Preliminary results have indicated that one must exercise care in choosing the value of background used and the portions of the data over which the exponentials are fit.

The advantages of this method, in addition to solving the difficulty illustrated in Fig. 5.1, are: (1) better statistical accuracy in the fitted value of the fundamental mode decay constant, since more data is utilized in the fit, and (2) the possibility of obtaining a higher mode decay constant (and associated B_n^2) for use in evaluating the coefficients m, n, and q in Eq. 5.3.

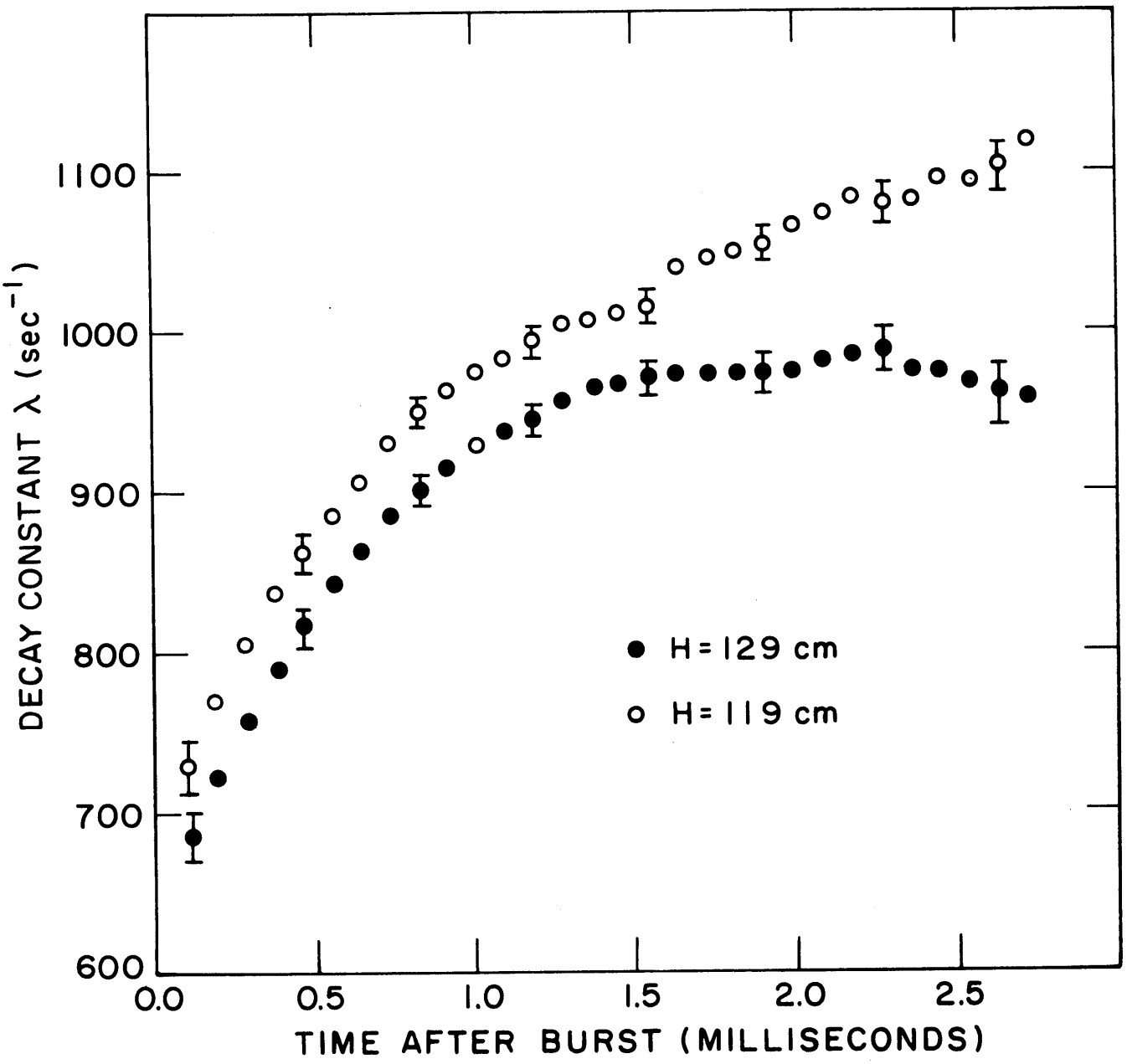

FIG. 5.1 VARIATION OF THE MEASURED DECAY CONSTANT WITH WAITING TIME

3. EFFECT OF THE CADMIUM PLATE

The derivation leading to Eqs. 5.1 and 5.2 assumes that the system is effectively bare in the thermal neutron energy range, and, to this end, a 20-mil cadmium plate clad in 1/8-inch aluminum has been inserted in the bottom of the lattice tank whenever pulsed neutron experiments have been performed. This provides an all-around black boundary since the sides and top of the lattice tank are already surrounded by cadmium. The installation of this plate is not desirable from an experimental standpoint because the lattice must be withdrawn from the tank to insert the plate. Withdrawing the lattice, (1) exposes a radiation source of fairly high level, 0.05 to 0.5 r/hr, depending on the recent operating history of the lattice facility; (2) results in the partial degradation of 1 to 2 gallons of D_2O per experiment, which must be removed before the facility can be operated again and which must eventually be reprocessed; and (3) consumes time while the system is being dried before use.

In an attempt to obviate the need for the plate in future experiments, measurements with and without the plate have been performed. If there is a significant return of neutrons from the graphite-lined cavity (hohlraum) under the lattice, then the decay constant λ will be decreased. It is still too early to report quantitative results, but there does appear to be a small but discernable return of neutrons.

This effect can be taken into account (4) by modifying the extrapolation distance d to take into account the return coefficient (albedo) of the cavity:

$$d = 0.71\,\lambda_{tr}\left(\frac{1+\beta}{1-\beta}\right), \tag{5.7}$$

where β is the experimentally determined albedo.

The data measured in the experimental assemblies listed in Table 5.1 are now being analyzed in accordance with the procedure described in section 5.2. Results will be published during the coming report period.

4. REFERENCES

(1) "Heavy Water Lattice Project Annual Report," NYO-10212 (MITNE-46), September 30, 1963.

(2) "Heavy Water Lattice Project Annual Report," MIT-2344-3 (MITNE-60), September 30, 1964.

(3) Malaviya, B. K., I. Kaplan, T. J. Thompson, and D. D. Lanning, "Studies of Reactivity and Related Parameters in Slightly Enriched Uranium Heavy Water Lattices," MIT-2344-1 (MITNE-49), May 1964.

(4) Glasstone, S., and M. C. Edlund, The Elements of Nuclear Reactor Theory, D. Van Nostrand Company, Inc., Princeton, N. J., 1952.

6. USE OF NEUTRON ABSORBERS IN THE DETERMINATION OF LATTICE PARAMETERS

J. Harrington, III

An extensive series of experiments has been carried out on subcritical lattices to which varying amounts of thermal neutron absorbers have been added. The purpose of these experiments is to obtain more precise measurements of lattice parameters, specifically, k_∞, η, τ, and L^2.

The analysis of the data is being carried out along the lines indicated in last year's report, under the heading, "Measurements on Poisoned Lattices." The final results of the present series of experiments will be published in detail in a separate report and summarized in the next annual report. In this section, the experiments carried out so far will be described and the results obtained to date presented.

1. DESCRIPTION OF LATTICES INVESTIGATED

Three lattices having widely varying moderator-to-fuel ratios have been investigated. Table 6.1 supplies the pertinent details on each, together with a designator assigned each lattice for convenience of reference.

For reasons discussed in the previous report, copper rods were chosen for use as thermal neutron absorbers. Two sets of rods of different diameters were purchased: 0.188-inch (A rods) and 0.144-inch (B rods). Support girders and top adapters, compatible with the fuel support mechanisms already in use, were designed and fabricated. The rods were clad with 0.0005 inch of electroless nickel, a uniform, hard plating which assured that no corrosion of aluminum hardware or contamination of heavy water took place while the rods were in the lattice.

The purity of the copper used, so-called OFHC copper, was found to be highly satisfactory. (See Table 6.2.)

TABLE 6.1

Description of Lattices Studied Using Added Neutron Absorbers

Lattice Designator	Lattice Pitch (in.)	Fuel Slug Diameter (in.)	Air Gap (in.)	Clad Thickness (in.)	Fuel Rod O. D. (in.)	Uranium Enrichment (weight %)	D_2O Purity (mole %)	Moderator to Fuel Volume Ratio
250	2.50	0.250	0.006	0.028	0.318	1.143	99.56	108.60
175	1.75	0.250	0.006	0.028	0.318	1.143	99.53	52.40
253	2.50	0.750	0.004	0.028	0.814	0.947	99.51	11.07

TABLE 6.2

Impurities Present in Copper Used in Experiments*
(Based on qualitative spectrographic analysis of two samples.)

Impurity	Weight Percentage (Max.)
Pb	0.01
Ag**	0.01
Ni	0.01-0.001
Na	0.001
Si	0.001
Mg	0.001-0.0001
Ca	0.0001
Fe	0.0001

*So-called OFHC (oxygen-free, high conductivity) copper.

**Subsequent quantitative analysis placed the actual amount of silver present at 0.0020 ± 0.0003%.

In most cases, the copper rods were spaced uniformly through the lattice, at intervals equal to the lattice pitch or an integral fraction thereof. In one assembly, however, only the central region contained copper. The purpose of the experiments carried out in this assembly was to explore the possibility of doing all the measurements in such two-region assemblies. Considerable economies in time and materials will result if this can be done.

Table 6.3 gives details on the nine different assemblies studied. The designator assigned to each indicates the host lattice, as well as the number and type of copper rods in a unit cell of the assembly. (In the 253A2B1 assembly, for instance, there were two A rods and one B rod for each fuel rod.) As may be seen from the table, the amount of moderator expelled from the lattices was slight, in no case exceeding 1.71%.

TABLE 6.3

Description of Assemblies Studied in Each Parent Lattice

Designator	Number of A Rods in Unit Cell	Number of B Rods in Unit Cell	Per Cent of Moderator Expelled from Unit Cell
250A2	2	0	1.04
250A1	1	0	0.52
250B2	0	2	0.62
250B1	0	1	0.31
175A1B1	1	1	1.71
175A1	1	0	1.08
253A2B1(2R)	(2)	(1)	(1.47)
253A2B1	2	1	1.47
253A2	2	0	1.12

(2R) signifies two-region assembly.

2. DESCRIPTION OF MEASUREMENTS

Measurements made include:

(1) the radial and axial macroscopic activation distribution, with bare and cadmium-covered gold foils as detectors,

(2) the axial activation distribution, with foils cut from the copper rods as detectors,

(3) the intracell activation distribution, with bare and cadmium-covered gold foils as detectors,

(4) R_{28}, the U^{238}-cadmium ratio in the fuel rods, and

(5) δ_{28}, the ratio of fissions in U^{238} to fissions in U^{235}.

The number and type of each experiment performed are shown in Table 6.4. The macroscopic distributions, as well as R_{28} and δ_{28}, were measured in exactly the same way as in lattices without added absorbers. (See secs. 2 and 4 of this report.) The intracell microscopic distribution measurement was also made in much the same manner as in lattices

TABLE 6.4

Number and Type of Experiments Done in Each Assembly

Designator	Radial Distribution Measurement		Axial Distribution Measurement		Microscopic Distribution Measurement	R_{28} Measurement	δ_{28} Measurement
	Bare foils	Cd-cov. foils	Bare foils	Cd-cov. foils			
250A2	3	1	4	2	2	4	3
250A1	2	1	2	2	2	2	3
250B2	2	1	2	2	2	4	3
250B1	2	1	4	2	2	4	3
175A1B1	2	1	3	3	2	4	3
175A1	2	1	2	2	2	8	0
253A2B1(2R)	1	1	3	3	0	0	0
253A2B1	1	2	3	2	2	2	2
253A2	1	0	3	1	2	0	0

(2R) signifies two-region assembly.

without added absorbers. Of course, establishment of the relative activation level inside the copper rods presented a new problem, but this was met by fabrication of a special set of experimental rods which can be disassembled to allow positioning of either a bare or a cadmium-covered foil within the rod. (See Fig. 6.1.) Foils were also placed on the surface of the copper rods.

3. ANALYSIS OF THE EXPERIMENTS AND RESULTS

The material bucklings of the various assemblies were established by least-squares fits to the measured radial and axial distributions. The analysis is identical to that made on similar data from clean lattices. The average values for the radial and the axial components of the material buckling for each assembly studied are listed in Table 6.5. The uncertainty assigned in each case is the standard deviation of the mean and is based on scatter of the data about the mean. The Student t correction for small sample size has been applied. Material bucklings and their standard deviations follow directly from the radial and axial components. The material bucklings of the clean lattices, which were measured by other project personnel, are also included in Table 6.5 for comparison. As can be seen from the table, the several experiments of each type in each assembly yield buckling values having a precision comparable to the clean lattice measurements.

Measurements of δ_{28} and R_{28} were carried out by H. Olsen, C. Robertson, H. Guéron, and S. Hellman. The analysis of the experimental data does not differ from that carried out on data from clean assemblies. The results are in Table 6.5; the uncertainties are again standard deviations of the mean.

The analysis of intracell foil activity distributions to obtain the thermal utilization involved a generalization of the method used in clean lattices. In such lattices, the thermal utilization is obtained by comparing the thermal activation distribution of small gold foils with a calculated distribution obtained with the THERMØS code. Use of the THERMØS code in its one-dimensional form involves the Wigner-Seitz approximation and treating the hexagonal unit lattice cell as circular. In clean lattices of the type considered here, this approximation is found to yield

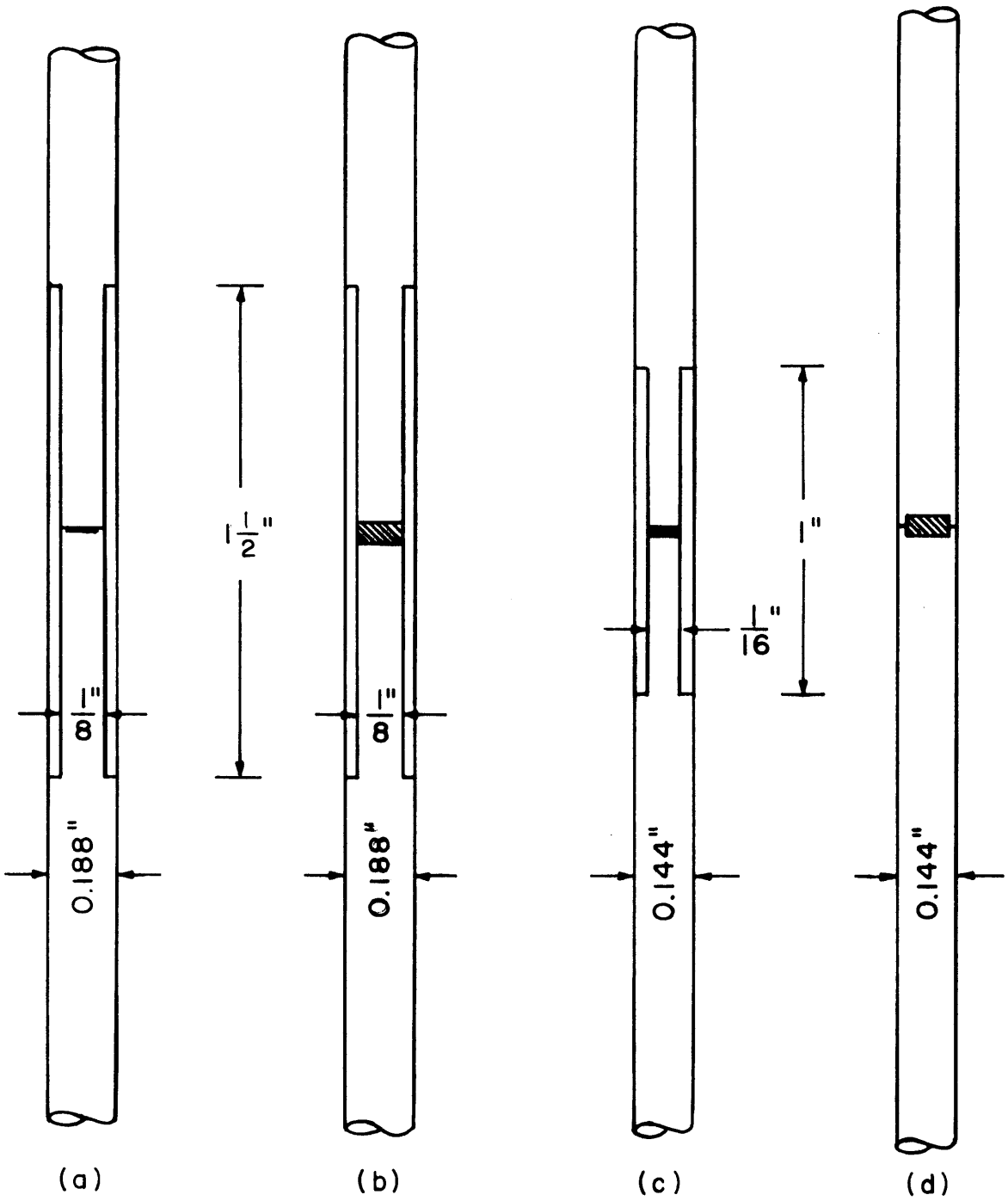

RODS ACCOMMODATE 1/16 INCH DIAMETER FOILS, OR 1/8 INCH DIAMETER CADMIUM BOXES WHICH ARE 0.060 INCH THICK

FIG. 6.1 CROSS-SECTION VIEW OF COPPER RODS USED IN INTRACELL DISTRIBUTION MEASUREMENTS

TABLE 6.5

Tabulation of Results to Date

Assembly	Radial Buckling (μB)	Axial Buckling (μB)	Material Buckling (μB)	Thermal Utilization	δ_{28}	R_{28}
250	2403 ± 16	1396 ± 7	+1007 ± 17	(0.9520)	0.01638 ± 14	5.268 ± 94
250A2	2385 ± 11	3068 ± 25	-683 ± 27	0.5328 ± 36	0.01733 ± 29	4.434 ± 29
250A1	2367 ± 23	2267 ± 6	+100 ± 24	0.6847 ± 6	0.01686 ± 95	4.821 ± 24
250B2	2395 ± 5	2443 ± 12	-48 ± 13	0.6462 ± 74	0.01705 ± 32	4.676 ± 42
250B1	2401 ± 11	1961 ± 22	+440 ± 25	0.7680 ± 5	0.01558 ± 47	5.048 ± 13
175	2418 ± 4	1013 ± 12	+1405 ± 13	(0.9678)	0.02045 ± 28	3.105 ± 23
175A1B1	2311 ± 8	2946 ± 10	-635 ± 13	0.6008 ± 48	0.02367 ± 393	2.690 ± 25
175A1	2316 ± 9	2288 ± 18	+28 ± 20	0.6936 ± 22	–	2.897 ± 24
253	2364 ± 8	1395 ± 7	969 ± 11	(0.9885)	0.06151 ± 207	1.736 ± 14
253A2B1	2305 ± 18	2197 ± 25	108 ± 31	0.8462 ± 3	0.06302 ± 308	1.693 ± 15
253A2	(2305)	1999 ± 7	306 ± 19	0.8767 ± 6	–	–

results in agreement with experiment if the reflecting condition at the cell boundary is properly treated (1, 2, 3, 4).

In a mixed lattice, however, the situation is not so simple. Each element may still be regarded as being centered in a cylindrical cell, but the size of the various cells is no longer known a priori, as Suich has pointed out (5). They can, however, be established a posteriori, on the basis of calculations, as in the case of Suich's work, or on the basis of measurements, as is done here. Using heterogeneous source-sink theory, Suich shows that the cross-sectional area to be assigned to the cell about each lattice element is directly proportional to the number of absorptions in the element. In his work, a weakly-absorbing moderator, a uniform slowing-down source across the cell, and invariance of the cell boundaries with neutron energy are assumed, all of which are considered applicable to the lattices considered here.

Thus, the following procedure was employed:

(1) Initial guesses of the relative absorption in the fuel and copper rods were made and cell areas assigned based on Suich's algorithm.

(2) The THERMØS code was used for calculation of hardened absorption cross sections for the fuel and copper rods.

(3) New guesses of the relative absorption in the fuel and copper rods were made using the hardened THERMØS cross sections and the measured activation distributions.

(4) Steps 1 through 3 were repeated until satisfactory convergence was obtained. In practice, a single iteration usually sufficed.

(5) The measured activation distributions and calculated cross sections from the final iteration were then used to calculate the relative thermal neutron absorption in each lattice material and to obtain the thermal utilization.

The activation distributions calculated with THERMØS show good agreement with the experimentally measured intracell foil activation data.

As may be seen from Table 6.4, two independent intracellular traverses have been made in each lattice, resulting in two independent values of the thermal utilization. The values are generally in excellent agreement; the average for each assembly is presented in Table 6.5. The standard deviations assigned merely reflect the spread between the two values.

4. CONCLUSIONS

As noted in the introduction, analysis of the data is continuing. The results obtained so far and reported in this section are quite encouraging and suggest that the goals stated in the introduction will be realized. As noted, a final report will be prepared and issued during the coming contract year.

5. REFERENCES

(1) Brown, P. S., T. J. Thompson, I. Kaplan, and A. E. Profio, "Measurements of the Spatial and Energy Distribution of Thermal Neutrons in Uranium, Heavy Water Lattices," NYO-10205 (MITNE-17), August 1965.

(2) Simms, R., I. Kaplan, T. J. Thompson, and D. D. Lanning, "Analytical and Experimental Investigations of the Behavior of Thermal Neutrons in Lattices of Uranium Metal Rods in Heavy Water," NYO-10211 (MITNE-33), October 1963.

(3) Honeck, H. C., "THERMØS, A Thermalization Transport Theory Code for Reactor Lattice Calculations," BNL-5826, September 1961.

(4) Honeck, H. C., "Some Methods of Improving the Cylindrical Reflecting Boundary Condition in Cell Calculations of the Thermal Neutron Flux," Trans. Am. Nucl. Soc., 5(2), 350, November 1962.

(5) Suich, J. E., "Calculation of Neutron Absorption Rates in D_2O-Moderated Mixed Lattices," Trans. Am. Nucl. Soc., 7(1), 32, June 1964.

7. SINGLE ROD EXPERIMENTS IN THE THERMAL ENERGY REGION

E. E. Pilat

1. THE BASIC EXPERIMENT AND ITS ANALYSIS

Since the experimental details have been adequately presented in earlier reports (1, 2), this report will concentrate on analysis of the data, which consists mainly of relative thermal fluxes as a function of horizontal distance from a single fuel rod immersed in heavy water in the MITR exponential facility. It has been verified experimentally (2) that the axial relaxation length in this system is independent of radius. Under the assumption that diffusion theory applies in the moderator, the equation describing the radial flux is:

$$\nabla_r^2\phi + (\gamma^2-\kappa^2)\phi + \eta\epsilon P \frac{J_{rod}}{D} G(r) = 0 \ , \qquad (7.1)$$

where:

$\phi(r)$ represents the radial flux dependence.

γ is the inverse axial relation length.

κ^2 is the inverse diffusion area of the moderator alone.

J_{rod} is the net neutron current into the fuel rod per unit length at the given height.

η is the neutron regeneration factor of the fuel rod (i.e., the number of fast neutrons produced directly per thermal absorption in the fuel rod including cladding). This depends on the spectrum of the thermal neutrons incident on the fuel rod, but the spectrum dependence is slight at thermal energies. The spectra both around the single fuel rod and in a lattice of such rods should be nearly Maxwellian, so that the single rod η will be nearly the same as the lattice η.

ϵ is the fast fission factor of the single fuel rod. This differs from the lattice ϵ by the omission of any interaction effect. Single rod δ_{28}'s have been measured for these rods by other workers at M.I.T. (3) and the ϵ's derived from such δ_{28} values can be used in Eq. 7.1.

P is the net escape probability from fast to thermal (i.e., the total number of neutrons slowing down to thermal at the given height per fast neutron born in the rod at the given height). This includes all neutron losses and gains in the slowing-down region below the fast fission threshold. These are radial out-leakage, net axial in-leakage, and resonance absorption in the single rod.

G(r) is the kernel giving the spatial (radial) distribution of neutrons slowing down to thermal, normalized so that

$$\int_A G(r)\, dA = 1 ,$$

where A is the cross-sectional area of the exponential assembly.

Three pieces of data are derived directly from this experiment. They are:

J_{rod} previously defined;

ϕ_o the value of the moderator flux, extrapolated to the center of the fuel rod; and

$(\eta\epsilon P)$ previously defined.

The values of J_{rod} and ϕ_o found are both relative values, but they both involve the same arbitrary constant and so their ratio,

$$\Gamma = \frac{\phi_o}{J_{rod}} ,$$

is uniquely determined. The quantity Γ was introduced in slightly different form by Galanin (4). The modification to the present conceptual definition in which ϕ_o is defined by using the moderator flux extrapolated to the rod center rather than the actual flux at the rod surface is due to Klahr (5, 6), who also gives experimental and theoretical evidence that Γ is independent of the spatial extent of the surrounding medium (i.e., independent of cell size). From Γ, one can infer the value of the thermal utilization in a lattice with any spacing of the same fuel rods in the same moderator, by using a formula given by Klahr (6) and derived by Galanin (4).

The data are analyzed by using an integrated form of Eq. 7.1:

$$-r\left(\frac{J_{rod}}{D}\right) + (\eta\epsilon P)\left(\frac{J_{rod}}{D}\right)\int_0^r dw \int_0^w 2\pi u G(u)\, du$$

$$= 2\pi \int_0^r \phi(w)\, dw - 2\pi r\phi(r) - 2\pi(\gamma^2-\kappa^2) \int_0^r dw \int_0^w u\phi(u)\, du\,. \qquad (7.2)$$

Equation 7.2 has been obtained from Eq. 7.1 by the following manipulations:

(1) Equation 7.1 was multiplied by the element of area $2\pi u\, du$ (in terms of the dummy variable u) before the first integration.

(2) The fuel rod has been replaced by a line source and sink at r = 0. The boundary condition here,

$$\lim_{\rho\to 0} 2\pi\rho \frac{d\phi}{d\rho} = \frac{J_{rod}}{D}\,,$$

was used in performing the first integration.

(3) The middle term on the right-hand side results from an integration by parts.

The doubly integrated form, Eq. 7.2, is used rather than Eq. 7.1 because Eq. 7.2 avoids the necessity for differentiating a set of discrete experimental data, always an error-prone operation.

Equation 7.2, with r equal to the radii at which the various measurements were made, is used to obtain $\left(\frac{J_{rod}}{D}\right)$ and $(\eta\epsilon P)\left(\frac{J_{rod}}{D}\right)$ by a least-squares fit to the data at the various radii. For this purpose, a computer program ONE-RØD has been written for the IBM 7094 at the M.I.T. Computation Center. The code calculates the right-hand side of Eq. 7.2 from the experimental data and uses the age theory line source kernel to evaluate the double integral on the left-hand side. Use of this computer program with data taken around a 1.01-inch-diameter, natural uranium rod indicates that a more exact kernel than that of age theory is desirable. The inexactness of the age theory kernel appears as a variation of $\eta\epsilon P$, depending upon the number and position of the data points used in the fit. However, values of J_{rod} appear to be fairly insensitive to the kernel used. Figure 7.1 shows how the output values of $\eta\epsilon P$ and $\frac{J_{rod}}{D}$ vary as the outermost radial data points are successively

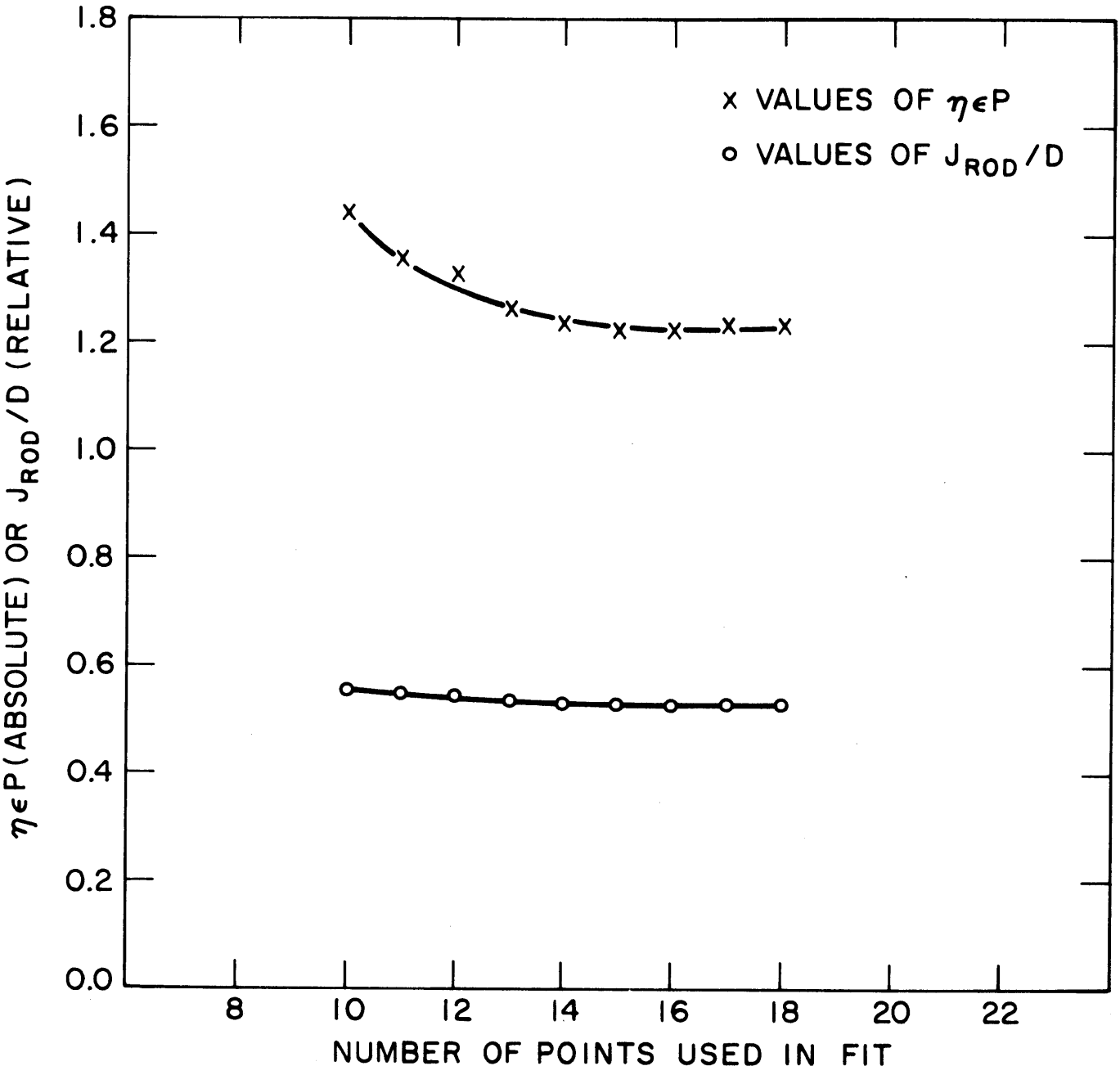

FIG. 7.1 VALUES OF $\eta\epsilon P$ AND J_{ROD}/D AS A FUNCTION OF THE NUMBER OF POINTS USED IN FITTING THE DATA (1.010 INCH DIAMETER NATURAL URANIUM ROD IN D_2O)

NOTE: THE NUMBER OF THE LAST POINT USED EQUALS THE NUMBER OF TOTAL POINTS USED. LOWER NUMBERS ARE NEARER TO ROD.

dropped to vary the number of points used in the fit. Work is in progress on finding, either experimentally or theoretically, a better kernel to use with the program.

The moderator flux extrapolated to the rod center, ϕ_o, is obtained by noting that if the measured activities are divided by $J_o(ar)$, the result is a linear function of r over a large range, which can thus be easily extrapolated to $r = 0$. The theoretical justification for this operation is the fact that the solution of Eq. 7.1 with the inner boundary condition previously given and the outer boundary condition,

$$\phi(R) = 0 \ ,$$

is of the form:

$$\phi(r) = J_o(ar)\, f_1(r) + Y_o(ar)\, f_2(r) \ .$$

It is found that for r not close to 0 or R,

$$|f_2(r)| \ll |f_1(r)| \ ,$$

$$|Y_o(ar)| \ll |J_o(ar)| \ ,$$

and that $f_1(r)$ is only a weak function of r. Thus, in the range considered,

$$\frac{\phi(r)}{J_o(ar)} = f_1(r) + \frac{Y_o(ar)}{J_o(ar)} f_2(r) \approx f_1(r) \ ,$$

and $f_1(r)$ is well represented here by a linear function. Figure 7.2 shows a typical plot of this kind.

2. PRELIMINARY RESULTS OF MEASUREMENTS AROUND A 1.010-INCH-DIAMETER, NATURAL URANIUM ROD

The characteristics of the rod are described in Ref. 7.

Analysis of the data by the methods just described gave the results shown in Table 7.1. Lattice thermal utilizations have been computed from Γ by using the formula given by Klahr. Aside from Γ and geometric dimensions, this formula requires values of the heavy water absorption cross section in the various lattices. Two sets of cross sections have been used; the first set was obtained by Brown (8) from

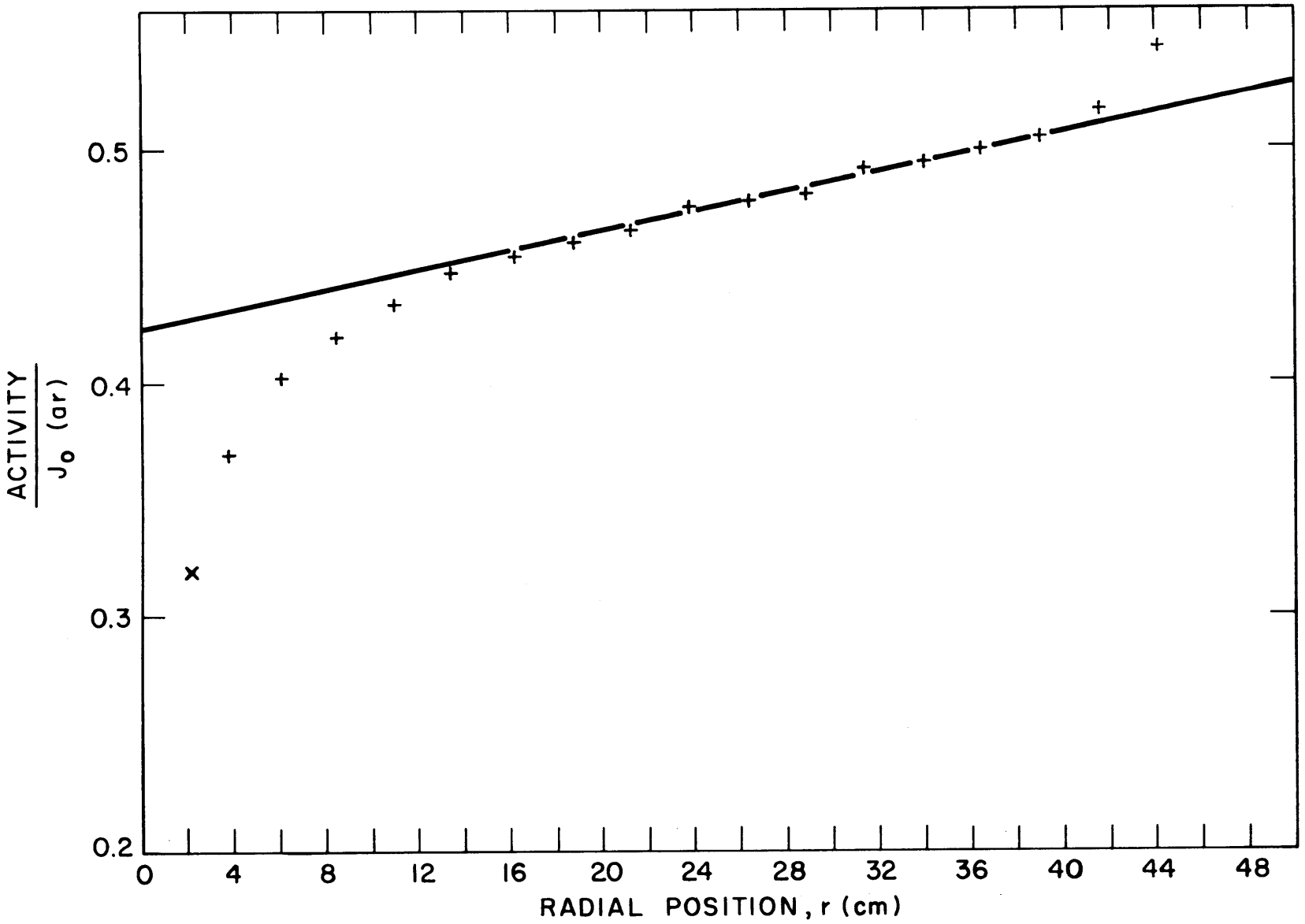

FIG. 7.2 ACTIVITY DIVIDED BY $J_0(ar)$ AS A FUNCTION OF RADIAL POSITION (1.010 INCH DIAMETER NATURAL URANIUM ROD IN D_2O)

TABLE 7.1
Natural Uranium, Single Rod Results

Quantity	Value	Source
ϕ_o	0.424	Fit to the linear portion of Fig. 7.1
J_{rod}	0.440	Computer program ØNE-ROD
Γ	0.964	Ratio of ϕ_o to J_{rod}

THERMØS code (9) calculations for the various lattices, and the second set is derived simply on the assumption that the spectrum is a hardened Maxwellian with an effective temperature 40°C above the moderator temperature of 20°C. Table 7.2 compares the values of f and 1 - f so obtained with the experimental values obtained by Brown (8). (In conformance with the previous definition of η, the thermal utilizations reported include the cladding as part of the fuel.) It is seen that not only do both sets of cross sections yield accurate values of f, but that even the values of 1 - f are in error by no more than 10%.

3. PRESENT WORK

Work is continuing on the attempt to find a more accurate line source slowing-down kernel. The problem of computing or measuring P is being considered. Data obtained from similar measurements around 1.027% and 1.143% enriched uranium rods of 0.25-inch diameter are now being analyzed.

TABLE 7.2

Lattice Thermal Utilizations Deduced from the Single Rod Experiment

Spacing (inches)	f (exptl.)	f From Γ and Brown's Σ's	f From Γ and Maxwellian Σ's	1 - f (exptl.)	1 - f From Γ and Brown's Σ's	1 - f From Γ and Maxwellian Σ's
4.5	0.9912	0.9919	0.9908	0.0088	0.0081	0.0092
5.0	0.9890	0.9897	0.9885	0.0110	0.0103	0.0115
5.75	0.9847	0.9861	0.9845	0.0153	0.0139	0.0155

4. REFERENCES

(1) "Heavy Water Lattice Project Annual Report," NYO-10212 (MITNE-46), September 30, 1963.

(2) "Heavy Water Lattice Project Annual Report," MIT-2344-3 (MITNE-60), September 30, 1964.

(3) Papay, L. T., "Fast Neutron Fission Effect for Single Slightly Enriched Uranium Rods in Air and Heavy Water," M.S. Thesis, M.I.T. Nuclear Engineering Department, June 1964.

(4) Galanin, A. D., "Thermal Coefficient in a Heterogeneous Reactor," P/666, PICG, 1955.

(5) Klahr, C. N., et al.,"Heterogeneous Reactor Calculation Methods," NYO-2680, June 1961.

(6) Klahr, C. N., et al., "Test and Verification of Heterogeneous Reactor Calculation Methods," NYO-3194-1, August 1964.

(7) Kaplan, I., D. D. Lanning, A. E. Profio, and T. J. Thompson, "Summary Report on Heavy Water, Natural Uranium Lattice Research," NYO-10209 (MITNE-35), July 1963.

(8) Brown, P. S., T. J. Thompson, I. Kaplan, and A. E. Profio, "Measurements of the Spatial and Energy Distributions of Thermal Neutrons in Uranium Heavy Water Lattices," NYO-10205 (MITNE-17), August 1962.

(9) Honeck, H. C., "THERMØS, A Thermalization Transport Theory Code for Reactor Lattice Calculations," BNL-5826, September 1961.

8. TWO-REGION LATTICES

J. Gosnell

The economic advantages of using a two-region assembly to investigate properties of a small central test region have often been discussed and do not need to be repeated here. As part of the M.I.T. Lattice Research Program, studies are being made to determine the validity of measurements made with such test regions.

1. ASSEMBLIES STUDIED

The flexibility of the M.I.T. lattice facility and the availability of several types of fuel rods allow examination of the effects of test region size, and differences in enrichment, rod diameter and pitch between the two regions. The assemblies chosen to isolate and examine each of these effects are listed in Table 8.1.

Experimental data from the first four assemblies were presented in the previous annual reports (1). The data on Assemblies V through VIII will be discussed in this report.

2. GOLD-CADMIUM RATIOS

Gold-cadmium ratios have been measured as a function of radius in each of the assemblies studied. These traverses provide an indication of spectral changes throughout both regions and of the approach to spectral equilibrium in the center of the test region.

In all cases, 0.125-inch-diameter, 0.010-inch-thick, gold foils were used and the traverses run on a chord passing through the center cell. Four traverses, two with bare foils and two with cadmium-covered foils, were run in each assembly. Since the foil holders employed are symmetrical, the cadmium ratio at each position is the average of four measurements. In most cases, the standard deviation of the mean was less than 1%.

Assemblies V and VI are similar in composition to Assemblies I and III, previously reported (1), differing only in fuel enrichment

TABLE 8.1

Two-Region Assemblies Tested in the M.I.T. Lattice Facility

Assembly Designation	Properties Common to Both Regions	Outer Reference Region	Inner Test Region
I	0.25-in.-diameter, 1.027% U-235 fuel	1.25-in. pitch	2 rings* - 2.50-in. pitch
II	0.25-in.-diameter, 1.027% U-235 fuel	1.25-in. pitch	3 rings - 2.50-in. pitch
III	0.25-in.-diameter, 1.027% U-235 fuel	1.25-in. pitch	4 rings - 2.50-in. pitch
IV	0.25-in.-diameter, 1.027% U-235 fuel	2.50-in. pitch	6 rings - 1.25-in. pitch
V	0.25-in.-diameter, 1.143% U-235 fuel	1.25-in. pitch	2 rings - 2.50-in. pitch
VI	0.25-in.-diameter, 1.143% U-235 fuel	1.25-in. pitch	4 rings - 2.50-in. pitch
VII	0.25-in.-diameter, 1.75-in. pitch	1.143% U-235 fuel	3 rings - 1.027% U-235 fuel
VIII	0.25-in.-diameter, 1.75-in. pitch	1.143% U-235 fuel	5 rings - 1.027% U-235 fuel
IX	2.50-in. pitch	0.25-in.-diameter, 1.027% U-235 fuel	4 rings - 0.75-in. diameter, 0.947% U-235 fuel
X	2.50-in. pitch	0.25-in.-diameter, 1.027% U-235 fuel	2 rings - 0.75-in.-diameter, 0.947% U-235 fuel
The above lattices have already been examined; the last remaining experiment proposed is:			
XI	5.00-in. pitch	0.75-in.-diameter, 0.947% U-235 fuel	2 rings - 1.0-in.-diameter, natural uranium fuel

*Rings about the central rod.

(1.143% vs. 1.027% U^{235}). The results for Assemblies V and VI are shown in Figs. 8.1 and 8.2. Figure 8.2 also shows the results reported previously for Assembly III. As expected, the spatial dependence of the cadmium ratio is quite similar for these two cases. In Assembly V, the full lattice value of the cadmium ratio is not reached in the test region, but within the larger test region of Assembly VI, the full lattice value is even slightly exceeded. The epicadmium and subcadmium components of the activities in Assembly VI are shown in Fig. 8.3.

The regions in Assemblies VII and VIII differ only (and slightly) in enrichment; the rod size and lattice pitch are the same. A slight decrease in cadmium ratio is observed between the 1.027% test regions and the 1.143% reference regions. The effect is, however, quite small, as can be seen in Figs. 8.4 and 8.5.

Assemblies IX and X were constructed with 0.25-inch-diameter, 1.027% enriched U^{235} rods in the test region and 0.75-inch-diameter, 0.947% enriched U^{235} fuel in the reference region. The cadmium ratios are shown in Figs. 8.6 and 8.7. In Assembly IX, the cadmium ratio in the first foil position has reached 98% of the full lattice value.

3. U^{238} CADMIUM RATIOS AND δ_{28} MEASUREMENTS

Measurements of R_{28}, the cadmium ratio of U^{238}, and of δ_{28}, the ratio of fissions in U^{238} to fissions in U^{235}, have been made in the central position of each assembly and, in some cases, as a function of radius as well. The data are being analyzed at the present time and will be reported later.

4. AXIAL RELAXATION LENGTHS

Bare gold axial traverses were made in the center position and in rings 3 and 8 of Assembly V. The ratio of the foil activity in each of these outer positions to the corresponding center traverse activity is shown in Fig. 8.8. From these results, together with previously reported experiments on Assemblies II, III and IV, it is concluded that the axial relaxation length is constant over the radius of the assembly. Thus, in the later assemblies, axial traverses were measured only in the center position, where the irradiation time required to achieve a given foil activity is lowest.

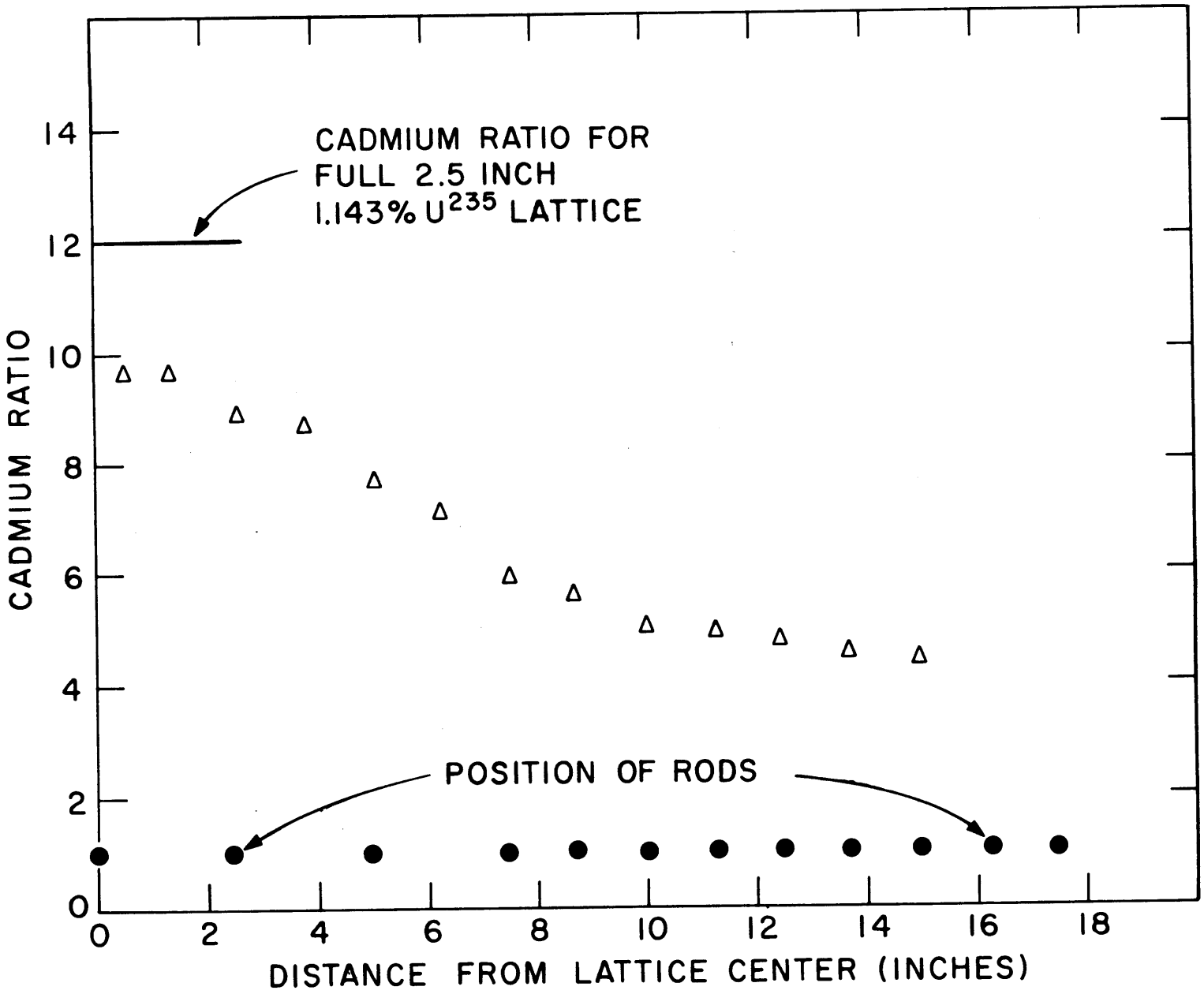

FIG. 8.1 GOLD CADMIUM RATIOS IN ASSEMBLY V

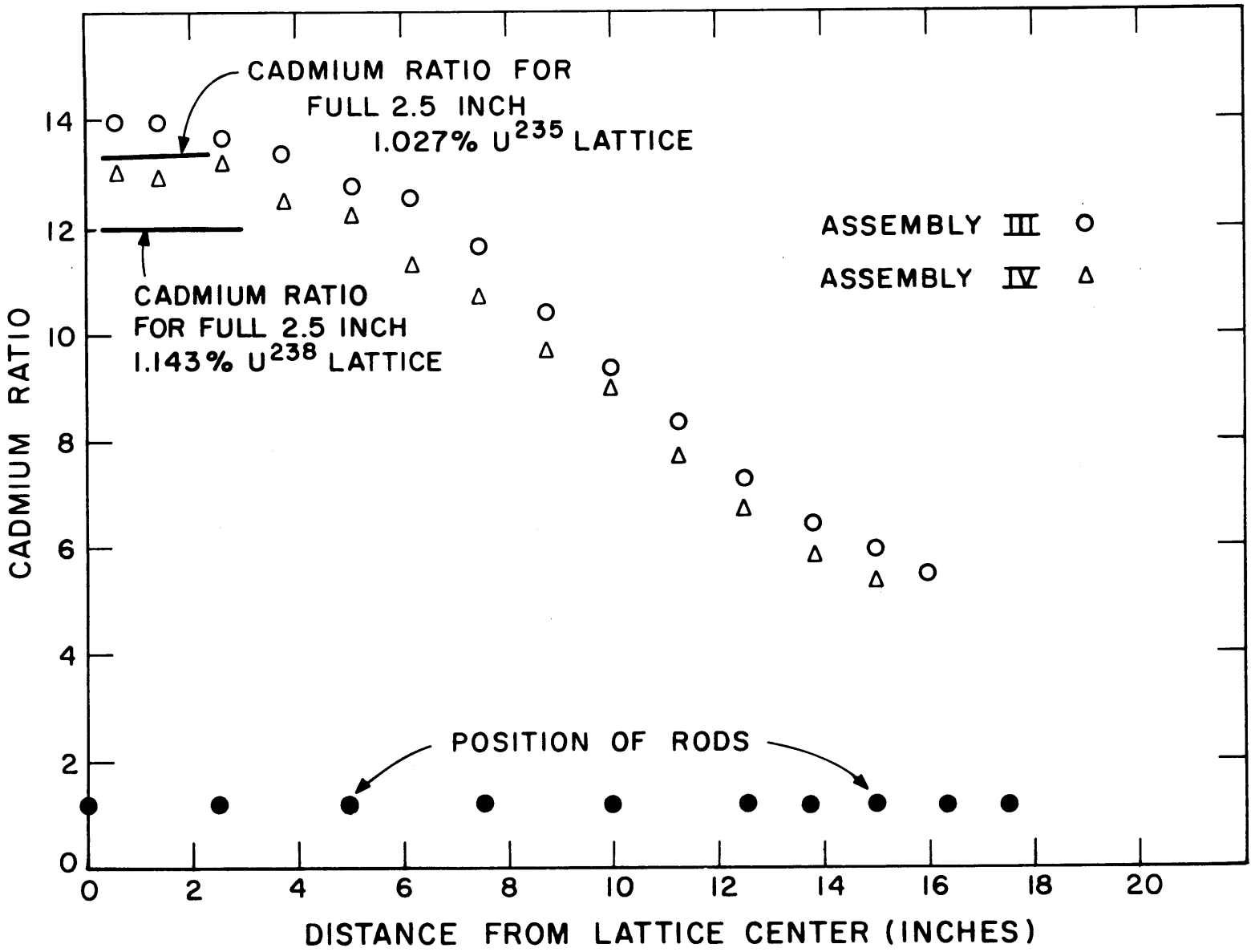

FIG. 8.2 GOLD CADMIUM RATIOS IN ASSEMBLIES III AND VI.
(AVERAGE STATISTICAL ERROR ~ 1%)

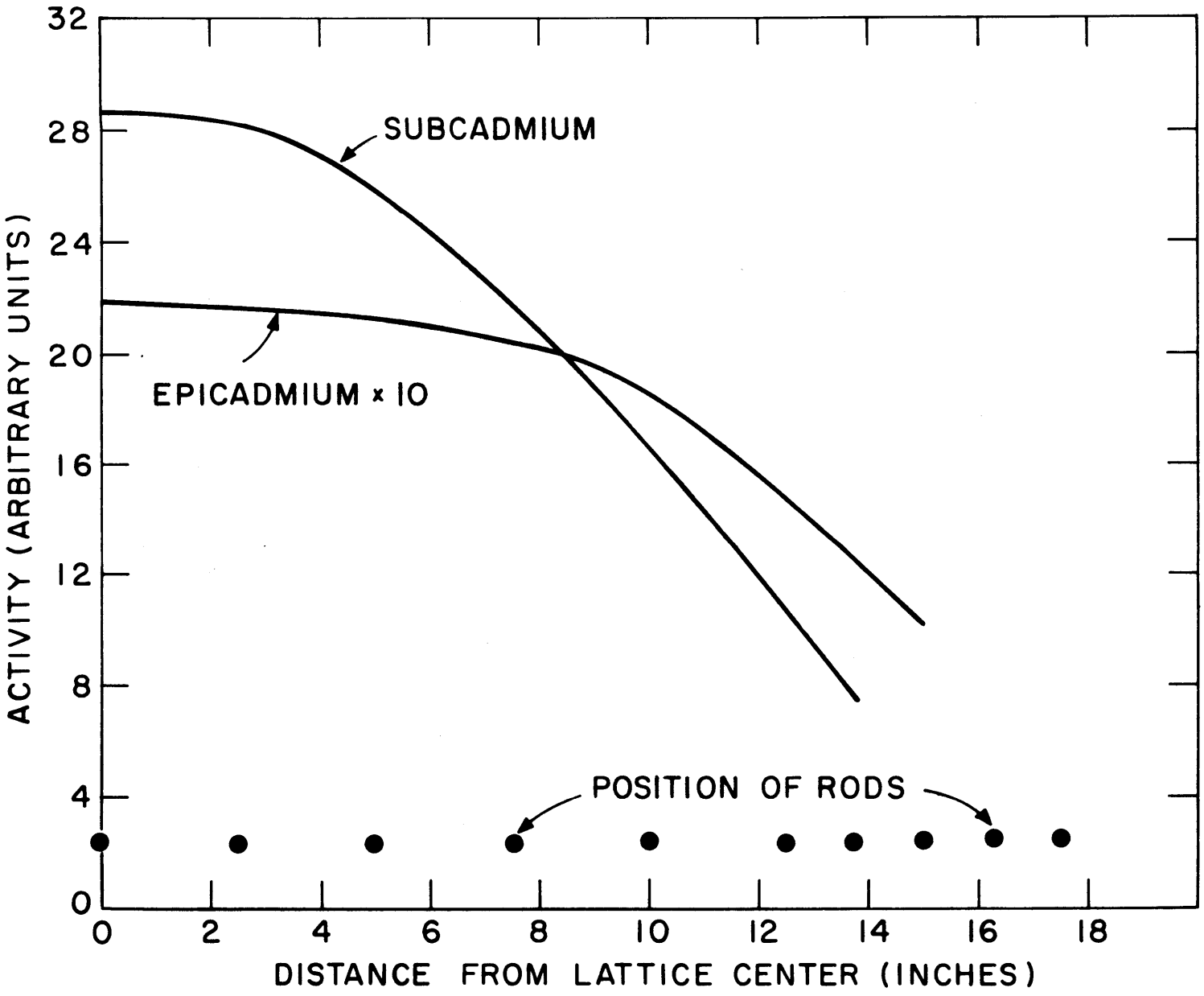

FIG. 8.3 GOLD FOIL ACTIVITIES IN ASSEMBLY VI

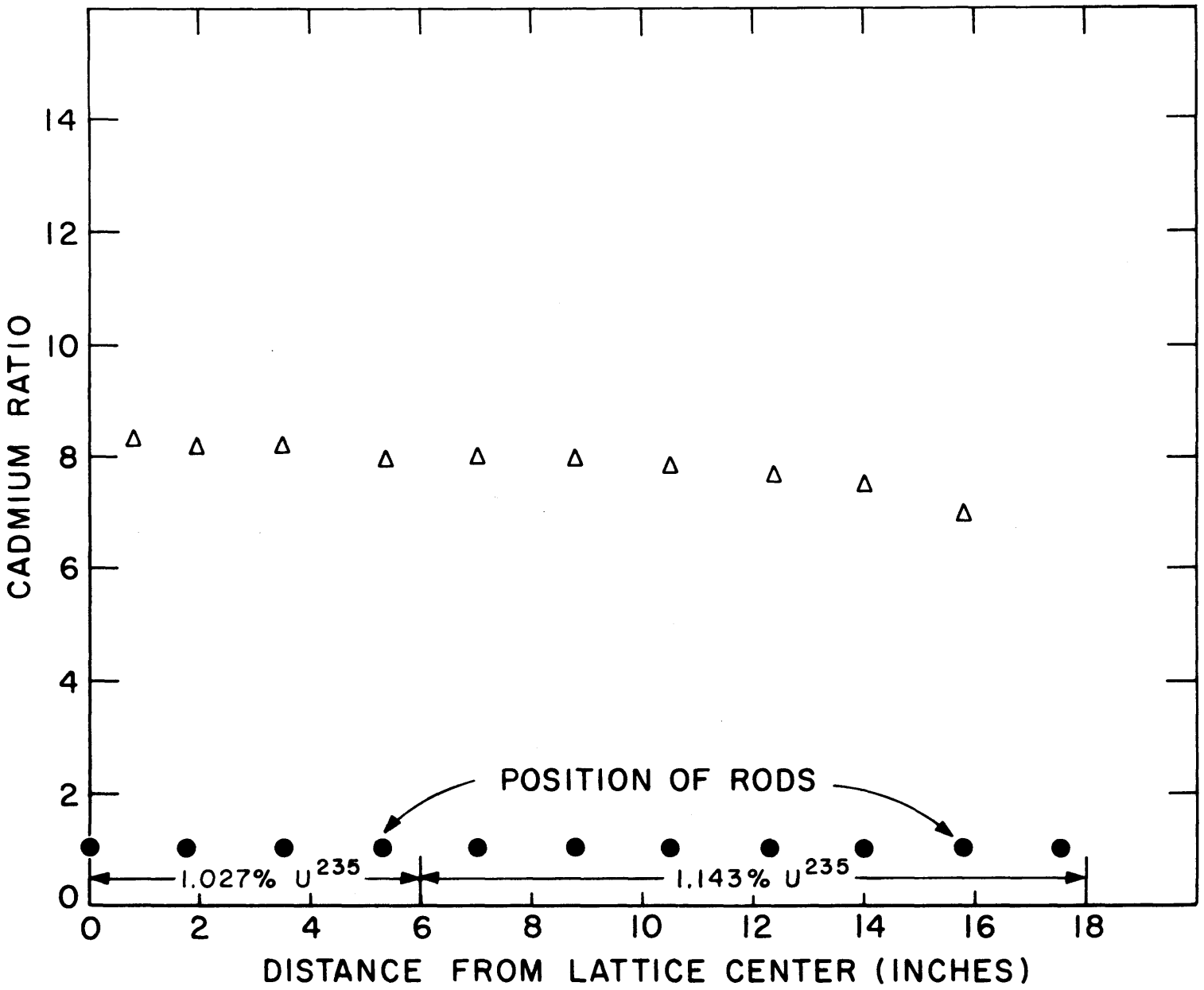

FIG. 8.4 GOLD CADMIUM RATIOS IN ASSEMBLY VII

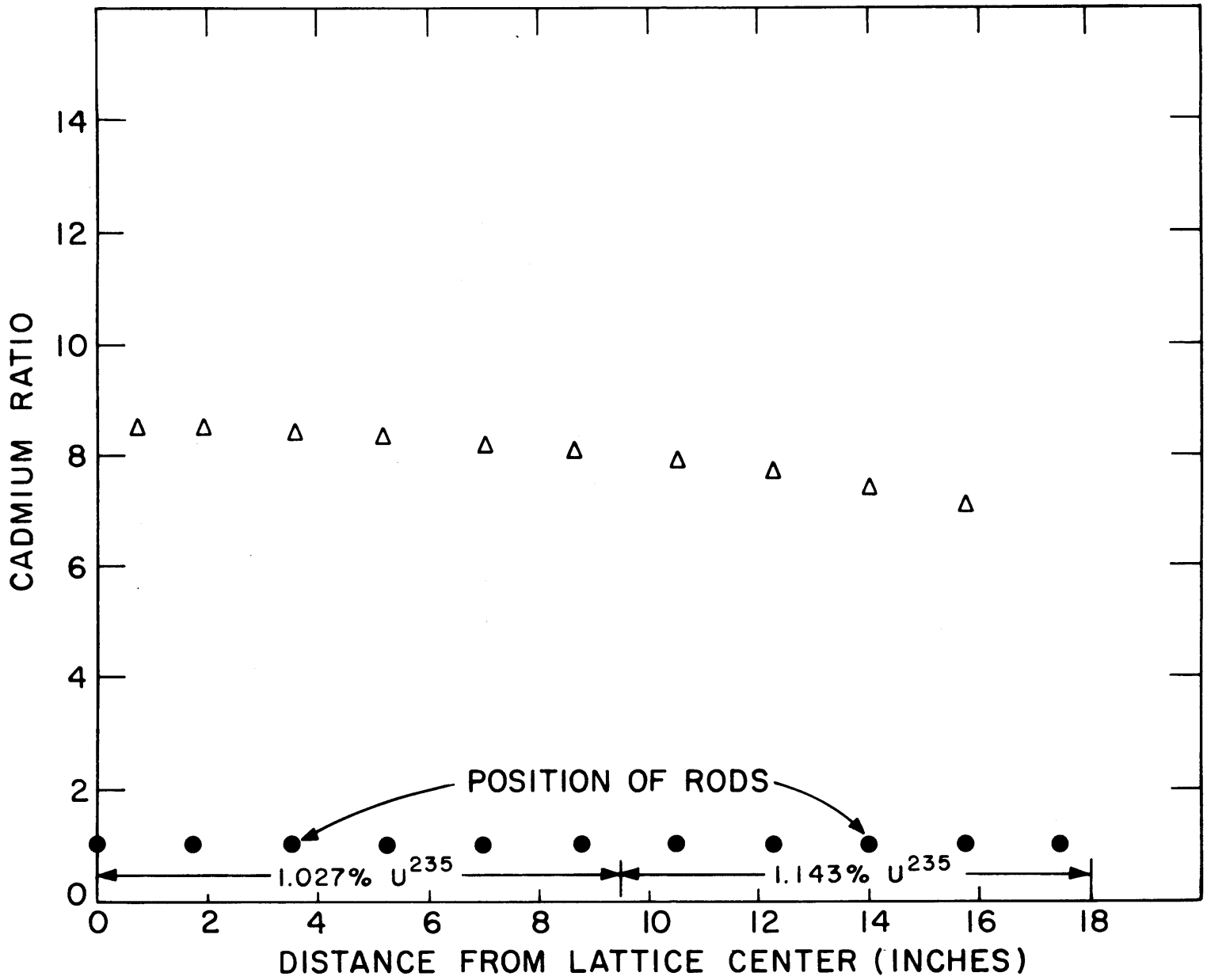

FIG. 8.5 GOLD CADMIUM RATIOS IN ASSEMBLY VIII

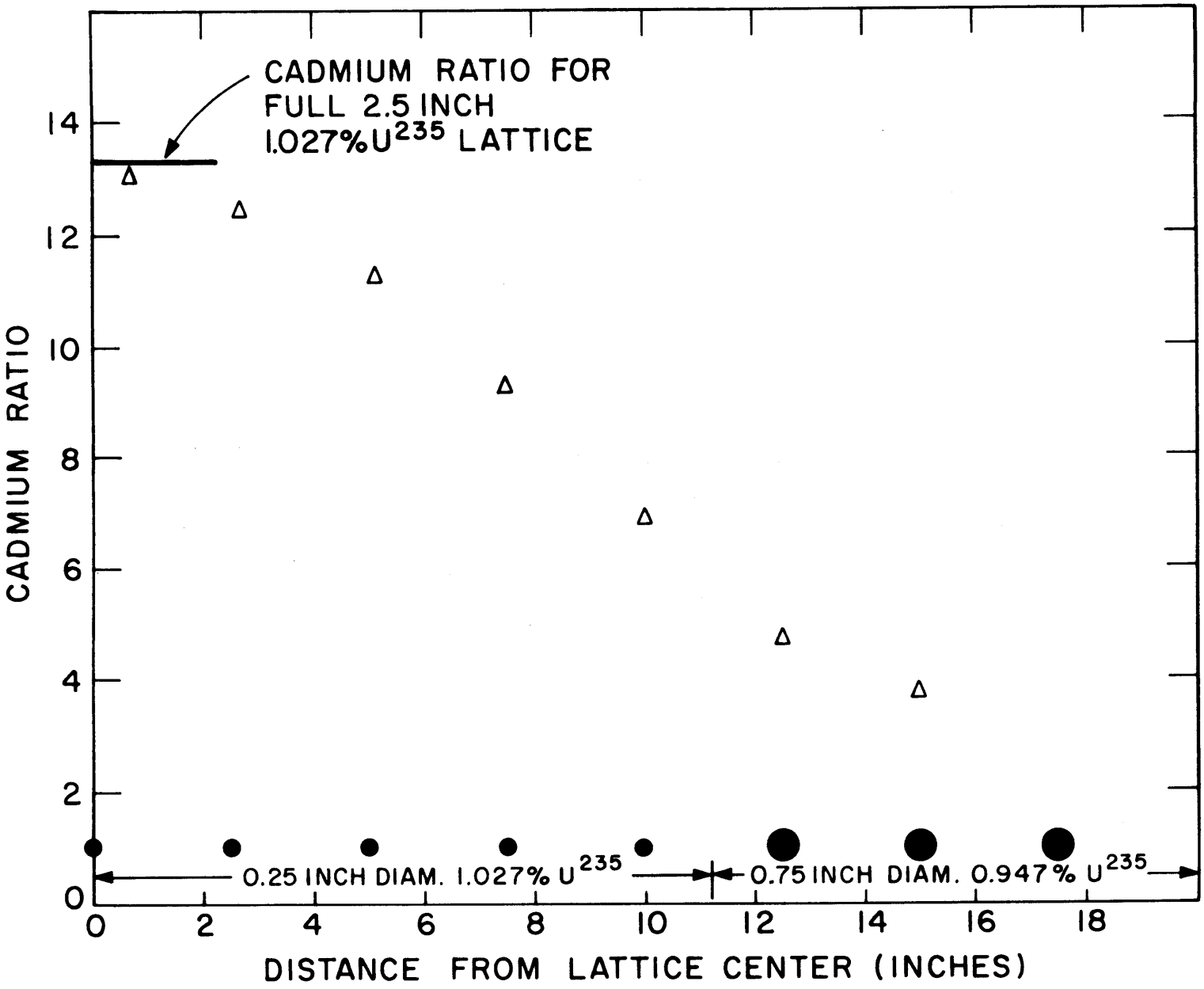

FIG. 8.6 GOLD CADMIUM RATIOS IN ASSEMBLY IX

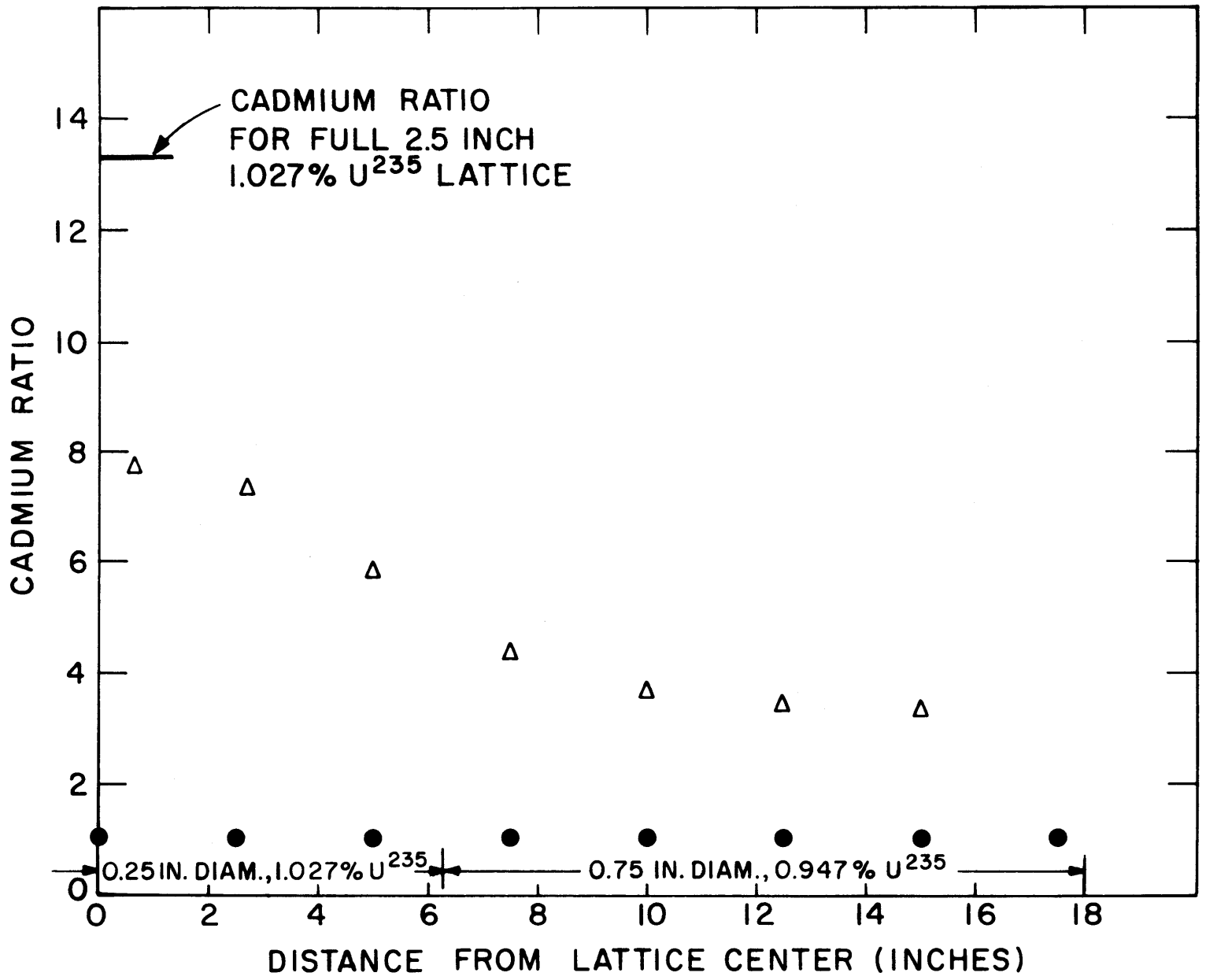

FIG. 8.7 GOLD CADMIUM RATIOS IN ASSEMBLY X

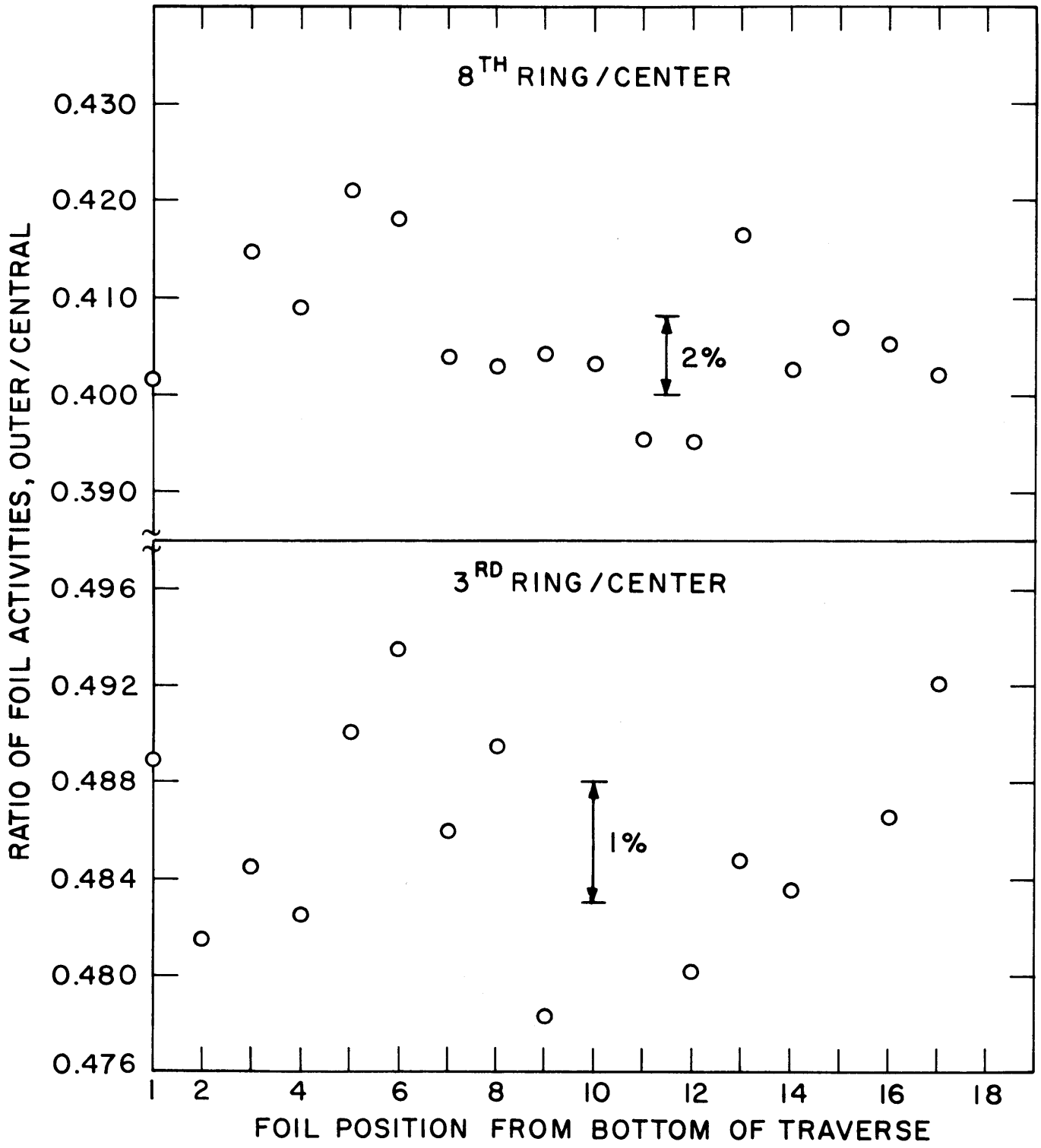

FIG. 8.8 RATIO OF AXIAL FOIL ACTIVITIES IN ASSEMBLY V AS A FUNCTION OF HEIGHT. (FIRST FOIL POSITION 22CM. ABOVE BOTTOM OF FUEL; FOIL POSITIONS ARE 2.0 INCHES APART)

TABLE 8.2

Axial Relaxation Lengths in Two-Region Assemblies

Assembly Designation	Axial Relaxation Length ($cm^{-2} \times 10^{-6}$)
V	991
VI	1112
VII	1006
VIII	1069
IX	1178
X	1200

Axial relaxation lengths were determined for each of the assemblies by least-squares fit of the appropriate foil activity traverses. The results are presented in Table 8.2. The uncertainty in these values is about $\pm$ 25 $\times 10^{-6}$ cm^{-2}.

5. MATERIAL BUCKLING

A model based on two-group diffusion theory is being developed to interpret the experimental data. Several approaches are being tried with the prime objective being to minimize the use of nonexperimental parameters; ideally, we would like to employ only the experimental radial and axial traverse data.

As noted earlier, eight assemblies have been studied to date and work is about to begin on the ninth. Data analysis is continuing, and it is expected that final results will be issued as a Sc.D. thesis and topical report during the next annual report period.

6. REFERENCES

(1) "Heavy Water Lattice Project Annual Report," MIT-2344-3 (MITNE-60), September 30, 1964.

9. OSCILLATING NEUTRON SOURCE EXPERIMENT

E. Sefchovich

1. INTRODUCTION

In reactor physics studies of lattices, the material buckling and diffusion coefficient have played an important role because of their relation to the diffusing and multiplying properties of the medium under consideration. Great emphasis has therefore been given to their accurate measurement.

The foil activation technique is the oldest and most widely used method for measuring buckling. The material buckling is determined from the flux distribution measured in exponential assemblies by means of the activation of suitably chosen foils. This is the so-called stationary method. This technique has, however, the disadvantages and inaccuracies normally encountered in all foil activation measurements. A large effort, however, has gone into reducing these inaccuracies and good results ($\pm 0.5\%$) are attainable (1).

In recent years, the pulsed neutron technique has been widely investigated. The pertinent theory has been described in the literature (2). In essence, the procedure is to introduce a pulse $\delta(t)$ at $t = 0$ and observe its decay in time at a given position in the assembly. The decay constant, λ, which is related to the geometric buckling and nuclear properties of the system, is then measured. The material buckling is obtained by repeating the measurement for different geometric bucklings and extrapolating to $\lambda = 0$, in which case the system is critical and the geometric buckling equals the material buckling. This technique has the advantage that, in addition to the buckling, the diffusion coefficient and cross sections can be obtained simultaneously. The main drawback lies in the difficulties inherent in varying the geometric buckling.

An alternative to the pulsed source method is the use of sinusoidal modulation. When a periodically varying neutron source is introduced into a medium, the time behavior of the neutron flux at any point in the medium also varies periodically with the source frequency. The flux

will, however, lag behind the source because of the finite time it takes neutrons to travel from the source to the point of interest. The amplitude of the neutron wave will also be attenuated because of the absorption and leakage of neutrons. Because the phase lag and the relaxation length of the amplitude of the wave depend on the nuclear properties of the system, their measurement can be used to determine the buckling and diffusion coefficient. A detailed mathematical derivation of the buckling and diffusion coefficient in terms of the phase change and relaxation length is given, in Ref. 3, in the one-group diffusion approximation. Perez and Uhrig (4) have extended the theory to include thermalization effects. DiPasquantonio (5) considered the problem in relation to the one-group Boltzman equation in the consistent P-1 approximation which leads to the Telegrapher's equation. In principle, this technique has the advantage that neither foil counting nor geometric buckling changes are involved.

Foil activation and pulsed neutron techniques are now used in M.I.T. lattice research. As a possible prelude to use of neutron wave techniques as well, an oscillator was built by Laurence E. Demick (6) to modulate the beam in the Medical Therapy Facility at the M.I.T. Reactor in a sinusoidal manner. The oscillator is described in more detail in the 1964 M.I.T. Heavy Water Lattice Project Annual Report (7). This section will report further on the evaluation being made of the method and the equipment.

2. SUMMARY OF RECENT EXPERIMENTAL WORK

During the early part of the present year, work was directed toward use of small surface-barrier detectors. It was found that use of a fully enriched U^{235} neutron converter would permit adequate discrimination against the inherent noise of the semiconductors. The semiconductors gave reproducible results as long as the total exposure was kept below a nvt of about 3×10^{12} n/cm^2.

However, studies showed that the rotary-type oscillator described in Ref. 7, because of its very nature, causes a lateral oscillation in the otherwise sinusoidal beam which is incident on the system being studied. This required that detectors having a larger lateral dimension be used

to average-out the effects of the lateral oscillations. The small surface-barrier detectors were therefore replaced by a BF_3 detector of larger size. This solved the problem, although the attenuation observed in the amplitude of the signal was greater than expected. The cause of this attenuation is currently under consideration.

3. DISCUSSION

In the present work, several problems became apparent which were not foreseen at the time the neutron source oscillator was designed and built.

The most prominent problem is that of the spatial variation of the transmitted flux. Ideally, an experiment of this type calls for a constant-area source transmitting a variable-intensity neutron beam. The present device, instead, varies the area through which a fixed intensity beam is transmitted. This gives rise to the spatial variation observed.

A constant-area source can indeed be obtained, although probably not by mechanical means. An accelerator can be altered to give a sinusoidal output, as has been done, for example, at the University of Florida(8). As the accelerator produces high energy neutrons, one must be careful, however, to properly account for their slowing down.

Alternatively, one could try to minimize the spatial effect and still use a mechanical device. It does not appear possible to accomplish much by using a single cylindrical rotor; instead, a device such as that shown in Fig. 9.1 appears to have possibilities. Instead of rotating one cylinder, an array of many small cylinders would be used. All cylinders must be synchronized so that their cadmium sectors, which cover one-quarter of the circumferential area, are at the same angular position at the same time. As shown in Fig. 9.1, each cylinder would tend to compensate for the pulse distortion introduced by its immediate neighbor.

It is considered that this study has laid the groundwork for future construction of an effective mechanical oscillator, should this become desirable.

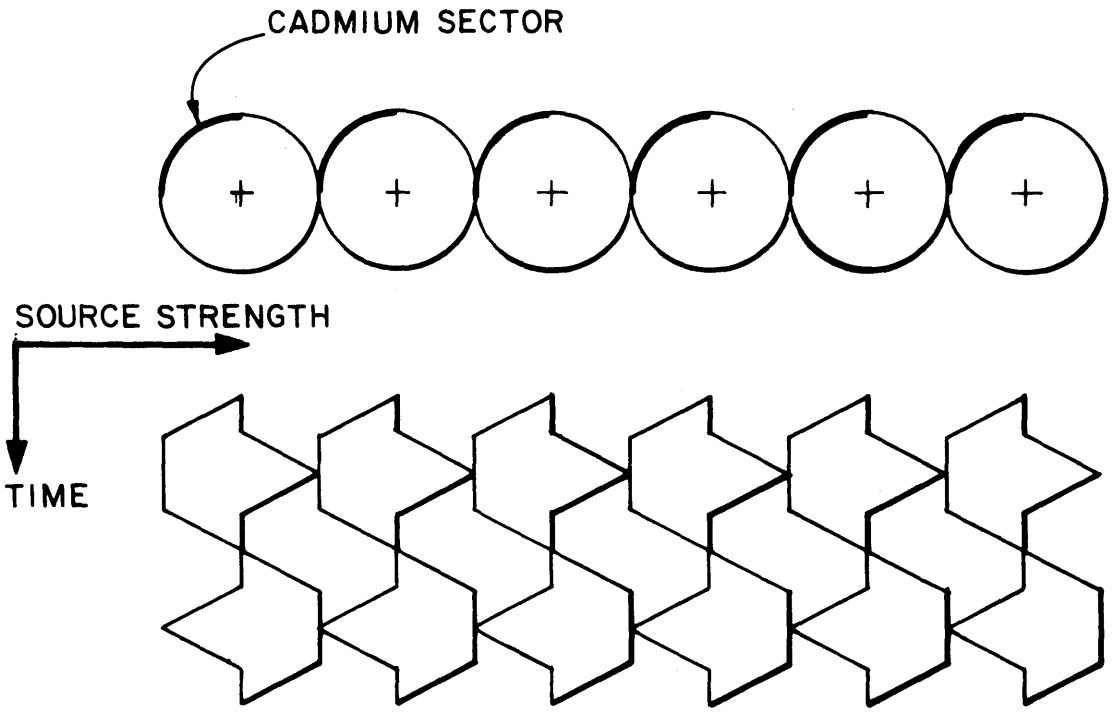

FIG. 9.1 IMPROVED CONFIGURATION SUGGESTED FOR A NEUTRON SOURCE OSCILLATOR

4. REFERENCES

(1) Palmedo, P. F., I. Kaplan, and T. J. Thompson, "Measurements of the Material Bucklings of Lattices of Natural Uranium Rods in D_2O," NYO-9660 (MITNE-13), January 1962.

(2) Isbin, H. S., Introductory Nuclear Reactor Theory, Reinhold Chemical Engineering Series, Chap. 9, 1963.

(3) Sefchovich, E., "Research with Miniature Lattices," in "Heavy Water Lattice Project Annual Report," NYO-10212 (MITNE-46), pp. 90-94, September 30, 1963.

(4) Perez, R. B., and R. E. Uhrig, "Propagation of Neutron Waves in Moderating Media," Nuclear Sci. and Eng., 17, pp. 90-100, 1963.

(5) DiPasquantonio, F., "Propagation of Monokinetic Neutron Waves in Dissipative Media," Energia Nucleare, 11 (9), 465, September 1964.

(6) Demick, L. E., "Modulation of a Thermal Neutron Beam," B.S. Thesis, M.I.T. Physics Department, 1963.

(7) Sefchovich, E., "Oscillating Neutron Source Experiment," in "Heavy Water Lattice Project Annual Report," MIT-2344-3 (MITNE-60), pp. 137-154, September 30, 1964.

(8) Uhrig, R. E., "Neutron Waves in a Subcritical Assembly," TID-7619, Proc. Univ. Conf. on Subcritical Assemblies, 1962.

10. MINIATURE LATTICE STUDIES

E. Sefchovich

The study of very small subcritical assemblies is of considerable practical interest because, if they can provide results of use in the design of full-scale reactor lattices, they offer a potentially large saving in cost and an increase in flexibility over larger subcritical or critical facilities. In order to establish their utility, it is necessary to show that they can provide reactor physics data comparable to that of the larger assemblies.

Earlier research in this area has produced useful results. Kouts and co-workers (1, 2) have studied the application of small lattices to light water moderated, slightly enriched uranium lattices. Their measurements included quantities related to ϵ, p and f. C. Wikdahl and F. Akerhielm (3) in Sweden obtained encouraging results for disadvantage factors in clusters and in single-rod assemblies. A more general study was carried out at M.I.T. by J. C. Peak (4). His investigation included the study of nine different lattices involving three different D_2O-H_2O mixtures, from about 80 to about 99 mole per cent D_2O, and three moderator-to-fuel volume ratios, namely, 12, 20.8 and 30. Peak also developed a theoretical model based on age-diffusion theory to extrapolate his results to critical assemblies.

The objective of the present study is to refine and extend the applicability of miniature lattice work. The present miniature lattice investigation will study lattices similar to those tested in the large exponential facility so that a definitive comparison of results can be made. The lattices to be studied are shown in Table 10.1. This research will include the measurement of macroscopic radial and axial gold traverses, microscopic intracell gold traverses, δ_{28}, ρ_{28}, δ_{25}, and C^*.

In the present report, we shall examine in some detail the problems which are encountered in using the miniature lattice, both

theoretically and experimentally. Some preliminary experimental results will also be presented.

TABLE 10.1

Lattices to be Studied

Fuel Rod Diameter (inches)	Fuel Enrichment (%)	Moderator	Lattice Pitch (inches)
0.25	1.143	D_2O	1.25
"	"	"	1.75
"	"	"	2.50
"	1.027	"	1.25
"	"	"	1.75
"	"	"	2.50

1. EXPERIMENTAL FACILITY

The small exponential tank is a right circular cylinder fabricated of 1/16-inch-thick aluminum, 21 inches high and 20 inches in diameter, with a removable 1/2-inch-thick aluminum base plate. The tank is equipped with a wheeled stand to provide mobility, plus appropriate piping to allow filling and draining. The fuel elements employed are 16-inch-long rods, and the required lattice spacings are obtained through the use of different grid plates. Figure 10.1 shows a sketch of the assembly.

The shielding consists of successive laminae of 1/4-inch borated plastic, 3 inches of paraffin, a layer of cadmium, and another 3 inches of paraffin. The shielding is completely lined with cadmium to minimize the reflection of neutrons back into the lattice. The tank, itself, is surrounded on sides and bottom by cadmium to approximate as closely as possible a bare assembly.

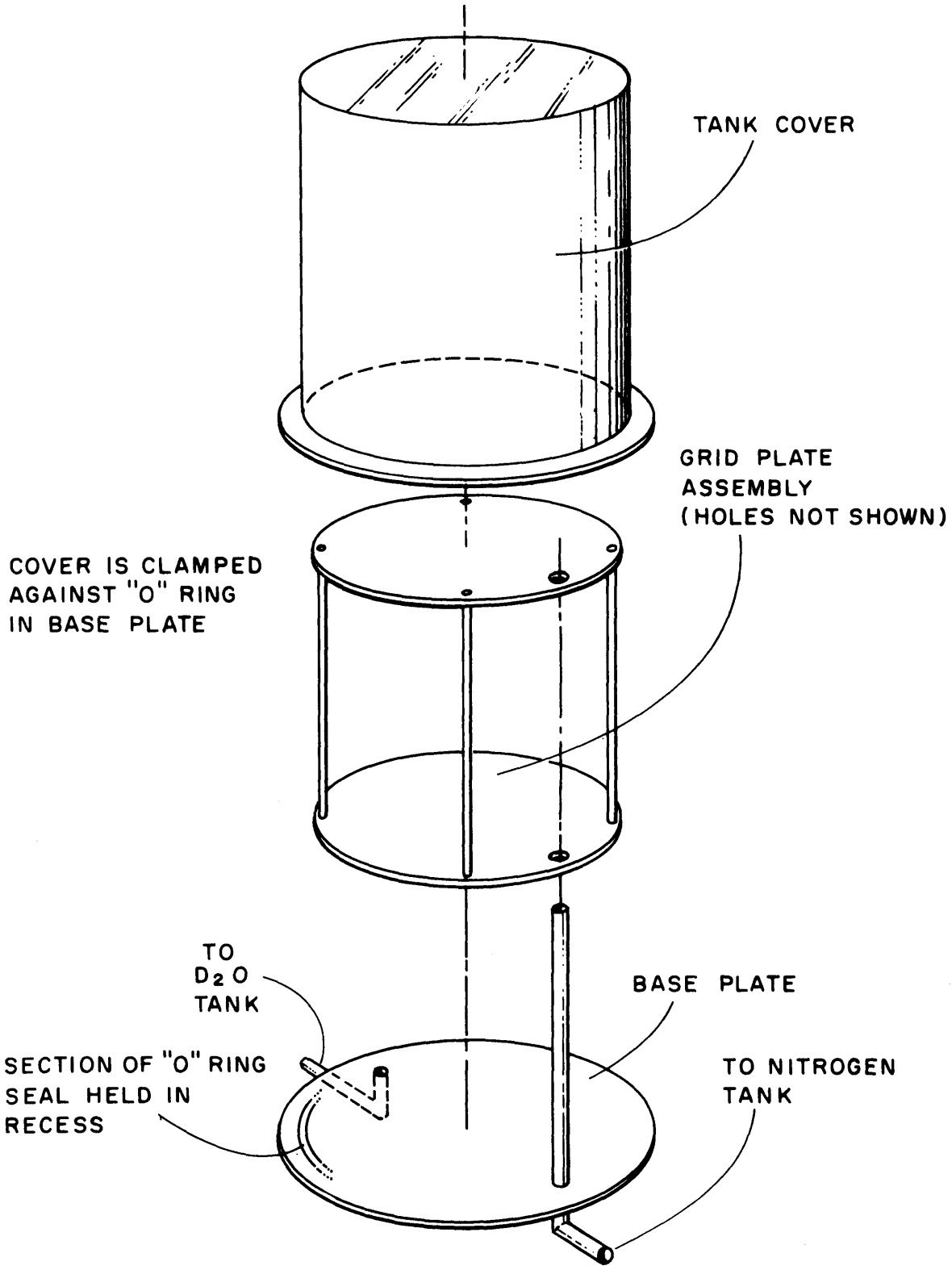

FIG. 10-1 SCHEMATIC OF THE M.I.T.
SMALL EXPONENTIAL ASSEMBLY

2. EXPERIMENTAL WORK

2.1 Experimental Techniques

One objective of the present study is to improve upon the techniques employed by Peak (4). Since the time of his research, much work at the M.I.T. Lattice Project has been devoted (5) to improving the accuracy of techniques for the measurement of lattice parameters. Thus, in the present work, axial and radial traverses are done according to the procedure of Palmedo (6), as improved by Harrington (7). Intracell measurements are made with the methods developed by Simms (8); and for δ_{28}, ρ_{28}, δ_{25} and C^*, the techniques developed by D'Ardenne (9) are used. In order to confirm the applicability of the preceding techniques to miniature lattice work, a complete set of measurements was made in a lattice duplicating the last lattice investigated by Peak: 1.143% enriched fuel, moderated by 80.2 mol% D_2O with a 0.880-inch lattice pitch. In brief, the results proved both that Peak's measurements were reproducible and that the present techniques gave the same results within experimental uncertainties. Several problems were encountered, however, which required modifications in the experimental design and procedures. For example, it was found that a layer of cadmium had to be placed around the tank and as much of the facility environment as possible because the laminated plastic shielding alone did not adequately prevent thermal neutron reflection back into the lattice. The final over-all arrangement has already been described in the preceding section.

2.2 Source Experiments

In interpreting measurements in the miniature lattice, it is necessary to take into account the presence of radial and axial harmonics in the flux shape. Hence, it is convenient to eliminate as many harmonic components as possible. Little can be done to remove axial harmonics. But, if we use a neutron source whose radial distribution is the same as the fundamental mode J_o function, we can in theory eliminate higher radial harmonics. An even more basic prerequisite is that the source be radially symmetric about the assembly centerline. From previous

experience (10), however, there was evidence that the source was asymmetric. Since the reactor core centerline is about 4 inches off center with respect to the medical beam port centerline, a certain asymmetry is, in fact, to be expected.

A series of experiments was undertaken to study and correct the radial and angular distribution of the source. An aluminum foil holder was built to position foils at 40 successive radial positions in a spiral pattern. The foil holder was then placed on top of the miniature lattice tank, aligned with the centerline of the neutron beam port, and irradiated.

Based on the results of this experiment, a series of steps was taken to improve the symmetry and to achieve a closer fit to a J_o function by placing aluminum discs of various sizes together with pieces of lucite in the collimator.

2.3 Preliminary Experimental Results

Before the study of the source just described, a series of measurements was made in a lattice constructed of 0.25-inch-diameter, 1.143% enriched fuel in a 1.25-inch pitch. This lattice is directly comparable to a similar lattice previously studied in the large exponential facility. Some preliminary experimental results are available and compare favorably with those obtained in the large lattice.

The first set of measurements on the above test lattice included axial and radial gold activity distributions, both subcadmium and epicadmium. As shown in Fig. 10.2, there is a range over which the cadmium ratio is constant.

The subcadmium radial distributions measured in this experiment corresponded quite well to a J_o shape. It is expected that with the improvements being made in the source distribution, an even better approximation will be obtained, thus allowing a more precise determination of the extrapolated radius.

Intracell gold activity distributions, both with bare foils and with cadmium-covered foils, have also been measured. Figure 10.3 shows the resulting subcadmium activity distribution between rods. The results obtained under similar conditions in the large exponential assembly are also shown. It is evident that both agree rather closely.

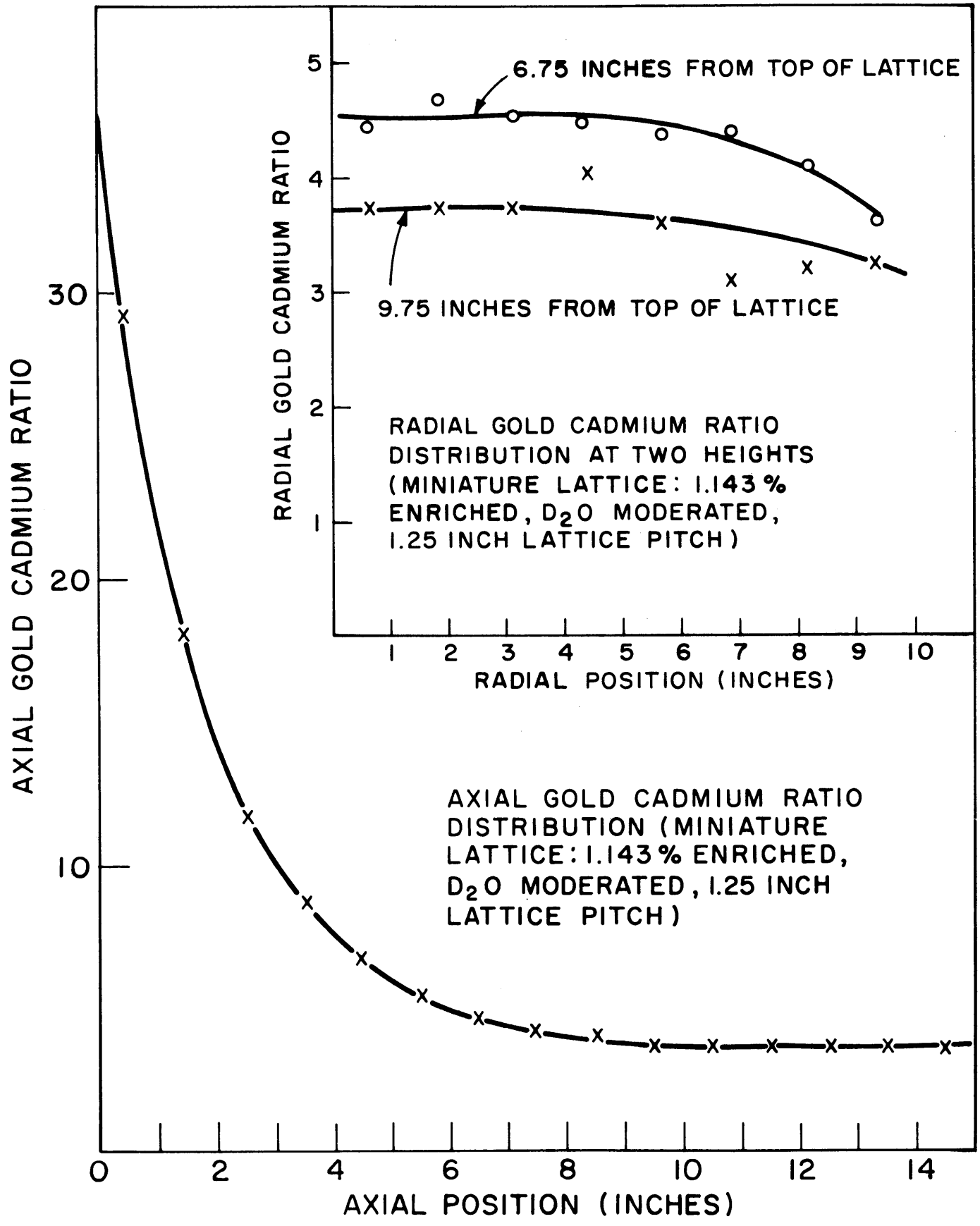

FIG. 10.2 AXIAL AND RADIAL CADMIUM RATIOS

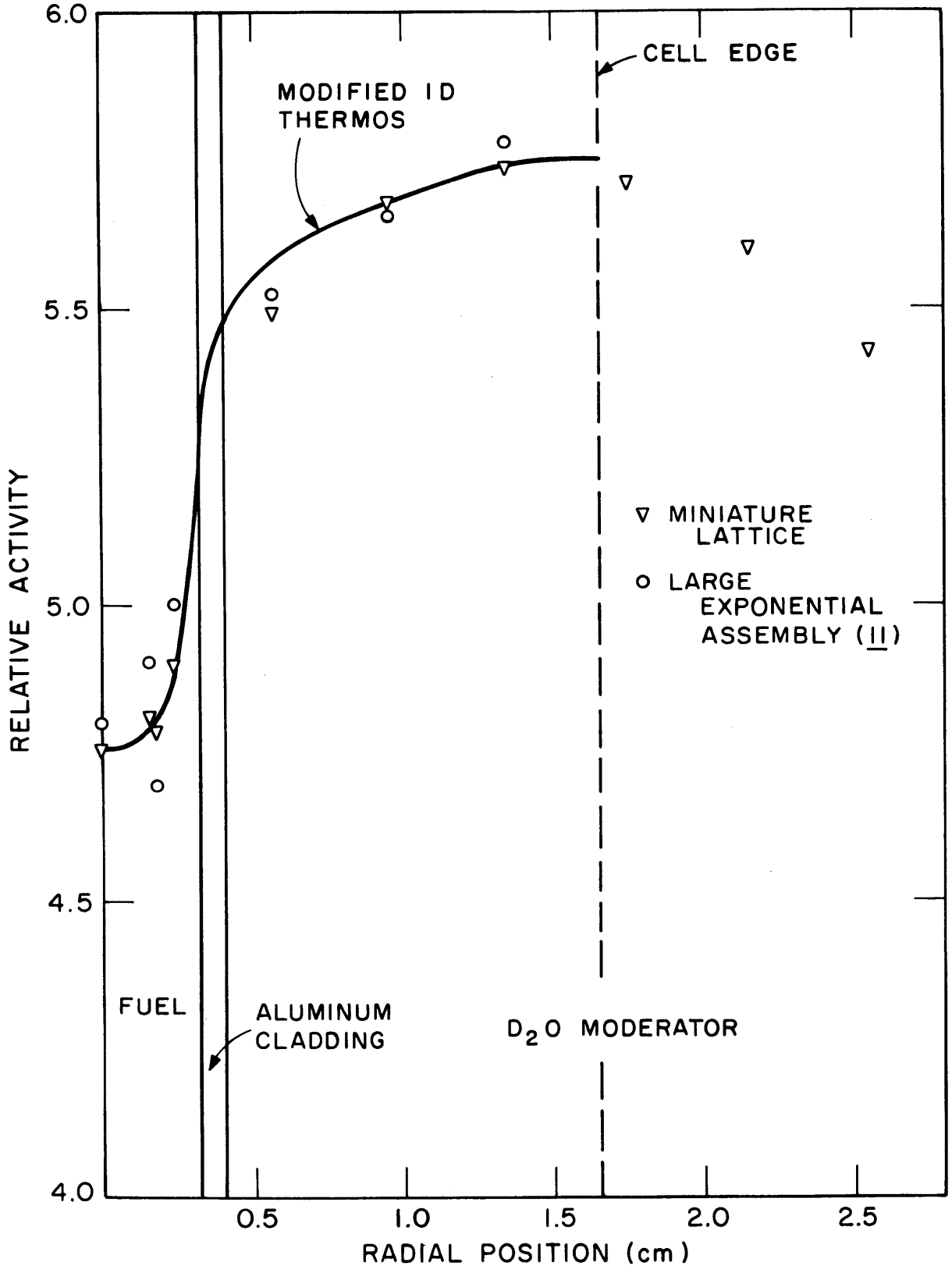

FIG. 10.3 INTRACELL SUBCADMIUM GOLD ACTIVITY DISTRIBUTIONS (MINIATURE LATTICE: 1.143% ENRICHED, D_2O MODERATED, 1.25 INCH LATTICE PITCH)

The distribution obtained with the THERMØS code, in the one-dimensional, modified version (8), is also shown. The miniature lattice results are in close agreement with this calculation.

Future plans include repetition of the preceding measurements in the same lattice, but with the improved source distribution, and then continuing with the rest of the lattices listed in Table 10.1.

3. THEORETICAL CONSIDERATIONS

The most important theoretical problem lies in developing a model which will permit extrapolation of miniature lattice results to those of a full-size critical assembly. There are a number of complications which make this a difficult problem. One arises from the fact that the neutron source is unidirectional rather than isotropic. This anisotropy may affect the comparison between theory and experiment in two ways. First, the spatial anisotropy of the source distribution may extend several mean-free paths into the lattice, thereby reducing the effective size of the lattice. Second, the energy spectrum of source neutrons is also different from that of lattice-born neutrons. This difference may extend deep into the assembly before a region is reached where the source neutrons have accumulated sufficient collisions to acquire the spectrum characteristic of the assembly under study.

Another problem arises from the fact that, in such small assemblies, end effects are important.

The above effects may be mitigated somewhat and the theoretical analysis simplified by proper design of the experiment. Source shaping has already been discussed, as have been the alterations made to delineate more precisely the neutronic boundaries of the system. Work is progressing on development of a model which will adequately account for the leakage and source effects on the measurements. At the present time, the possibility of using the GAM-I code (12) in conjunction with THERMØS in an age-diffusion treatment of the problem is being investigated. More work is required before the adequacy of this approach can be established.

4. REFERENCES

(1) Kouts, H., et al., "Exponential Experiments with Slightly Enriched U-Rods in Ordinary Water," P/600, ICPUAE, 1955.

(2) Kouts, H., et al., "Physics of Slightly Enriched Normal Water Lattices; Theory and Experiment," P/1841, ICPUAE, 1958.

(3) Wikdahl, C. E., and F. Akerhielm, "Measurement of Disadvantage Factor in a Small Mock-Up," P/162, ICPUAE, 1958.

(4) Peak, J., I. Kaplan, and T. J. Thompson, "Theory and Use of Small Subcritical Assemblies for the Measurement of Reactor Parameters," NYO-9661 (MITNE-15), February 1962.

(5) "Heavy Water Lattice Project Annual Report," NYO-10,212 (MITNE-46), September 30, 1963. Also, "Heavy Water Lattice Project Annual Report," MIT-2344-3 (MITNE-60), September 30, 1964.

(6) Palmedo, P. F., I. Kaplan, and T. J. Thompson, "Measurement of the Material Buckling of Lattices of Natural Uranium Rods in D_2O," NYO-9660 (MITNE-13), January 1962.

(7) Harrington, J., "Measurement of the Material Bucklings of a Lattice of Slightly Enriched Uranium Rods in Heavy Water," M.S. Thesis, M.I.T. Nuclear Engineering Department, July 1963.

(8) Simms, R., I. Kaplan, T. J. Thompson, and D. D. Lanning, "Analytical and Experimental Investigation of the Behavior of Thermal Neutrons in Lattices of Uranium Metal Rods in Heavy Water," NYO-10,211 (MITNE-33), October 1963.

(9) D'Ardenne, W. H., T. J. Thompson, D. D. Lanning, and I. Kaplan, "Studies of Epithermal Neutrons in Uranium, Heavy Water Lattices," MIT-2344-2 (MITNE-53) in press.

(10) Sefchovich, E., "Oscillating Neutron Source Experiment" in "Heavy Water Lattice Project Annual Report," MIT-2344-3 (MITNE-60), pp. 137-154, September 30, 1964.

(11) Clikeman, F., J. Barch, A. Supple, N. Berube, and B. Kelley, "Material Buckling and Intracellular Thermal Neutron Distributions" in "Heavy Water Lattice Project Annual Report," MIT-2344-3 (MITNE-60), pp. 155-164, September 30, 1964.

11. RETURN COEFFICIENT MEASUREMENTS

D. M. Goebel

To facilitate the interpretation of lattice experiments, it is desirable to have well-defined boundary conditions. In the M.I.T. lattice, this is effected for thermal neutrons by wrapping the sides of the core tank with 0.020-inch-thick cadmium (1). However, epicadmium neutrons can still leak into and out of the core. In order to determine the extent and consequences of this "room return" effect, a series of experiments was made using a detector design developed by Weinstock and Phelps at the Brookhaven National Laboratory (2). The results of these experiments yielded the return coefficient for the M.I.T. lattice as a function of vertical distance along the core tank.

The following sections summarize the results of the M.S. thesis work of the author (3).

1. DESCRIPTION OF DETECTOR

The detector used in these experiments consisted of a solid cylinder of indium (99.99% pure), 2 inches in diameter by 1 inch thick (Fig. 11.1). It was surrounded by 0.020-inch-thick cadmium, thereby precluding the possibility of activation by thermal neutrons. Two depressions, approximately 0.780 inch in diameter by 0.020 inch deep, were milled on the flat faces of the cylinder. Each depression held two indium foils, 0.750 inch in diameter by 0.010 inch thick. The foils were numbered 1 through 4, as shown, with foil number 1 nearest to the lattice core for all runs.

Data were recorded at 3.0-inch intervals, as depicted in Fig. 11.2. When a run was terminated, the detector was dismantled and a foil, 0.387 inch in diameter, was cut from the center of each irradiated foil. This procedure made it possible to avoid effects that might be caused by neutron-streaming or by the presence of burrs on the irradiated foil.

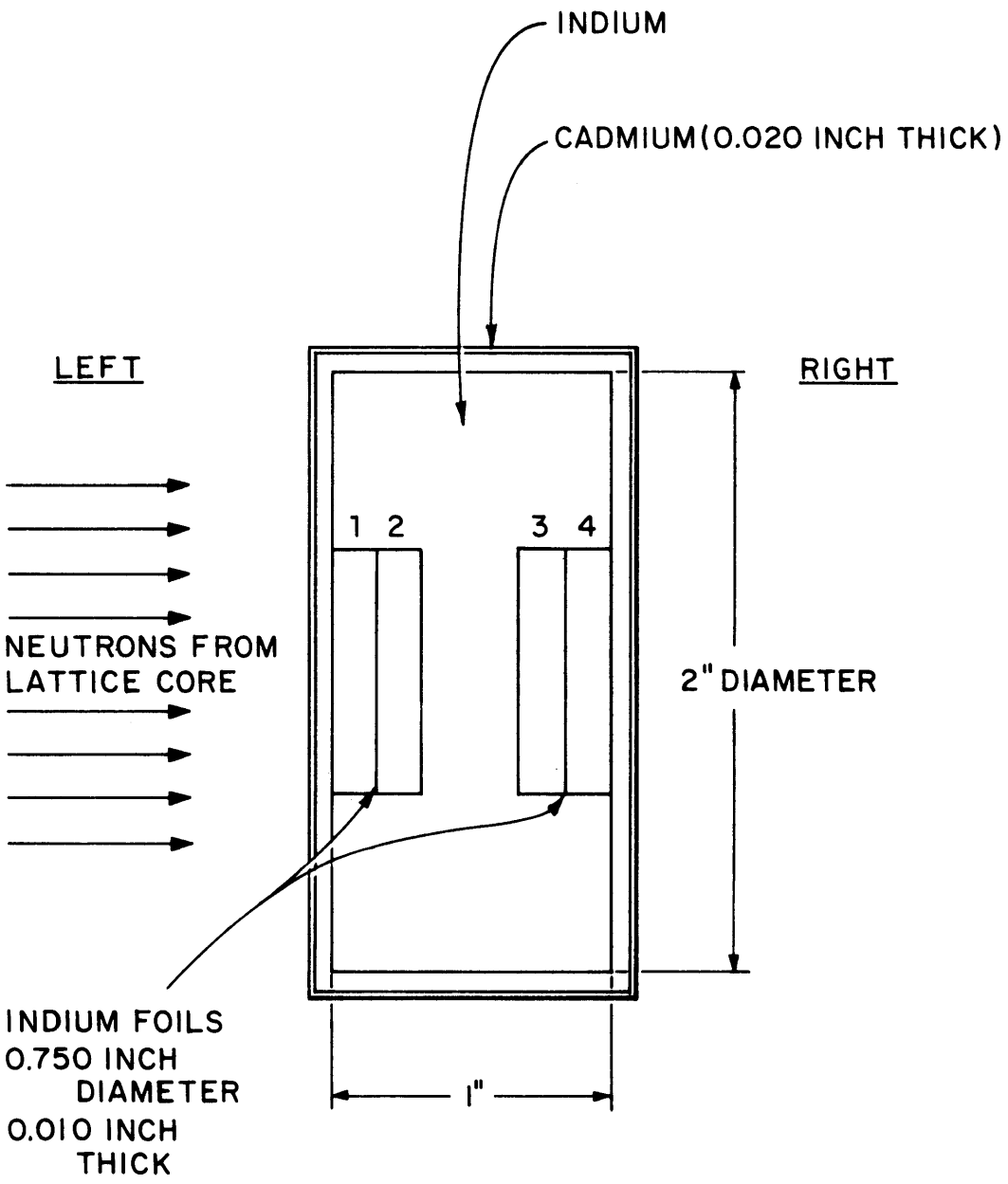

FIG. II.1 SCHEMATIC SIDE VIEW OF INDIUM DETECTOR

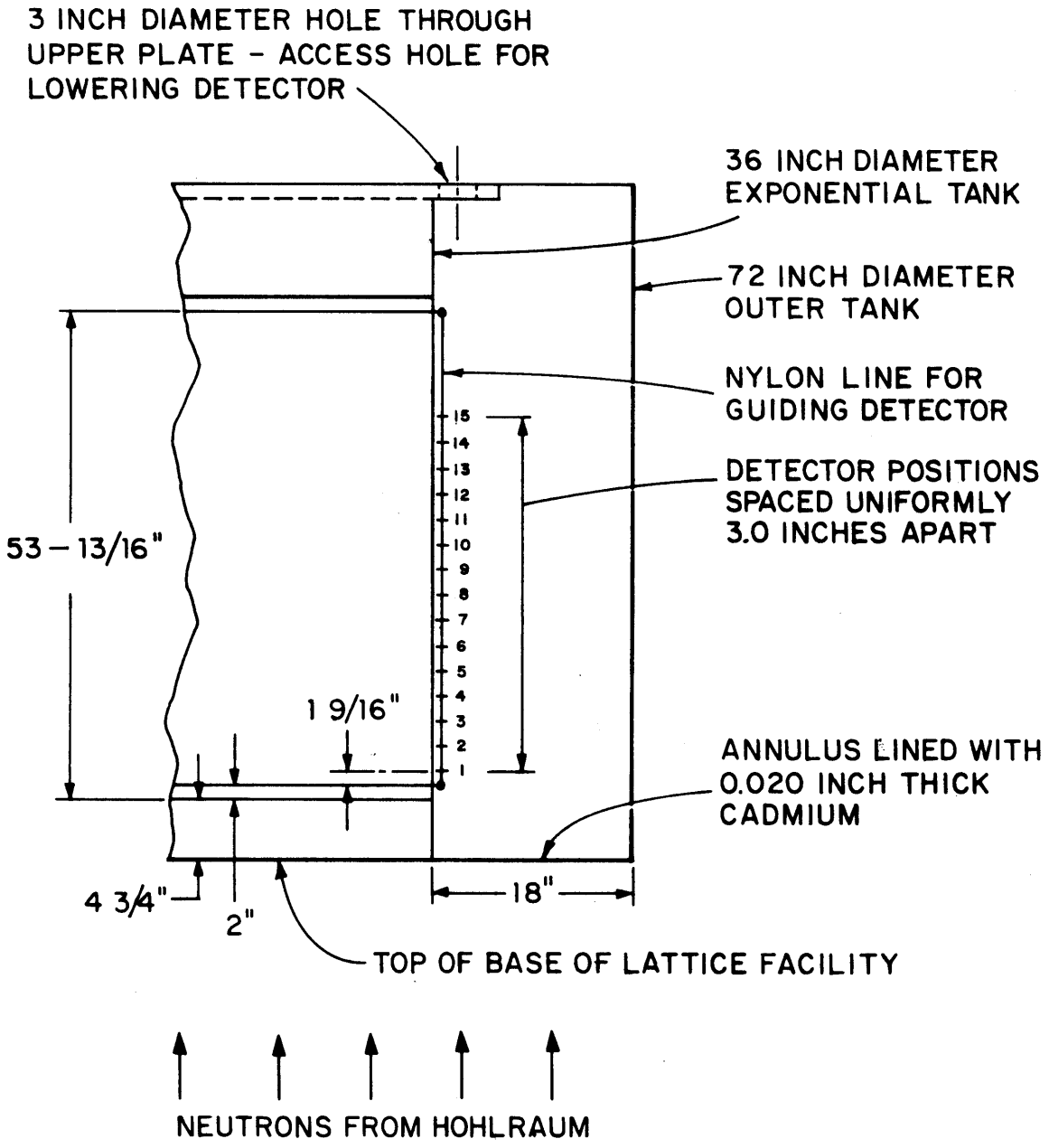

FIG. 11.2 DETECTOR LOCATION NUMBERS FOR EXPERIMENTAL RUNS

For reasons which will be explained in the following section, each side of each of the four indium foils was then γ-counted with an NaI(Tl) scintillator. Two runs were made at each location.

2. DATA ANALYSIS

In analyzing the data, it is necessary to consider the neutron currents incident on each side of each foil (Fig. 11.1). We wish to determine the albedo-like quantity, β:

$$\beta = \frac{\left(\begin{array}{l}\text{activity of the right side of foil number 4}\\ \text{due to the room-reflected neutron component}\end{array}\right)}{\left(\begin{array}{l}\text{activity of the left side of foil number 1}\\ \text{due to the neutron leakage from the core}\end{array}\right)} \qquad (11.1)$$

In the following derivation, the subscript L implies that the quantity so denoted refers to neutrons which travel from left to right, while the subscript R implies that the quantity so denoted refers to neutrons which travel from right to left. Also, the small letter ℓ with a subscript from 1 to 4 refers to the activity of the left side of foil 1 to foil 4, while the small letter r with a subscript from 1 to 4 refers to the activity of the right side of foil 1 to foil 4. Finally, the subscript m identifies a measured quantity.

We first define a transmission factor for a single outer foil:

$$f_1 = \frac{\ell_{2,L}}{\ell_{1,L}}, \qquad (11.2)$$

where $\ell_{1,L}$ and $\ell_{2,L}$ are the activities of the left side of foils 1 and 2, respectively, for neutrons entering from the left, and $\ell_{2,L}/\ell_{1,L}$ is the ratio of neutrons which pass through the first foil and activate the second, i. e., the transmission through foil number 1 of neutrons leaving the lattice core.

If it is assumed that the contributions to the observed activities of the left side of foils 1 and 2 by neutrons entering from the right are negligibly small, then

$$\frac{\ell_{2,L}}{\ell_{1,L}} = \frac{\ell_2^m}{\ell_1^m}.$$

This is a reasonable assumption, since neutrons which enter the block from the right are attenuated by the indium resonances while traversing the 1-inch-thick indium block shielding detector foils 1 and 2. Thus, the activity produced by these neutrons is negligibly small compared with the activation produced by the neutrons leaving the lattice core.

Next, the assumption is made that any neutron which traverses the entire block of indium, traveling from left to right, will activate the right side of foil number 4 to the same extent that it activates the right side of foil number 3, i.e.,

$$r_{3,L} = r_{4,L} \cdot \tag{11.3}$$

This is also a reasonable assumption because any neutrons which have penetrated the block must have energies at which the indium cross section is small and for which the attenuation is therefore low (2).

The following expression may now be written for the measured activity ratio r_4^m / r_3^m:

$$\frac{r_4^m}{r_3^m} = \frac{r_{4,L} + r_{4,R}}{r_{3,L} + r_{3,R}} ,$$

or

$$\frac{r_4^m}{r_3^m} = \frac{\frac{r_{4,L}}{r_{4,R}} + 1}{\frac{r_{4,L}}{r_{4,R}} + \frac{r_{3,R}}{r_{4,R}}} . \tag{11.4}$$

The quantity $\frac{r_{3,R}}{r_{4,R}}$ is the transmission through foil number 4 of those neutrons which travel from right to left, i.e., the component reflected back by the lattice facility surroundings. If it is now assumed that the spectral distributions of the outgoing and the returning components in the indium resonance activation region are identical, then:

$$\frac{r_{3,R}}{r_{4,R}} = \frac{\ell_2^m}{\ell_1^m} ,$$

and Eq. 11.4 becomes:

$$\frac{r_4^m}{r_3^m} = \frac{\frac{r_{4,L}}{r_{4,R}} + 1}{\frac{r_{4,L}}{r_{4,R}} + \frac{\ell_2^m}{\ell_1^m}} \,. \tag{11.5}$$

Equation 11.5, together with the relation $r_{4,L} + r_{4,R} = r_4^m$, gives an expression for $r_{4,R}$. Then, β is given by:

$$\beta = \frac{r_{4,R}}{\ell_1^m} = \frac{\left(\frac{r_4^m - r_3^m}{1 - \frac{\ell_2^m}{\ell_1^m}} \right)}{\ell_1^m} \,. \tag{11.6}$$

The activities obtained by γ-counting the indium foils were fed into a computer program, ACTCOR, which corrected the observed activities to the saturated activity and normalized for foil weight. The output from ACTCOR was fed into a second computer program, BETA, which determined the return coefficient, β, by solving Eq. 11.6. In both computer programs, the statistical fluctuations were determined in the usual manner (4), assuming a Poisson distribution.

3. EXPERIMENTAL RESULTS

During the period in which the investigation was made, the core consisted of 361 cylindrical rods of metallic uranium enriched to 1.143 wt % U^{235}. The rods were each 0.25 inch in diameter, 48.0 inches long, and were arranged in a triangular lattice with a spacing of 1.75 inches. The moderator was D_2O with a purity of 99.6%.

Two series of runs were made: the first with fuel and moderator in the core; the second with only moderator present. By combining the return effects measured in the fueled runs (β_{F+M}) with those measured in the moderator runs (β_M), it was possible to determine the return coefficient due to lattice-fuel-generated neutrons only (β_F).

To understand how this combined return coefficient was determined, it is necessary to recall one of the basic assumptions made in sec. 11.2.

It was assumed that any neutron traveling from left to right (i.e., leaves the core and travels outward) which activates the right side of foil number 3 will also activate the right side of foil number 4 to the same extent (see Fig. 11.1). Then it may be said that:

$$r_4^m - r_{4,R} = r_{4,L} = r_{3,L} , \tag{11.7}$$

where r_4^m is the total activity of the right side of foil number 4, $r_{4,R}$ is that portion of the activity which is due to the returning component of neutrons, and $r_{4,L}$ is that portion of the activity which is due to the leaving component of neutrons. For foil 3, the following relation holds:

$$r_{3,R} = r_3^m - r_{3,L} = r_3^m - r_{4,L} . \tag{11.8}$$

Thus, if $r_{3,R}$ and $r_{4,R}$ are determined for both the fuel-plus-moderator and the moderator-only runs, a net value $R_{3,F}$ and $R_{4,F}$, due to lattice-fuel-generated neutrons, may be obtained as follows:

$$r_{3,R,F+M} - r_{3,R,M} = R_{3,F} , \tag{11.9}$$

and

$$r_{4,R,F+M} - r_{4,R,M} = R_{4,F} , \tag{11.10}$$

where the additional subscripts F+M and M refer to fuel-plus-moderator and moderator runs, respectively.

Note that both $R_{3,F}$ and $R_{4,F}$ are functions only of the epithermal and fast leakage flux generated within the lattice core by the fuel. That is, $r_{4,R,F+M}$ consists of reflected neutrons due to:

(1) leakage neutrons generated by the fuel, including those originating as fission neutrons in the lattice fuel and a small number produced by the (γ,n) reaction between gamma rays produced in the lattice fuel and the D_2O moderator,

(2) source neutrons which leak out, including those originating as hohlraum neutrons and a small number produced by the (γ,n) reaction between the D_2O moderator and gamma rays which do <u>not</u> originate in the lattice fuel, and

(3) neutrons due to any external source which might be present.

On the other hand, $r_{4,R,M}$ contains only contributions from the latter two sources. Then $r_{4,R,F+M} - r_{4,R,M}$ contains only the contribution from the reflection of the fuel-generated neutrons (fission or (γ,n)) which leak out. The same considerations would be true for $R_{3,F}$.

Now, with these values of $R_{3,F}$ and $R_{4,F}$, we may determine the return coefficient β_F by using Eq. 11.6 as before. But ℓ_1 and ℓ_2 will be replaced by $L_{1,F} = \ell_{1,F+M} - \ell_{1,M}$ and $L_{2,F} = \ell_{2,F+M} - \ell_{2,M}$, to be consistent with the above considerations.

In the new notation, then, the defining equation for the return coefficient due to lattice-fuel-generated neutrons becomes:

$$\beta_F = \frac{\dfrac{R_{4,F} - R_{3,F}}{1 - \dfrac{L_{2,F}}{L_{1,F}}}}{L_{1,F}} . \qquad (11.11)$$

The values of β_M and β_{F+M} calculated, using Eq. 11.6 and the value of β_F from Eq. 11.11, are listed in Tables 11.1, 11.2 and 11.3 and plotted in Fig. 11.3. As shown in Fig. 11.3, the return coefficient increases with height. This can be attributed to the following factors:

(1) Epicadmium neutrons from the hohlraum and other parts of the lattice environment can leak into the lattice tank. In particular, the 18-inch-wide annular void between the inner and outer lattice tanks (see Fig. 11.2) provide a path through which neutrons can stream. Thus, in the moderator-only run, we find $\beta_M > 1.0$ high on the tank wall. All this signifies is that externally produced fast neutrons stream up the void and scatter into the tank in greater number than those which penetrate several feet of D_2O inside the tank and then scatter out.

(2) Most of the fission neutrons from the lattice fuel rods are produced near the bottom of the lattice tank: as a rough approximation, this source decreases exponentially with height. Again, fast neutrons can leak out of the lattice, stream up the annular void, and re-enter the lattice at a higher position. Thus the value of β_F, which measures the return of lattice-generated neutrons, also increases with height.

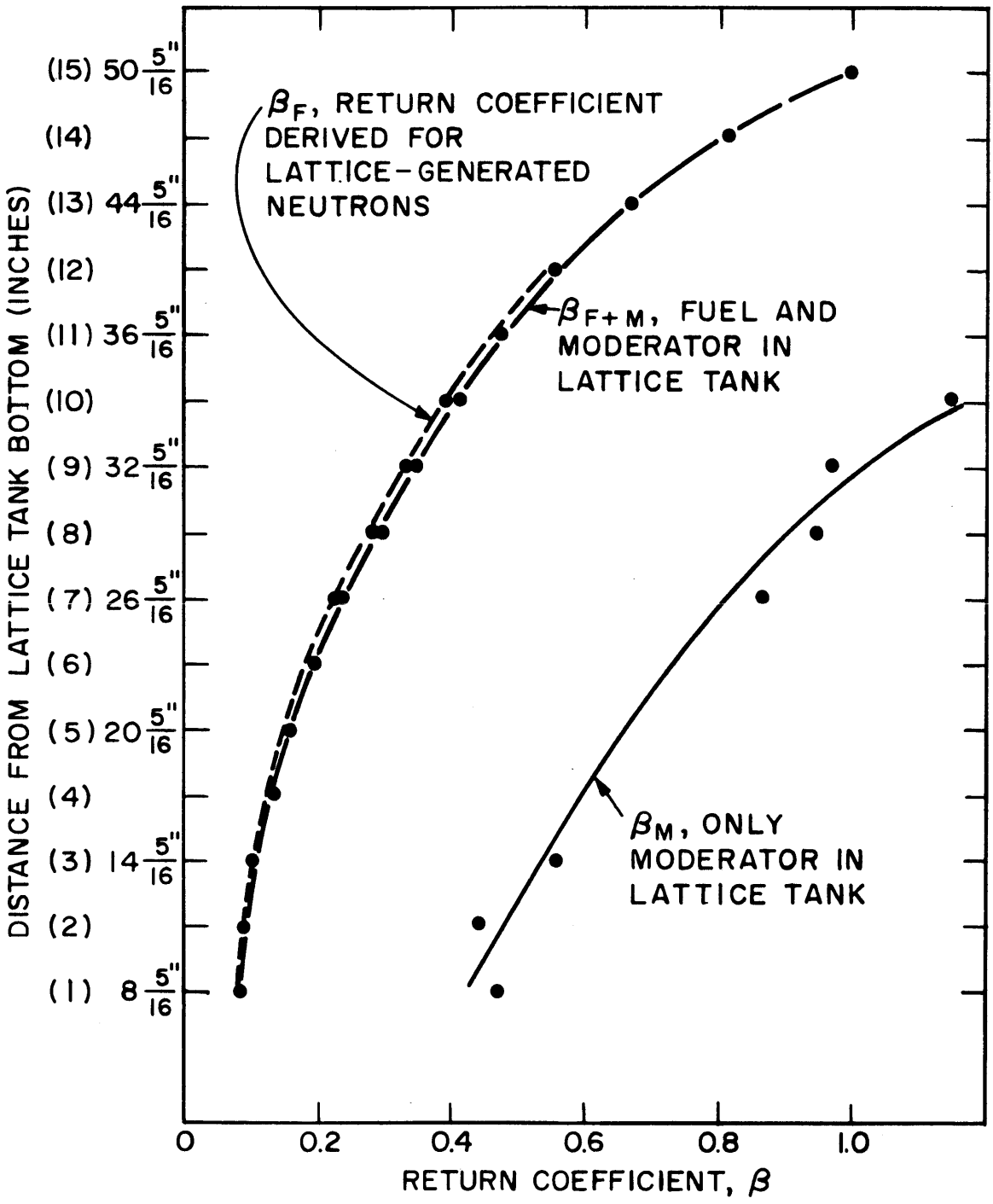

FIG. II.3 RETURN COEFFICIENTS AS A FUNCTION OF HEIGHT ALONG THE LATTICE CORE TANK

TABLE 11.1

Values of β and the Standard Deviation
for the Fuel + Moderator Runs

Location	β_{F+M}	$\beta_{S.D.}$
1	0.08973	0.00046
2	0.09663	0.00043
3	0.10652	0.00057
4	0.13224	0.00062
5	0.15702	0.00069
6	0.19449	0.00096
7	0.23014	0.00136
8	0.29418	0.00185
9	0.34530	0.00226
10	0.41141	0.00307
11	0.47714	0.00261
12	0.55801	0.00321
13	0.67166	0.00371
14	0.81493	0.00434
15	1.00340	0.00628

TABLE 11.2

Values of β and the Standard Deviation in β for the Moderator Runs

Location	β_M	$\beta_{S.D.}$
1	0.47208	0.01065
2	0.44015	0.00909
3	0.55506	0.01130
7	0.86337	0.01999
8	0.94228	0.02169
9	0.96642	0.02347
10	1.15384	0.02786

TABLE 11.3

Values of β for Neutrons Produced by the Lattice Fuel

Location	β_F
1	0.08640
2	0.09390
3	0.10391
7	0.22868
8	0.28320
9	0.33346
10	0.39674

To better illustrate the effects just described, we show in Fig. 11.4 and Fig. 11.5 the corrected foil activities used to compute β_{F+M} in Fig. 11.3. Figure 11.4 displays the foil activation produced by the epicadmium neutron current leaving the lattice tank $\left(\ell_1^m\right)$ and Fig. 11.5 shows the foil activation due to the epicadmium current into the tank $(r_{4,R})$. As can be seen, both ℓ_1^m and $r_{4,R}$ are largest near the bottom of the tank due to the high source strength in this region. As we move up the tank wall, ℓ_1^m attenuates but $r_{4,R}$ tends toward a constant value which is indicative of a relatively uniform current of background and backscattered neutrons entering the lattice tank.

4. DETERMINATION OF THE EFFECT ON LATTICE MEASUREMENTS PRODUCED BY THE NEUTRON RETURN PHENOMENON

To determine the consequences of the return effect on lattice measurements, data from radial buckling measurements made at various heights were analyzed. Since the return coefficient increases with height, a similar increase in the activities of the outer foils in the radial buckling measurements might be expected. Investigation of the change in activity of these outer foils as a function of radial distance from the inside edge of the core tank would thus indicate the relative effect of the return phenomenon.

Scheduling considerations did not permit making these radial measurements on the same lattice used for the return coefficient measurements, but it was possible to use similar data obtained earlier on another lattice. This latter lattice (to be referred to as the reference lattice) had the same characteristics as the lattice used for the return coefficient measurements, except that the enrichment was 1.027 wt % U^{235} in lieu of 1.143 wt % U^{235}. Although the comparison will not be exact, the possible existence of a general trend may be established.

The particular radial buckling measurements investigated involved the irradiation of cadmium-covered gold foils (99.9% pure), 0.125 inch in diameter and 0.010 inch thick. The distances above the bottom of the lattice tank and the run numbers involved are given in Table 11.4. The radial buckling (α) values obtained are also shown. These values of α

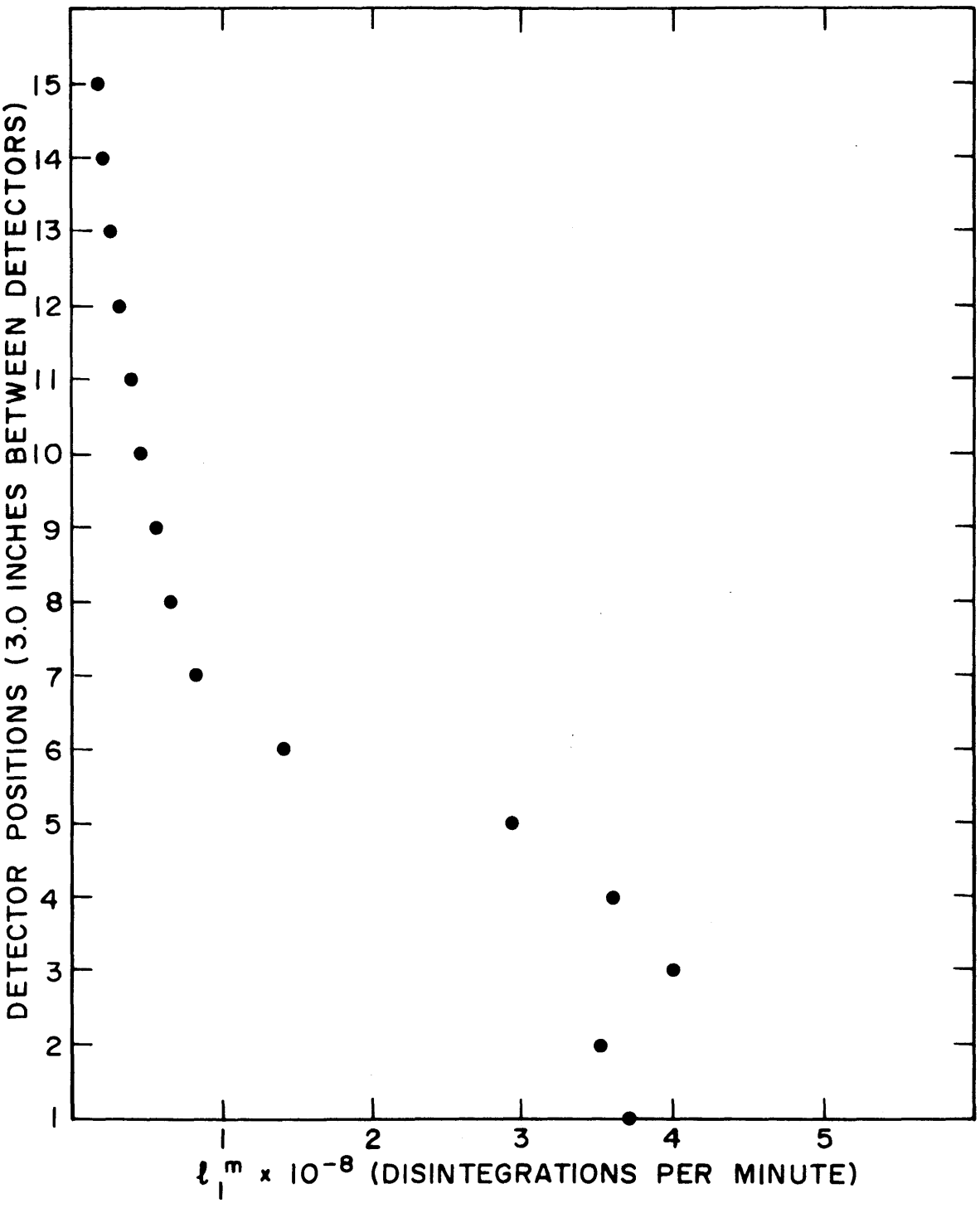

FIG. II.4 ACTIVITY OF THE LEFT SIDE OF FOIL NO. 1 DUE TO NEUTRONS LEAVING THE LATTICE TANK (FUEL AND MODERATOR RUN)

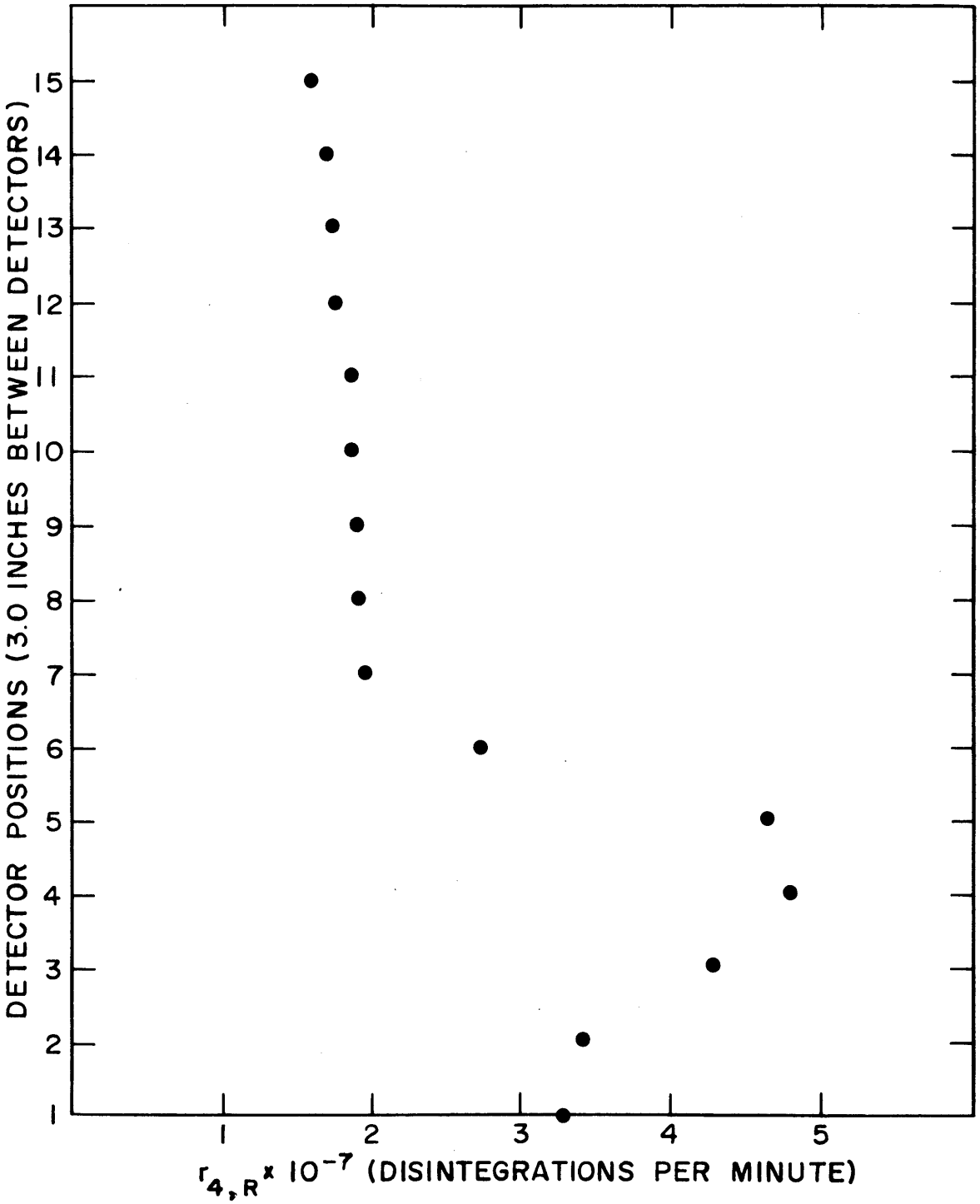

FIG. II.5 ACTIVITY OF THE RIGHT SIDE OF FOIL NO. 4 DUE TO NEUTRONS ENTERING THE LATTICE TANK (FUEL AND MODERATOR RUN)

TABLE 11.4

Radial Buckling Values at Various Distances Above the Lattice Tank Bottom for the Reference Lattice

Run Number	Distance (inches)	Radial Buckling (μB) (no points dropped)
12	21.795	2374.0
13	21.795	2384.3
17	25.181	2379.4
18	25.181	2387.8
40	28.173	2358.3
45	28.173	2405.8
47	28.173	2393.4

have been computed by considering all the measured data (i.e., no points were dropped). The measurements were made in a direction parallel to the girders (Fig. 11.6).

To determine the relative activities of the outside foils used in the buckling measurements, it is necessary to normalize the activity of the outermost foil to that of the central foil. Since the reference lattice was a rod-centered lattice, there was no central foil; but there were two foils approximately equidistant from the center. Consequently, the activity of the outermost foil was normalized to the arithmetic average of these two foils. The outer foil was located nearest the black plug to the right of the girders, visible in Fig. 11.6. This black plug marks the location of the return coefficient measurements. Note that the radial buckling measurements were not made along the same radius vector as the return coefficient measurements. Although Palmedo (5) and others have shown that the lattice facility is symmetric as far as radial buckling measurements are concerned, we are interested here in a small effect involving only the outermost foils in a radial traverse. The fast neutron return is not necessarily the same for all circumferential positions around the lattice tank. Nevertheless, the results will be valid as far as establishment of a general trend is concerned.

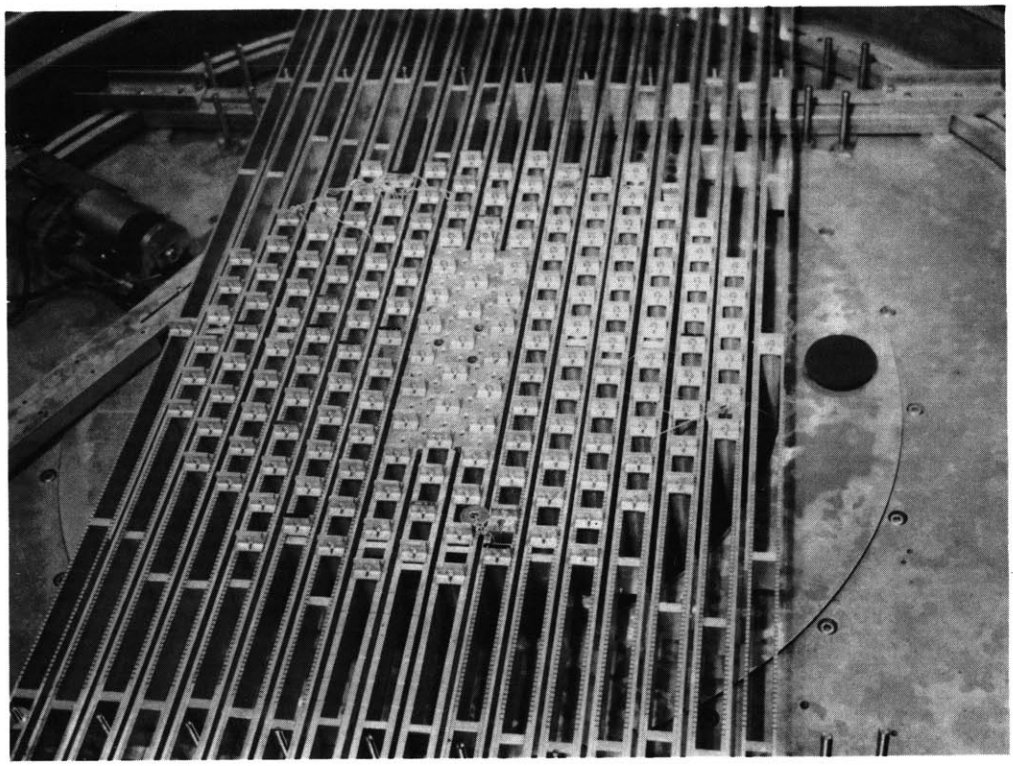

FIG. II.6 VIEW OF LATTICE TANK WITH CORE INSERTED

The results of normalizing the activity of the outer foil to that of the two central foils and then normalizing these results such that the activity of the outer foil at the lowest vertical distance is taken as unity, are given in Table 11.5.

TABLE 11.5

Relative Activities of the Outer, Cadmium-Covered Foil at Various Heights in the Reference Lattice

Distance from Tank Bottom (inches)	Distance of Foil from Tank Edge (inches)	Relative Activities Normalized to Lowest Position
21.795	1.30	1.000
25.181	1.30	1.284
28.173	1.30	1.345

The results listed in Table 11.5 indicate that the relative activity of the outer foil in a radial buckling measurement definitely increases with an increase in vertical distance from the lattice tank bottom, which conforms to the expected trend.

To determine how many of the foils in a radial buckling measurement are affected by this return coefficient, the above procedure was repeated for several interior foil positions; the results are presented in Table 11.6.

TABLE 11.6

Relative Activities of Radial Buckling Foils as a Function of Radial and Vertical Position

Distance from Tank Bottom (inches)	Distance of Foil from Tank Edge (inches)	Relative Activities Normalized to Lowest Position
21.795	2.95	1.000000
25.181	2.95	1.128880
28.173	2.95	1.134014
21.795	4.80	1.000000
25.181	4.80	1.065686
28.173	4.80	1.079060

From Table 11.6, it is seen that the magnitude of the return effect decreases quickly with distance from the core edge and that only the increase in the activities of the end foil and, to a lesser extent, the second foil in from the core edge is strongly affected.

Although not strictly correct, it is of interest to compare the relative increase in activity with the increase in the return coefficient. In Fig. 11.7, the distance from the core edge, at a constant height, is plotted against the normalized activity. The data were then extrapolated to the core edge and the resulting value of the normalized activity compared with the return coefficient, normalized to unity at the lowest position, to correspond to the similar normalization procedure performed on the foil activities. This comparison is made in Table 11.7. In examining this comparison, the existence of differences in the lattice cores utilized for the two types of measurements and the differences in the relative directions of the measurements must be kept in mind. Although a quantitative explanation of the differences between the normalized activities and the normalized return coefficients cannot be given for the reasons stated previously, it has been definitely established that:

(1) the neutron return coefficient increases with height, and

(2) the activity of the outer foil in a radial buckling measurement increases with height.

TABLE 11.7

Normalized Foil Activities and Normalized Return Coefficients as a Function of Height

Distance from Tank Bottom (inches)	Normalized Activity	Normalized Epithermal Neutron Return Coefficient
21.795	1.000	1.000
25.181	1.360	1.235
28.173	1.440	1.558

The final point to consider is the effect on the over-all results of measurements made within the lattice core. The measurement of particular interest is the radial buckling, and it can be seen from Table 11.4

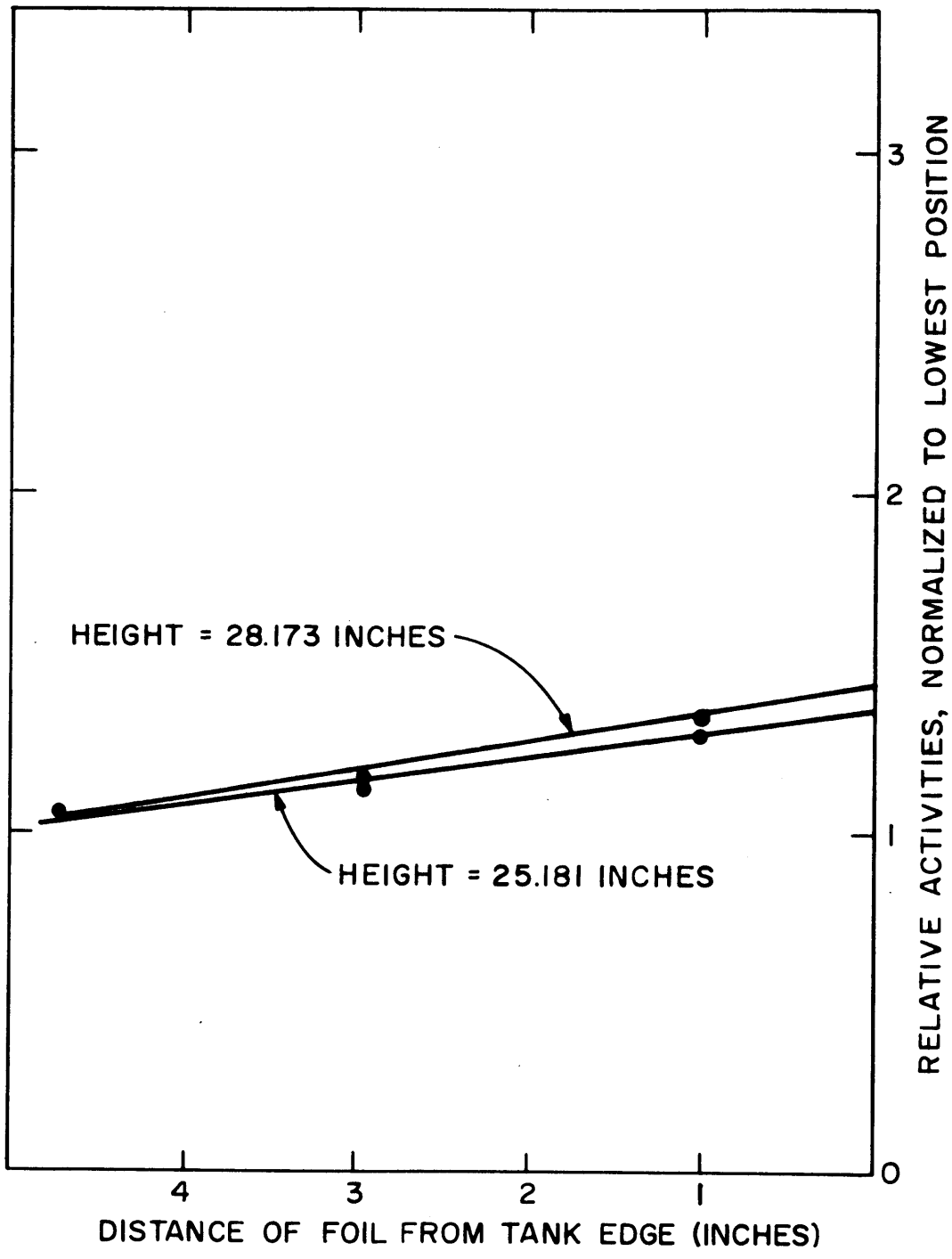

FIG. II.7 FOIL ACTIVITY AS A FUNCTION OF DISTANCE FROM CORE EDGE

that values of α, as a function of height, do not appear to be systematically affected by the neutron return effect. In this tabulation, none of the experimental points have been dropped. It must also be remembered, however, that the highest vertical distance at which buckling measurements were made in the reference lattice corresponds to a height approximately midway between positions 7 and 8 used for the return coefficient measurements, where $\beta_{F+M} \simeq 0.27$ (ref. Fig. 11.3). As the height is increased beyond this point, β_{F+M} increases markedly. Hence, the values of the radial buckling obtained might also change. This point is presently under investigation, but it should be noted that it has not been the practice to make any of the standard lattice measurements above this height and, further, that the standard data analysis procedure usually involves dropping the outer data points.

5. REFERENCES

(1) "Heavy Water Lattice Research Project Annual Report," NYO-9658, September 30, 1961.

(2) Weinstock, E. V., and J. P. Phelps, "A Simple Detector for the Measurement of Room-Scattered Neutrons," submitted as a letter to the editor of Nuclear Sci. and Eng., 18 (4), 525-532, April 1964.

(3) Goebel, D. M., "Return Coefficient Measurements for the M.I.T. Enriched Uranium-D_2O Lattice," M.S. Thesis, M.I.T. Nuclear Engineering Department, May 1965.

(4) Evans, R. D., The Atomic Nucleus, McGraw-Hill Book Company, Inc., 1955.

(5) Palmedo, P. F., I. Kaplan, and T. J. Thompson, "Measurements of the Material Bucklings of Lattices of Natural Uranium Rods in D_2O," NYO-9660 (MITNE-13), January 20, 1962.

12. MEASUREMENT OF THE DIFFUSION COEFFICENT IN AN ANISOTROPIC MEDIUM

E. E. Pilat, H. Guéron, and D. D. Lanning

An experiment has been conducted to provide a test of Benoist's theory of diffusion (1) in an anisotropic medium, unencumbered by the presence of either strong distributed absorption or fission sources and under conditions of anisotropy considerably more extreme than those encountered in most practical reactors. Measurements of the effective thermal neutron diffusion coefficient were made in heavy water containing a regular vertical array of air-filled, Type 1100 aluminum tubes representing a voided volume fraction of 16%. The experiment yielded a ratio of radial diffusion coefficient to moderator diffusion coefficient of 1.29 ± 0.02 compared to the theoretical ratio of 1.28 (2).

1. THEORY

According to Benoist's theory (1), the expression for the total flux in a finite assembly of identical unit cells consists not only of the usual product of a macroscopic function (satisfying the external boundary conditions) and a microscopic function (having the periodicity of the unit cells), but also contains an additive term proportional both to the gradient of the macroscopic function and to a geometric factor depending only on the dimensions of the unit cell. From this constant of proportionality, C_o, the ratio D_R/D_M of radial diffusion coefficient to the diffusion coefficient in moderator alone is determined by the relation:

$$\frac{D_R}{D_M} = \frac{2\pi C_o}{S} + 1 \ , \tag{12.1}$$

where S is the cross-sectional area of the cell. Since D_R is of the same order of magnitude as D_M, a given percentage error in C_o will appear as a much smaller percentage error in the value of D_R determined in this way.

The constant C_o can be determined from microscopic foil activation measurements around a lattice rod. In principle, C_o can also be determined from macroscopic buckling measurements, but this method did not prove successful in the present study.

2. THE EXPERIMENT

The aluminum tubes used to construct the test lattice were about 2.25 inches in diameter and were arrayed on a square 5-inch spacing in 99.5% D_2O within the 3-foot-diameter exponential facility of the M.I.T. reactor (3). Figure 12.1 shows the lattice configuration employed and Figs. 12.2 and 12.3 show the foil arrangements used. Cadmium plugs were inserted in the bottom of the air-filled tubes to minimize streaming of neutrons up the tubes from the extended source beneath the tank. The D_2O level during the run was 48 inches. The measurements whose results are shown in Table 12.1 were made with gold foils of 0.25-inch or 0.125-inch diameter and 10-mil thickness. The foils were counted on an automatic sample changer, and the ACTIVE code (4) for the IBM 7094 was used to correct the activities for foil weight differences, decay, and deadtime.

3. RESULTS

It has already been noted that, while there are two possible ways to obtain C_o, the method using the macroscopic buckling data proved too insensitive to yield useful results. Thus, we will consider only the more useful of the two methods.

The formula for computing C_o from the activation of two foils on opposite sides of a rod (both lying along the same radius vector from the center of the tank) is:

$$C_o = \frac{A_\beta J_o(B_r r_F) - A_F J_o(B_r r_\beta)}{B_r G\{A_F J_1(B_r r_\beta) + A_\beta J_1(B_r r_F)\}}, \tag{12.2}$$

where

A = foil activity,

r = distance from center of tank,

subscript F refers to the "front" foil position (i.e., that nearer to the tank center),

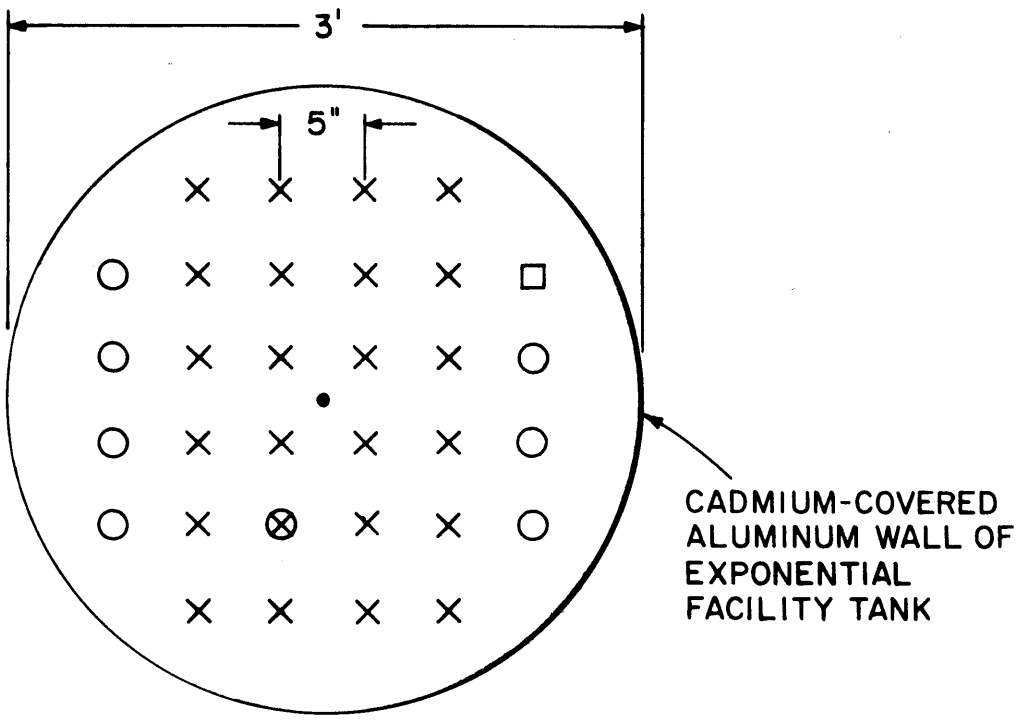

- • CENTER OF LATTICE AND OF TANK
- × 2.290 INCH O.D. , 2.188 INCH I.D., 54 INCH LONG TUBES
- ⊗ 2.290 INCH O.D. , 2.188 INCH I.D., 71.5 INCH EXPERIMENTAL TUBE
- ○ 2.10 INCH O.D. , 2.00 INCH I.D., 54 INCH LONG TUBES
- □ NO TUBE IN THIS POSITION

TUBES ARE ALL TYPE 1100 ALUMINUM

FIG 12.1 LATTICE ARRANGEMENT FOR RADIAL DIFFUSION COEFFICIENT MEASUREMENT

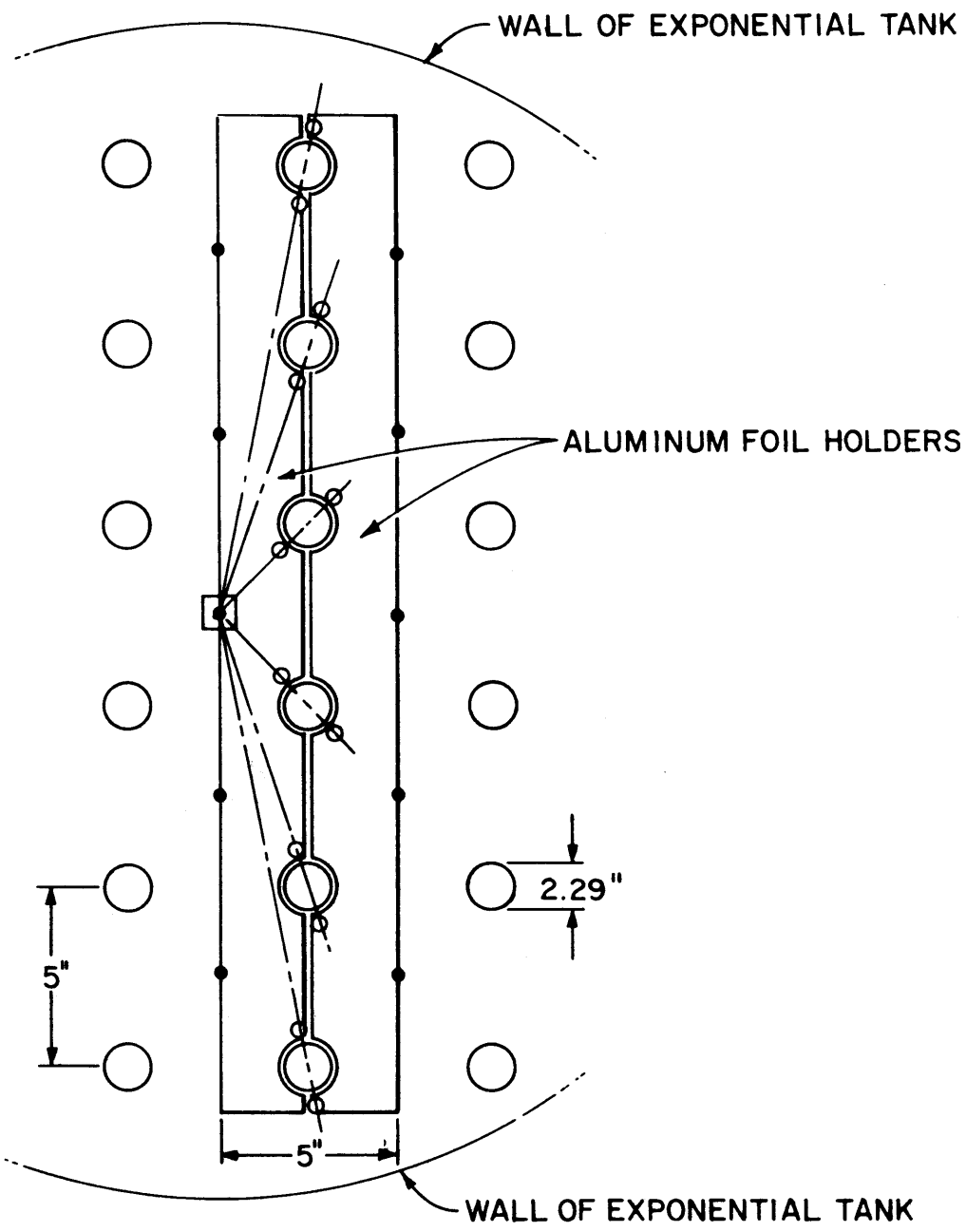

○ AIR-FILLED ALUMINUM TUBES

• GOLD FOILS FOR RADIAL TRAVERSES IN CENTER OF MODERATOR BETWEEN TUBES

o GOLD FOILS FOR RADIAL TRAVERSES ADJACENT TO TUBES

□ CENTER OF EXPONENTIAL TANK

FIG. 12.2 POSITIONS OF RADIAL TRAVERSES

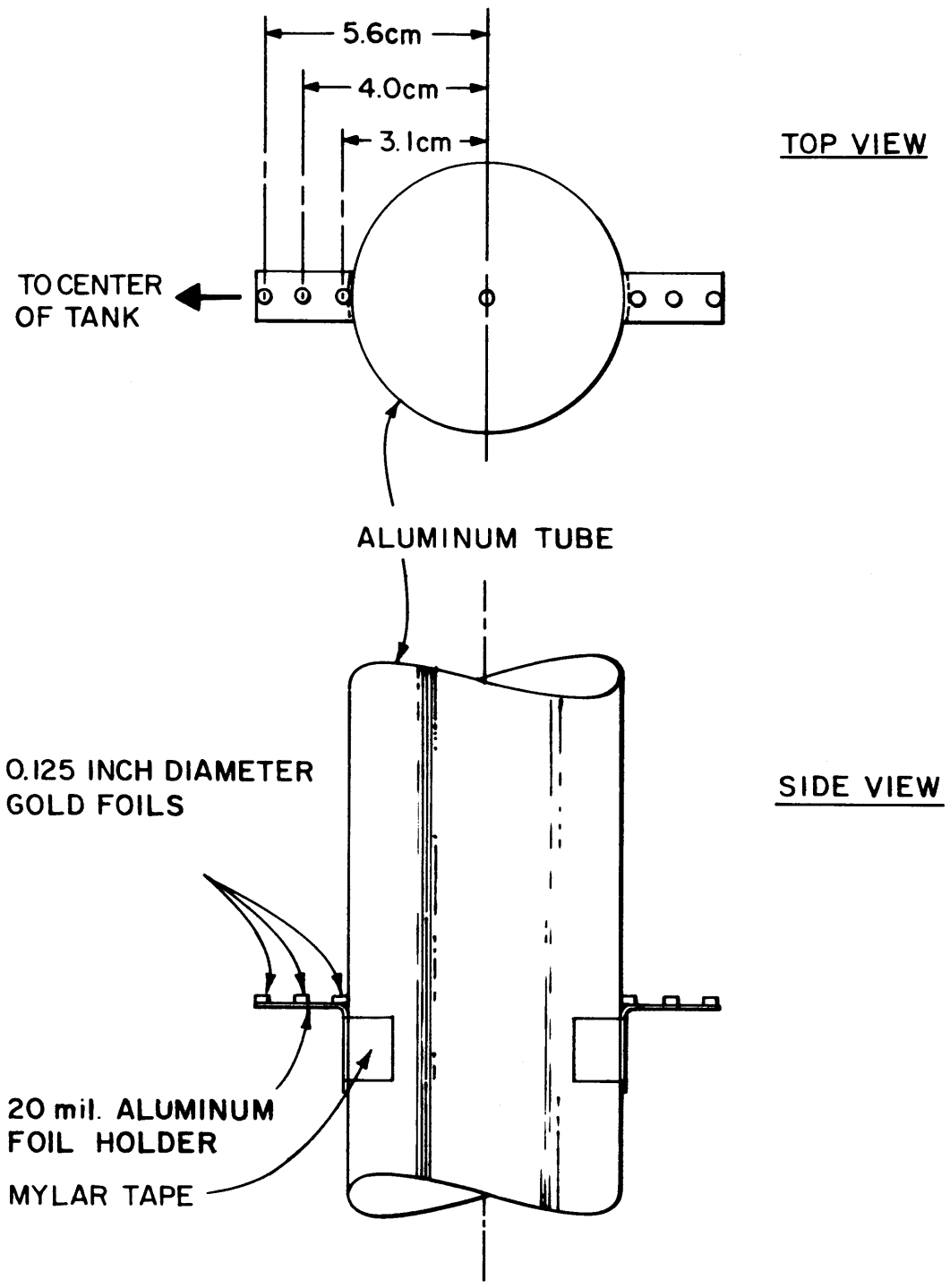

FIG. 12.3 POSITIONS OF MEASUREMENTS AT DIFFERENT POINTS WITHIN CELL.

TABLE 12.1

Experiments Used in Determining the Radial Diffusion Coefficient

Experiment Number	Foil Arrangement	Purpose
1	(a) 2 radial traverses in center of moderator channels, midway between tubes.	To determine the radial buckling B_r^2 and thus the macroscopic function $J_o(B_r r)$.
	(b) 2 radial traverses adjacent to tubes. (See Fig. 12.2.) Foil pairs 180° apart.	To fit activity to the function $J_o(B_r \pm \epsilon)$ and thus obtain ϵ.
2	Foil pairs 180° apart on outer surface of the experimental tube located halfway between center and edge of lattice. (See Fig. 12.1.) Seven pairs were spaced every 5 inches vertically.	(a) To find the axial relaxation length, λ, along the tube. (b) To find C_o, using each pair of foils at a given height.
3	Every 2.5 inches vertically in the moderator, midway between tubes.	To find the axial relaxation length, λ', in the moderator.
4	3 pairs of foils at distances of 1/16 inch, 9/16 inch, 17/16 inch from outside of experimental tube and 180° apart. (See Fig. 12.3.)	To determine C_o at several different radial positions in the unit cell.

subscript β refers to the "back" foil position (i.e., that farther from the tank center),

B_r^2 = radial buckling,

$G = \frac{1}{\rho} - \frac{\rho}{b^2}$,

ρ = distance of foils from center of tube, and

b = radius of equivalent circular cell.

The four experiments listed in Table 12.1 provided the data for calculation of C_o from Eq. 12.2. The results are summarized in Table 12.2. Application of Eq. 12.1 to the mean value $\overline{C}_o = 7.5 \pm 0.5$ cm^2 gives $D_R/D_M = 1.29 \pm .02$, in excellent agreement with the theoretical ratio of 1.28.

4. ERROR ANALYSIS

Since the effect being investigated is small, it is particularly important to minimize experimental error. The locations for the foil positions shown in Fig. 12.2 were chosen with this in mind, since the anisotropic effect is maximized for foil pairs positioned 180° apart around the tube and lying on a radius vector from the center of the lattice. Even so, unavoidable uncertainties in foil position must be carefully considered.

The quantities r_β, r_F, ρ, b (and therefore G) are known well enough so they contribute negligible uncertainty to C_o. The error in C_o thus arises from uncertainties in A_β, A_F, and B_r. These are independent quantities, so the total expected standard deviation in C_o is:

$$\sigma_{C_o} = \left[\left(\frac{\partial C_o}{\partial A_\beta} \right)^2 \sigma_{A_\beta}^2 + \left(\frac{\partial C_o}{\partial A_F} \right)^2 \sigma_{A_F}^2 + \left(\frac{\partial C_o}{\partial B_r} \right)^2 \sigma_{B_r}^2 \right]^{1/2} . \qquad (12.3)$$

The errors in A_β and A_F arise primarily from errors in <u>vertical</u> placement of the foils. (To first order, horizontal misplacement has no effect, since at the foil positions, the derivative of flux is zero in the <u>horizontal</u> direction tangent to the tube.) Since the axial (vertical) flux dependence goes as $e^{-\lambda z}$,

TABLE 12.2

Experimental Results

Experiment Number as Described in Table 12.1	Summary of Results
1 (a) Radial buckling	$B_r^2 = 2301 \pm 13 \times 10^{-6}\ cm^{-2}$ $B_r = 0.04797\ cm^{-1}$
(b) The constant ϵ	The flux shape is so weak a function of ϵ that this constant could not be determined.
2 (a) Axial λ along tube	$\lambda = 21.8 \pm 0.2$ cm
(b) C_o vs. height	Height above cadmium discs at bottom of tube (cm) / C_o (cm^2) 99.1 / 7.60 86.4 / 7.57 73.7 / 9.08 61.0 / 8.92 48.3 / 4.96 35.6 / 7.62 22.9 / 6.70 Average ± standard deviation of the mean = 7.5 ± 0.5
3 Axial λ' in moderator	$\lambda' = 22.0 \pm 0.2$ cm
4 C_o vs. radial position	Foil distance from center of cell (cm) / C_o (cm^2) 3.1 / 6.3 4.0 / 8.0 5.6 / 22.0

$$\sigma_A = \sqrt{\left(\frac{\partial A}{\partial z}\right)^2 \sigma_z^2} \approx \lambda A \sigma_z \ . \tag{12.4}$$

Since A_β and A_F have similar values (within a few per cent) as do $\frac{\partial C_o}{\partial A_\beta}$ and $\frac{\partial C_o}{\partial A_F}$, denote both A_β and A_F by A and express σ_{C_o} as:

$$\sigma_{C_o} \approx \left[2\left(\frac{\partial C_o}{\partial A}\right)^2 (\lambda A)^2 \sigma_z^2 + \left(\frac{\partial C_o}{\partial B_r}\right)^2 \sigma_{B_r}^2 \right]^{1/2} \ . \tag{12.5}$$

With typical values for A, using the experimental value of λ given in Table 12.2, and assuming σ_z = 2 mm for the uncertainty in foil position:

$$\sigma_{C_o} \approx \sqrt{2(1.7) + 0.01} = \cancel{2.3}\ 1.9 \text{ cm}^2 \ . \tag{12.6}$$

This is the expected standard deviation in one measurement and compares reasonably well with the actual standard deviation of one measurement which, from the seven measurements of run 2, is 1.4 cm^2. Equation 12.6 shows that the experiment is sensitive to the vertical placement of the foils and insensitive to the particular value of the radial buckling. The sensitivity to vertical placement occurs because C_o is approximately proportional to the difference in the activities of the front and back foils, and this difference is a small fraction of the total activity. Thus, the results in Table 12.2 are <u>not</u> indicative of any true axial dependence of C_o.

Although the standard deviation in C_o appears relatively large, Eq. 12.1 shows that the resultant error in D_R/D_M, a ratio close to unity, is reduced by a factor approximately equal to $2\pi/S \approx 0.03$. Thus, good precision can be obtained in the final results.

The three values of C_o obtained from experiment 4 are not necessarily indicative of any radial dependence in C_o, since there are at least two factors which greatly increase the uncertainty in the values at larger radii. First, the total magnitude of the heterogeneous effect decreases as one moves toward the cell edge, making the measurement increasingly sensitive to foil misplacement. Second, the theory was derived on the

basis of a cylindrical unit cell, so that measurements made near the cell edge may show the effects of the actual cell shape, which is not accounted for in the theory.

5. ACKNOWLEDGEMENT

The authors wish to acknowledge the assistance of Dr. Pierre Benoist who helped plan this experiment during the Fall 1964 Semester, which he spent at M.I.T. as a visiting lecturer in reactor physics.

6. REFERENCES

1. P. Benoist, Thèse, Série A, No. 4233, No. d'Ordre 5084, January 1964.
2. Ibid., pp. 117, 161.
3. "Heavy Water Lattice Research Project Annual Report," NYO-9658, September 30, 1961.
4. ACTIVE, an IBM 7090 code to reduce activation data, written by R. Simms, revised by F. C. Clikeman, private communication, November 1964.

13. EPITHERMAL NEUTRON STUDIES

W. H. D'Ardenne

The last Heavy Water Lattice Project Annual Report (1) and the Sc.D. thesis of the author (2, 3) have described in some detail the results of a comprehensive study of epithermal neutron behavior in the MITR lattice facility. In this section, attention will be confined to an additional result obtained through further analysis. Specifically, the dependence of ERI^{28} on the fuel-to-moderator ratio is to be examined.

1. THEORY

Following the approach of Petrov as reported by Dresner (4), one can write the following expression for the effective resonance integral for fuel rods in a lattice having a small fuel-to-moderator volume ratio:

$$ERI^{28}_{LAT} = \int \frac{\Sigma_a(u)}{N} \frac{\phi(u)}{\phi} du \ , \tag{13.1}$$

where

$\Sigma_a(u)$ = the effective absorption cross section of the fuel rods,

N = resonance absorber atom density in the fuel rod,

$\phi(u)$ = flux at lethargy u,

ϕ = flux in the absence of absorption, in which case, $\phi(u) = \phi$ = constant in the asymptotic slowing-down approximation.

The relation among $\phi(u)$, ϕ and $\Sigma_a(u)$ can be approximated by:

$$\frac{\phi(u)}{\phi} = \frac{V_m \Sigma_{sm}}{V_m \Sigma_{sm} + V_f \Sigma_a(u)} \ , \tag{13.2}$$

where

V_m = moderator volume in lattice cell,

V_f = fuel volume in lattice cell,

Σ_{sm} = scattering cross section of pure moderator.

Substitution of 13.2 into 13.1 gives:

$$ERI^{28}_{LAT} = \int \frac{\Sigma_a(u)}{N}\left(1 + \frac{V_f}{V_m}\frac{\Sigma_a(u)}{\Sigma_{sm}}\right)^{-1} du \,. \qquad (13.3)$$

Further, since $\frac{V_f}{V_m}\frac{\Sigma_a(u)}{\Sigma_{sm}} \ll 1$, the term $1 + \frac{V_f}{V_m}\frac{\Sigma_a(u)}{\Sigma_{sm}}$ in Eq. 13.3 can be expanded in a series approximation with the result:

$$ERI^{28}_{LAT} = \int \frac{\Sigma_a(u)}{N} du - \left\{\int \frac{\Sigma_a(u)}{N}\frac{\Sigma_a(u)}{\Sigma_{sm}} du\right\}\frac{V_f}{V_m} + \left\{\int \frac{\Sigma_a(u)}{N}\left[\frac{\Sigma_a(u)}{\Sigma_{sm}}\right]^2 du\right\}\left(\frac{V_f}{V_m}\right)^2 - \ldots \qquad (13.4)$$

Equation 13.4 shows that to first order, ERI^{28}_{LAT} should be a linear function of V_f/V_m.

2. EXPERIMENTAL RESULTS

The linear relationship predicted in Eq. 13.4 can be tested by using the experimental data for ERI^{28}_{LAT} reported by the author in references 2 and 3 and reproduced in Table 13.1.

TABLE 13.1

Effective Resonance Integral of U^{238} Lattices
of 0.25-Inch-Diameter, 1.027% Enriched Fuel Rods

Rod Spacing (inches)	Volume Ratio Fuel-to-Moderator V_F/V_M	ERI^{28} barns	$ERI^{28}_{\infty} - ERI^{28}_{LAT}$ barns
1.25	0.0388	14.0 ± 1.1	4.3
1.75	0.0191	16.2 ± 1.3	2.1
2.50	0.0092	17.3 ± 1.4	1.0
∞(a)	0.0000	18.3 ± 0.9	0.0

(a) From reference 5, as discussed in reference 2.

In Fig. 13.1, the values of ERI^{28} are plotted versus the fuel-to-moderator ratio. As can be seen, the relationship is indeed linear. It should be noted that the values of ERI^{28}_{LAT} listed in Table 13.1 were calculated using the ERI^{28}_{∞} value reported for a 1/E spectrum:

$$\frac{ERI^{28}_{LAT}}{ERI^{28}_{\infty}} = \left(\frac{\rho_{28}}{\rho_{Au}}\right)_{LAT} \left(\frac{\rho_{Au}}{\rho_{28}}\right)_{1/E}, \tag{13.5}$$

where ρ is the ratio of epicadmium to subcadmium foil activity. For this reason, the standard deviation of the data points shown in Fig. 13.1 is mainly due to the ± 0.9 uncertainty contributed by ERI^{28}_{∞}. Thus, the confirmation of linearity using only the three data points for $V_f/V_m > 0$ would be even more precise.

The results of this section support the conclusions of section 4 as to the possibility of extending the use of single rod measurements in the determination of lattice parameters.

3. REFERENCES

(1) "Heavy Water Lattice Research Project Annual Report," MIT-2344-3 (MITNE-60), September 30, 1964.

(2) D'Ardenne, W. H., "Studies of Epithermal Neutrons in Uranium Heavy Water Lattices," Ph.D. Thesis, M.I.T. Nuclear Engineering Department, August 1964.

(3) D'Ardenne, W. H., T. J. Thompson, D. D. Lanning, and I. Kaplan, "Studies of Epithermal Neutrons in Uranium, Heavy Water Lattices," MIT-2344-2 (MITNE-53), August 1964 (in press).

(4) Dresner, L., Resonance Absorption in Nuclear Reactors, p. 92, Pergamon Press, New York, New York, 1960.

(5) Reactor Physics Constants, ANL-5800 (Second Edition), July 1963.

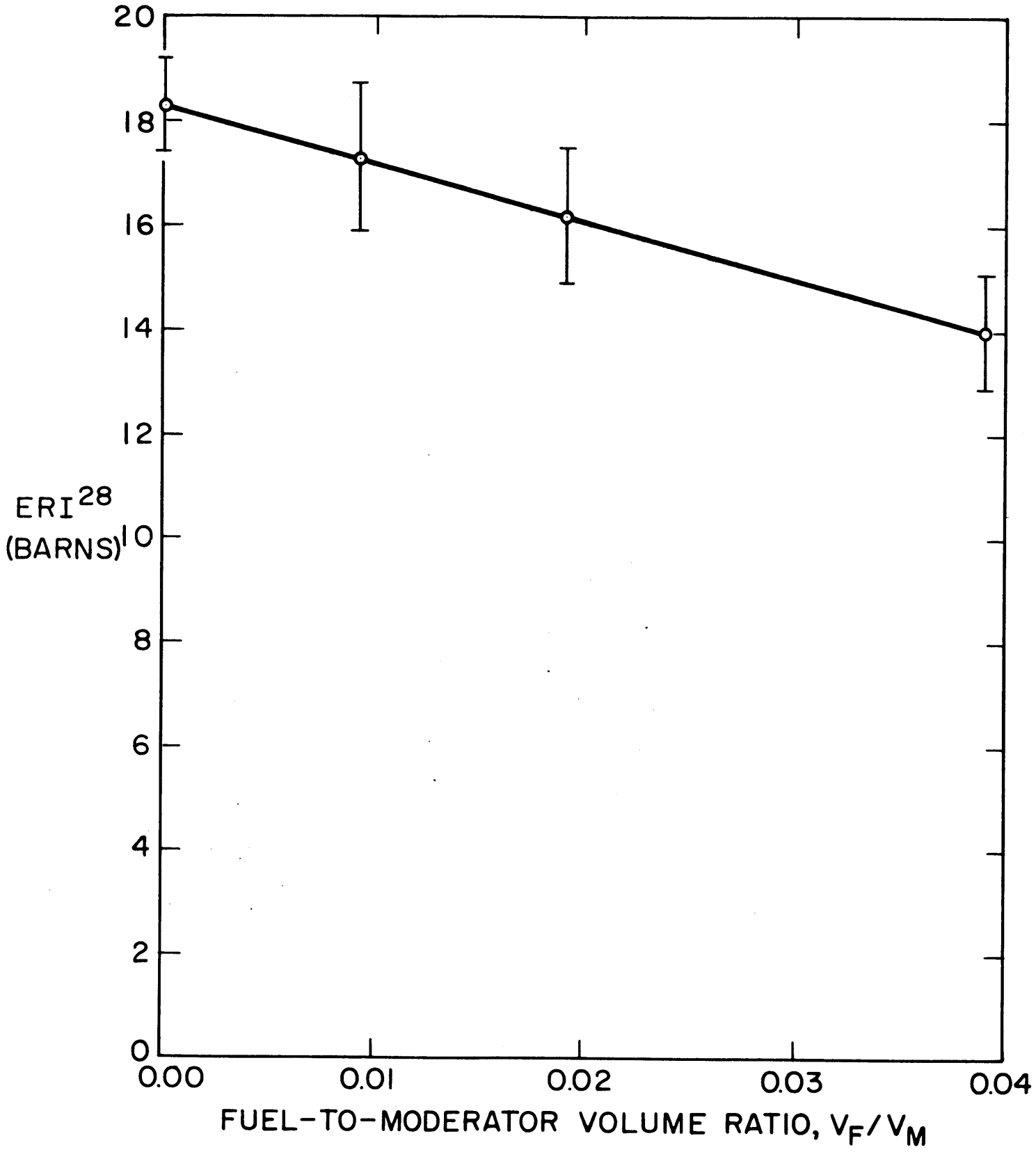

FIG. 13.1 VARIATION OF ERI^{28} AS A FUNCTION OF FUEL-TO-MODERATOR RATIO

Appendix A

BIBLIOGRAPHY OF HEAVY WATER LATTICE PROJECT PUBLICATIONS

In this appendix are tabulated all publications directly associated with work performed in the M.I.T. Heavy Water Lattice Project. Sc.D. theses are listed first, followed by M.S. theses, and then by other publications. For convenience, publications since the last annual progress report, dated September 30, 1964, are listed separately.

1. DOCTORAL THESES ON MITR HEAVY WATER LATTICE PROJECT

Madell, John T.
Spatial Distribution of the Neutron Flux on the Surface of a Graphite-Lined Cavity
Sc.D. Thesis, M.I.T. Nucl. Eng. Dept., January 1962
(Thesis Supervisors: I. Kaplan and T. J. Thompson)

Weitzberg, Abraham
Measurements of Neutron Capture in U-238 in Lattices of Uranium Rods in Heavy Water
Ph.D. Thesis, M.I.T. Nucl. Eng. Dept., January 1962
(Thesis Supervisors: I. Kaplan and T. J. Thompson)

Palmedo, Philip F.
Measurements of the Material Bucklings of Lattices of Natural Uranium Rods in D_2O
Ph.D. Thesis, M.I.T. Nucl. Eng. Dept., January 1962
(Thesis Supervisors: I. Kaplan and T. J. Thompson)

Wolberg, John R.
A Study of the Fast Fission Effect in Lattices of Uranium Rods in Heavy Water
Ph.D. Thesis, M.I.T. Nucl. Eng. Dept., February 1962
(Thesis Supervisors: I. Kaplan and T. J. Thompson)

Peak, John
Theory and Use of Small Subcritical Assemblies for the Measurement of Reactor Parameters
Ph.D. Thesis, M.I.T. Nucl. Eng. Dept., April 1962
(Thesis Supervisors: I. Kaplan and T. J. Thompson)

Simms, Richard
Analytical and Experimental Investigations of the Behavior of Thermal Neutrons in Lattices of Uranium Metal Rods in Heavy Water
Ph.D. Thesis, M.I.T. Nucl. Eng. Dept., October 1963
(Thesis Supervisors: I. Kaplan and T. J. Thompson)

Malaviya, Bimal K.
Studies of Reactivity and Related Parameters in Subcritical Lattices
Ph.D. Thesis, Physics Dept., Harvard University, May 1964
[Thesis Supervisors: I. Kaplan and D. D. Lanning
(T. J. Thompson, on sabbatical leave)]

D'Ardenne, Walter H.
Studies of Epithermal Neutrons in Uranium Heavy Water Lattices
Ph.D. Thesis, M.I.T. Nucl. Eng. Dept., August 1964
[Thesis Supervisors: I. Kaplan and D. D. Lanning
(T. J. Thompson, on sabbatical leave)]

2. M.S. THESES ON MITR HEAVY WATER LATTICE PROJECT

Quinteiro Blanco, Manuel
Design and Construction of an Automatic Neutron Flux Scanner for the M.I.T. Heavy Water Lattice Facility
M.S. Thesis, M.I.T. Nucl. Eng. Dept., February 1962
(Thesis Supervisor: T. J. Thompson)

Kielkiewicz, Marian S.
A Study of the Fast Fission Effect for Single Natural Uranium Rod
M.S. Thesis, M.I.T. Nucl. Eng. Dept., September 1962
(Thesis Supervisor: T. J. Thompson)

Kim, Hichull
Measurements of the Material Buckling of Lattice of Enriched Uranium Rods in Heavy Water
M.S. Thesis, M.I.T. Nucl. Eng. Dept., June 1963
(Thesis Supervisor: T. J. Thompson)

Harrington, Joseph
Measurement of the Material Buckling of a Lattice of Slightly Enriched Uranium Rods in Heavy Water
M.S. Thesis, M.I.T. Nucl. Eng. Dept., July 1963
(Thesis Supervisor: T. J. Thompson)

Bliss, Henry E.
Measurements of the Fast Effect in Heavy Water, Partially Enriched Uranium Lattices
M.S. Thesis, M.I.T. Nucl. Eng. Dept., May 1964
(Thesis Supervisor: D. D. Lanning)

Goebel, David M.
Return Coefficient Measurements for the M.I.T. Enriched Uranium-D_2O Lattice
M.S. Thesis, M.I.T. Nucl. Eng. Dept., May 1965
(Thesis Supervisor: D. D. Lanning)

Papay, Lawrence T.
Fast Neutron Fission Effect for Single Slightly Enriched Uranium Rods in Air and Heavy Water
M.S. Thesis, M.I.T. Nucl. Eng. Dept., June 1965
(Thesis Supervisor: D. D. Lanning)

Robertson, Cloin G.
Measurements of Neutron Utilization for Lattices of Slightly Enriched Uranium Rods
M.S. Thesis, M.I.T. Nucl. Eng. Dept., June 1965
(Thesis Supervisor: D. D. Lanning)

Hellman, Sanford P.
Measurements of δ_{28} and ρ_{28} in a 2.5-Inch Triangular Lattice of 0.75-Inch Metallic Uranium Rods (0.947 wt% U^{235}) in a Heavy Water Moderator
M.S. Thesis, M.I.T. Nucl. Eng. Dept., September 1965
(Thesis Supervisor: T. J. Thompson)

3. LATTICE PROJECT PUBLICATIONS

3.1 Prior to September 30, 1964

J. T. Madell, T. J. Thompson, A. E. Profio, and I. Kaplan
Spatial Distribution of the Neutron Flux on the Surface of a Graphite-Lined Cavity
NYO-9657, MITNE-18, April 1962

A. Weitzberg, I. Kaplan, and T. J. Thompson
Measurements of Neutron Capture in U-238 Lattices of Uranium Rods in Heavy Water
NYO-9659, MITNE-11, January 8, 1962

P. F. Palmedo, I. Kaplan, and T. J. Thompson
Measurements of the Material Bucklings of Lattices of Natural Uranium Rods in D_2O
NYO-9660, MITNE-13, January 20, 1962

J. R. Wolberg, T. J. Thompson, and I. Kaplan
A Study of the Fast Fission Effect in Lattices of Uranium Rods in Heavy Water
NYO-9661, MITNE-15, February 21, 1962

J. Peak, I. Kaplan and T. J. Thompson
Theory and Use of Small Subcritical Assemblies for the Measurement of Reactor Parameters
NYO-10204, MITNE-16, April 9, 1962

P. S. Brown, T. J. Thompson, I. Kaplan, and A. E. Profio
Measurements of the Spatial and Energy Distribution of Thermal Neutrons in Uranium, Heavy Water Lattices
NYO-10205, MITNE-17, August 20, 1962

K. F. Hansen
Multigroup Diffusion Methods
NYO-10206, MITNE-19, April 1962

I. Kaplan
Measurements of Reactor Parameters in Subcritical and Critical Assemblies: A Review
NYO-10207, MITNE-25, August 1962

I. Kaplan, D. D. Lanning, A. E. Profio, and T. J. Thompson
Summary Report on Heavy Water, Natural Uranium Lattice Research
NYO-10209, MITNE-35, July 1963
(Presented at the IAEA Symposium on Exponential and Critical Experiments, Amsterdam, September 2-6, 1963)

J. R. Wolberg, T. J. Thompson, and I. Kaplan
Measurement of the Ratio of Fissions in U-238 to Fissions in U-235 Using 1.60-Mev Gamma Rays of the Fission Product LA-140
NYO-10210, MITNE-36, 1963
(Presented at the IAEA Symposium on Exponential and Critical Experiments, Amsterdam, September 2-6, 1963)

R. Simms, I. Kaplan, T. J. Thompson, and D. D. Lanning
Analytical and Experimental Investigations of the Behavior of Thermal Neutrons in Lattices of Uranium Metal Rods in Heavy Water
NYO-10211, MITNE-33, October 1963

B. K. Malaviya, I. Kaplan, T. J. Thompson, and D. D. Lanning
Studies of Reactivity and Related Parameters in Slightly Enriched Uranium Heavy Water Lattices
MIT-2344-1, MITNE-49, May 1964

W. H. D'Ardenne, T. J. Thompson, D. D. Lanning, and I. Kaplan
Studies of Epithermal Neutrons in Uranium, Heavy Water Lattices
MIT-2344-2, MITNE-53, August 1964 (in press)

T. J. Thompson, I. Kaplan, and A. E. Profio
Heavy Water Lattice Project Annual Report
NYO-9658, September 30, 1961

I. Kaplan, A. E. Profio, and T. J. Thompson
Heavy Water Lattice Project Annual Report
NYO-10208, MITNE-26, September 30, 1962

I. Kaplan, D. D. Lanning, and T. J. Thompson
Heavy Water Lattice Project Annual Report
NYO-10212, MITNE-46, September 30, 1963

J. T. Madell, T. J. Thompson, A. E. Profio, and I. Kaplan
Flux Distribution in the Hohlraum Assembly
Trans. Am. Nucl. Soc. 3, 420 (December 1960)

A. Weitzberg and T. J. Thompson
Coincidence Technique for U-238 Activation Measurements
Trans. Am. Nucl. Soc. 3, 456 (December 1960)

J. T. Madell, T. J. Thompson, I. Kaplan, and A. E. Profio
Calculation of the Flux Distribution in a Cavity Assembly
Trans. Am. Nucl. Soc. 5, 85 (June 1962)

A. Weitzberg, J. R. Wolberg, T. J. Thompson, A. E. Profio, and I. Kaplan
Measurements of U-238 Capture and Fast Fission in Natural Uranium, Heavy Water Lattices
Trans. Am. Nucl. Soc. 5, 86 (June 1962)

P. S. Brown, P. F. Palmedo, T. J. Thompson, A. E. Profio, and I. Kaplan
Measurements of Microscopic and Macroscopic Flux Distributions in Natural Uranium, Heavy Water Lattices
Trans. Am. Nucl. Soc. 5, 87 (June 1962)

B. K. Malaviya and A. E. Profio
Measurement of the Diffusion Parameters of Heavy Water by the Pulsed-Neutron Technique
Trans. Am. Nucl. Soc. 6, 58 (June 1963)

B. K. Malaviya, T. J. Thompson, and I. Kaplan
Measurement of the Linear Extrapolation Distance of Black Cylinders in Exponential Experiments
Trans. Am. Nucl. Soc. 6, 240 (November 1963).

P. S. Brown, I. Kaplan, A. E. Profio, and T. J. Thompson
Measurements of the Spatial and Spectral Distribution of Thermal Neutrons in Natural Uranium Heavy Water Lattices
BNL-719, Vol. 2, 305-17, 1962

R. Simms, I. Kaplan, T. J. Thompson, and D. D. Lanning
The Failure of the Cell Cylindricalization Approximation in Closely Packed Uranium, Heavy Water Lattices
Trans. Am. Nucl. Soc. 7, 9 (June 1964)

3.2 Publications (Including Theses) Since September 30, 1964

D. D. Lanning, I. Kaplan, and F. M. Clikeman
Heavy Water Lattice Project Annual Report
MIT-2344-3, MITNE-60, September 30, 1964

B. K. Malaviya, D. D. Lanning, A. E. Profio, T. J. Thompson and I. Kaplan
Measurement of Lattice Parameters by Means of the Pulsed-Neutron Technique
Paper presented at the ANS Winter Meeting, San Francisco, November 1964

B. K. Malaviya, I. Kaplan, D. D. Lanning, and T. J. Thompson
Studies of the Reactivity Worth of Control Rods in Far Subcritical Assemblies
Trans. Am. Nucl. Soc. 8, 282 (June 1965)

Goebel, David M.
Return Coefficient Measurements for the M.I.T. Enriched Uranium-D_2O Lattice
M.S. Thesis, M.I.T. Nucl. Eng. Dept., June 1965
(Thesis Supervisor: D. D. Lanning)

Papay, Lawrence T.
Fast Neutron Fission Effect for Single Slightly Enriched Uranium Rods in Air and Heavy Water
M.S. Thesis, M.I.T. Nucl. Eng. Dept., June 1965
(Thesis Supervisor: D. D. Lanning)

Robertson, Cloin G.
Measurements of Neutron Utilization for Lattices of Slightly Enriched Uranium Rods
M.S. Thesis, M.I.T. Nucl. Eng. Dept., June 1965
(Thesis Supervisor: D. D. Lanning)

Hellman, Sanford P.
Measurements of δ_{28} and ρ_{28} in a 2.5-Inch Triangular Lattice of 0.75-Inch Metallic Uranium Rods (0.947 wt% U^{235}) in a Heavy Water Moderator
M.S. Thesis, M.I.T. Nucl. Eng. Dept., September 1965
(Thesis Supervisor: T. J. Thompson)

3.3 Forthcoming Publications

H. E. Bliss, D. D. Lanning, J. Harrington, I. Kaplan, B. K. Malaviya, and T. J. Thompson
Studies of Subcritical Lattices with Distributed Neutron Absorbers by Means of the Pulsed Neutron Source Technique
ANS Winter Meeting, Washington, D.C., November 15, 1965

E. E. Pilat, H. Guéron, and D. D. Lanning
Measurement of Diffusion Coefficient in a Highly Anisotropic Medium
ANS Winter Meeting, Washington, D. C., November 15, 1965

W. H. D'Ardenne, I. Kaplan, D. D. Lanning, and T. J. Thompson
Reactor Physics Measurements in Slightly Enriched Uranium D_2O Lattices
ANS Winter Meeting, Washington, D. C., November 15, 1965